Identification and Characterization of a Novel Population of Memory B cells in the Human Intestine

Laura Comerma Blesa

Doctoral Thesis UPF - 2016

THESIS DIRECTOR

Prof. Andrea Cerutti
iCREA
Fundación IMIM
Mount Sinai School of Medicine

THESIS CODIRECTOR

Dra. Giuliana Magri
Fundación IMIM

upf. Universitat Pompeu Fabra Barcelona

ACKNOWLEDGEMENTS

This thesis is the result of four years of intense and passionate work that had changed me in a way I would have never imagined. From MD to PhD, I am really proud of where I now stand.

Undoubtedly, this thesis has been possible thanks to many people.

First and foremost, I want to thank Professor Andrea Cerutti for giving me the opportunity of joining his group. I always had a great interest for research, but it is only now that I understand its true value. Thank you for sharing your vision and for your guidance throughout these years. It has changed my perspective about science and I am sure it will further impact my career. I will always be grateful for that.

Giuliana, thanks for all the science and hard work. It has been quite an experience! We've shared moments of stress, scientific discussions and laughs at late hours. For sure my mind has been recolonized with a huge number of priceless memories and ideas.

Sabrina, thank you for helping me so many times with your energy and joy, you are unique! Jordi, thanks for sharing that special sense of humor and for being always the voice of reason. David, thanks for your optimism and for that always-smiling-back. Nerea, thanks for listening and caring, I can’t wait to meet the new addition to the family. Marc, thanks for being patient and supportive during the multiple iterations and refinement of the NGS data. Ada and Dani, these busy months haven’t let us time for anything else than a quick coffee or breakfast but I hope this can change soon. To Eva and Erika, thanks for solving any sorting problems, even by phone late at night, and your always positive and helping attitude. To the

former members and friends of the Cerutti Lab, Irene, Linda, Mau, Carol and Jordi, thank you for making my transition from the hospital to the lab much easier, and for all the fun dinner reunions.

To the pathology department, thanks for being always there. It still feels like home when I visit to take samples, ask for tips about protocols or to just have some coffee with good friends.

To my family, thanks for caring so much about what I do, for looking at me with admiration without knowing that the feeling is mutual, and for all the efforts you invested in me. I will never be able to give back enough.

And most importantly, to my husband, Karim, I can only say thank you. You know that there are not enough words to describe how much I appreciate your unconditional support. I wouldn't be here if it weren't for you.

ABSTRACT

B cells inhabiting the gut-associated lymphoid tissue enhance tolerance against intraluminal antigens by mounting homeostatic humoral responses dominated by non-inflammatory IgA. We found that IgM^+IgD^- memory (ME-M) B cells formed a large reservoir of intestinal antigen-selected IgM^+ lymphocytes distinct from antigen-naïve IgM^+ lymphocytes. In humans, ME-M B cells colonized the intestine early in life, persisted throughout adulthood and inhabited mucosal sites of antigen entry, including Peyer's patches (PPs) and isolated lymphoid follicles (ILFs). Intestinal ME-M B cells shared some commonalities with splenic $IgM^+IgD^{low}CD27^+$ marginal zone B cells, including phenotypic traits, multiple IgVH gene families and a pronounced reactivity against microbial carbohydrates and lipids. However, ME-M B cells expressed a gut-specific gene signature and an IgVH gene mutation profile consistent with a germinal center origin from gut inductive sites. Accordingly, ME-M B cells showed strong reactivity against mucus-embedded commensal antigens. Furthermore, ME-M B cells generated IgM^+ or IgA^+ plasma cells (PC) in response to T cell-dependent or T cell-independent signals and organized clonally coordinated IgM and IgA responses in ileum and colon. IgM^+ PC emerging from ME-M B cells released IgM antibodies that along with IgA, coated bacteria and fungi embedded within the mucus layer of the gut mucosa. In summary, our findings suggest that human PPs and ILFs contain plastic collections of pre-selected lymphocytes capable to accommodate sudden antigenic changes of the microbiota via rapid production of IgM or IgA.

RESUM

Les cèl·lules B del teixit limfoide associat a la mucosa intestinal promouen la tolerància davant antígens intraluminals mitjançant respostes humorals homeostàtiques dominades per IgA anti-inflamatòria. Hem descovert que les cèl·lules B de memòria $IgM^{+}IgD^{-}$ (ME-M) formen una gran reserva intestinal de limfòcits preseleccionats diferents dels limfòcits IgM^{+} verges. En els éssers humans, les cèl·lules B ME-M colonitzen l'intestí als inicis de la vida i hi perduren durant l'edat adulta localitzades en llocs propers a l'entrada d'antígens, com les plaques de Peyer (PP) i els fol·licles limfoides aïllats (ILF). Les cèl·lules B ME-M intestinals comparteixen una sèrie de característiques amb les cèl·lules B $IgM^{+}IgD^{lleu}CD27^{+}$ de la zona marginal de la melsa, incloent trets fenotípics, múltiples famílies de gens IgVH i una reactivitat pronunciada contra hidrats de carboni i lípids microbians. No obstant això, les cèl·lules B ME-M expressen una signatura gènica específica de la mucosa intestinal i un perfil de mutació en els gens IgVH consistent amb un origen als centres germinals de les zones inductives del intestí. D'acord amb això, les cèl·lules B ME-M mostren una forta reactivitat enfront d'antígens comensals localitzats al moc intestinal. A més, les cèl·lules B ME-M generen cèl·lules plasmàtiques (PC) IgM^{+} o IgA^{+} en resposta a senyals dependents i independents de cèl·lules T, i organitzen respostes clonals coordinades IgM i IgA en l'ili i el còlon. PC IgM^{+} derivades de cèl·lules B ME-M, produeixen anticossos IgM que, juntament amb IgA, recobreixen bacteris i fongs localitzats al moc intestinal. En resum, els nostres resultats suggereixen que en humans, les PP i els ILF contenen col·leccions plàstiques de limfòcits preseleccionats amb capacitat per a acomodar canvis antigènics sobtats de la microbiota a través de la producció rápida d'IgM o IgA.

PREFACE

Mucosal organs are under constant exposure to external attacks and regulate our relationship with the external environment. In the gut, commensal bacteria live peacefully in the intestinal lumen without generating any adverse effects. Most importantly, commensal microbes stimulate the maturation of the gut immune system and form an ecological niche that prevents the growth of pathogens. Conversely, the gut lumen provides commensals with a stable and energy rich habitat. In this mutualistic relationship, microbial signals stimulate the intestinal mucosa to generate a non-inflammatory homeostatic balance dominated by the IgA^+ plasma cell pool. IgA blocks the penetration of invading pathogens to our body through a process known as "immune exclusion" and also modulates the interaction of commensal bacteria with the mucosal immune system by mitigating associated inflammatory responses. Whereas the plasma cell compartment provides long-term protection through continuous secretion of low levels of antibodies, memory B cells allow for a rapid and robust recall response upon antigenic changes in the microbial environment.

ABBREVIATIONS

AHR	Aryl hydrocarbon receptor
AID	Activation-induced cytidine deaminase
APRIL	A proliferation-inducing ligand
ASC	Antibody-secreting cells
BAFF	B-cell activating factor
Bcl-6	B cell lymphoma-6
BCMA	B cell maturation antigen
BCR	B cell receptor
Blimp-1	B lymphocyte-induced maturation protein 1
CCL	Chemokine ligand
CCR	Chemokine receptor
CD40L	CD40 ligand
CFSE	Carboxyfluorescein diacetate succinimidyl ester
CP	Cryptopatches
CR	Complement receptor
CSR	Class switch recombination
CT	Circle transcripts
CVID	Combined variable immunodeficiency
CXCL	C-X-C chemokine ligand
CXCR	C-X-C chemokine receptor
DAPI	4′-6-diamidine-2′-phenylindole
DC	Dendritic cell

EBV	Epstein–Barr virus
ELISA	Enzyme-Linked ImmunoSorbent Assay
FAE	Follicular-associated epithelium
FCRL	Fc receptor–like
FDC	Follicular dendritic cell
FFPE	Formalin-fixed and paraffin-embedded
GALT	Gut-associated lymphoid tissue
GC	Germinal center
GLT	Germline transcripts
GM-CSF	Granulocyte macrophage colony-stimulating factor
GPR	G protein-coupled receptor
HIGM	Hyper-IgM syndrome
ICOS	Inducible co-stimulator
IEC	Intestinal epithelial cells
Ig	Immunoglobulin
IgH	Immunoglobulin heavy chain
IGHJ	Immunoglobulin heavy chain joining region
IGHV	Immunoglobulin heavy chain variable region
IL	Interleukin
ILC	Innate lymphoid cell
ILF	Isolated lymphoid follicle
IRF4	Interferon regulatory factor 4
KREC	Kappa-deleting recombination excision circle
LP	Lamina propria
LT	Lymphotoxin

LTi	lymphoid tissue inducer
LTo	Lymphoid tissue organizer
MAdCAM-1	Mucosal addressin cell adhesion molecule 1
MALT	Mucosa-associated lymphoid tissues
ME-A	Immunoglobulin A class-switched memory
ME-G/E	IgG/IgE memory
ME-M	$IgM^{+}IgD^{-}$ memory
ME-SW	Switched memory
MHC	Major histocompatibility complex
MLN	Mesenteric lymph nodes
MRC	Marginal reticular cell
MZ	Marginal zone
N	Naive
NCR	Natural cytotoxicity receptor
NGS	Next generation sequencing
NK	Natural killer
PAX5	Paired box 5
PB	Plasmablast
PC	Plasma cell
PC-A	Immunoglobulin A-secreting plasma cell
PD-1	Programmed cell death-1
PDL2	Programmed cell death 1 ligand 2
pIgR	Polymeric immunoglobulin receptor
PP	Peyer's patches
RAG	Recombination activating gene

RANKL	Receptor activator of nuclear factor κ-B ligand
RMA	Robust multi-array average
RORγt	Retinoic acid-related orphan receptor γt
SC	Stromal cells
SED	Subepithelial dome
SHM	Somatic hypermutation
SIgA	Secretory immunoglobulin A
SIgAD	Selective immunoglobulin A deficiency
Siglec	Sialic acid binding immunoglobulin-like lectin
SIgM	Secretory immunoglobulin M
SPF	Specific pathogen free
TACI	Transmembrane activator and calcium-modulating cyclophilin-ligand interactor
TCR	T cell receptor
TD	T cell-dependent
T_{FH}	T follicular helper
T_{FR}	T follicular regulatory
TGF-β	Transforming growth factor β
TI	T cell-independent
TLR	Toll-like receptor
TNF	Tumor necrosis factor
T_{REG}	T regulatory
TSLP	Thymic stromal lymphopoietin
VCAM-1	Vascular cell adhesion molecule 1
XBP1	X-box-binding protein 1

CONTENTS

ABSTRACT vii
PREFACE xi
ABBREVIATIONS xiii

CHAPTER 1 INTRODUCTION 1

I. Humoral Systemic Immune Responses 3
1. Systemic Immunity 3
2. B Cell Development 3
3. B Cell Activation and Differentiation 5
A. T Cell-Dependent B cell responses 5
a. Germinal Center 7
i. Germinal Center Components 9
ii. Germinal Center Reaction 10
B. T Cell-Independent B Cell Responses 15
C. Humoral Memory 18
a. Memory B Cells 19
b. Plasma Cells 21

II. Mucosal Immune Responses 22
1. Mucosal Immunology 22
2. Anatomy and Histology of the Gut 23
A. Regional Differences along the Gut 24
3. Immunological Components of the Gut Mucosa 25
A. Mucosal Barrier: Mucus and Epithelial Cells 25
B. Gut-Associated Lymphoid Tissue 26
a. Peyer's Patches 26
b. Isolated Lymphoid Follicles 27
C. Lamina Propria 28
4. Mesenteric Lymph Nodes 32
5. Gut Microbiota 33
6. IgA Responses in the Gut 34
A. IgA Structure and Function 35
B. IgA Induction 37

a. T Cell-Dependent IgA Induction 38
b. T Cell-Independent IgA Induction 41
7. Clinical Relevance 44

CHAPTER 2 AIMS 47

CHAPTER 3 MATERIALS AND METHODS 51

CHAPTER 4 RESULTS 69

CHAPTER 5 DISCUSSION 137

CHAPTER 6 CONCLUSIONS 159

ANNEX I References 167

ANNEX II Publications 195

CHAPTER 1
INTRODUCTION

I. Humoral Systemic Immune Responses

1. Systemic Immunity

The immune system comprises the physical structures and biological processes that protect our body against disease, through the recognition and clearance of antigens, the elimination of abnormal host's cells capable of inducing inflammation or tumor growth[1], and the generation of multiple layers of innate and adaptive defenses with increasing specificity[2]. Any alteration on these functions can lead to the onset of autoimmunity, inflammation or cancer[3].

Components of the **innate immune system** are able to react to pathogen invasion at the site of injury or infection within minutes. Granulocytes, monocytes, macrophages, dendritic cells (DCs) and natural killer (NK) cells recognize and respond to microbes through nonspecific germline-encoded pattern recognition receptors, including the Toll-like receptors (TLRs)[4,5].

B and T cells from the **adaptive immune system** recognize microbes through specific somatically recombined antigen receptors known as B cell receptor (BCR) and T cell receptor (TCR), respectively. A remarkable feature of B and T cell responses is that they generate protective antibodies and long-lived memory cells that patrol our body for years after the initial antigen encounter and mount very rapid and robust secondary responses upon reinfection[6].

2. B Cell Development

B cells are a subset of lymphocytes that produce immunoglobulin (Ig) molecules, commonly known as **antibodies** that target specific antigenic determinants (or epitopes) associated with intruding microbes. B cells

were originally described in the bursa of Fabricius, the site of B cell maturation in birds and chickens[7]. Coincidentally, this nomenclature is also appropriate for several mammalian species, where the bone marrow is the major site of B cell development.

In humans, B cells develop from hematopoietic stem cells in the fetal liver during gestation and in the bone marrow after birth[8]. Each newly generated B lymphocyte carries a transmembrane Ig receptor comprised of two identical Ig heavy chain (H) molecules and two identical Ig light chain (L) molecules, which can be either Igκ or Igλ[9].

The IgH and IgL chain molecules include an antigen-binding variable region encoded by recombined V_HDJ_H and V_LJ_L genes, respectively. The V, D and J segments of these genes are organized in multiple families within the IgH and IgL loci and their assembly into in-frame V_HDJ_H and V_LJ_L exons requires an antigen-independent diversification process known as V(D)J recombination[10,11]. These DNA recombination events require recombination activating gene (RAG) 1 and RAG2 endonucleases and are associated with D gene diversification by nucleotide addition via the enzyme terminal deoxyribonucleotidil transferase. Finally, the assembly of the IgL chain with the IgH chain is followed by the expression of a fully competent IgM receptor that functions as a **surface BCR**[12].

At this point, self-reactive clones are extinguished by apoptosis or receptor editing[13,14], whereas non-autoreactive immature B cells leave the bone marrow as transitional B cells that co-express IgM and IgD through a process of alternative splicing of a long RNA containing VHDJH as well as Cμ and Cδ exons[15]. **Transitional B cells** are typically short-lived and express high levels of the developmentally regulated molecules CD24 and CD38, but not the memory B cell molecule CD27[16]. These transitional B cells become fully **mature naïve B cells** expressing unmutated V(D)J

genes, IgM, IgD and CD19, but not CD24, CD27 and CD38, after colonizing peripheral lymphoid organs (Fig. 1).

3. B Cell Activation and Differentiation

After encountering native antigens in secondary lymphoid organs such as the spleen, lymph nodes and mucosa-associated lymphoid tissues (MALT), mature naïve B cells become activated and undergo further differentiation (Fig. 2).

A. T Cell-Dependent B cell responses

In secondary lymphoid tissues naive B cells are found in primary follicles with interspersed interfollicular areas, enriched in T cells and DCs. In the primary follicle[17], naïve B cells recognize and internalize protein antigens through the surface IgM and IgD receptors[18,19] and after receiving activating signals from the BCR, down-regulate the expression of surface IgD and process the internalized antigen to form an major histocompatibility complex (MHC) class II-peptide complex. After downregulating CXC chemokine receptor (CXCR) 5 and through the upregulation of chemokine receptor (CCR) 7[20], B cells are able to follow chemotactic gradients established by its ligands, chemokine ligand (CCL) 19 and CCL21, and migrate to the follicular T-B border, an area between the B cell follicle and the T cell zone[17,21]. At the T-B border, they form long-lived interactions with antigen-specific T cells to become fully activated[22,23] (Fig. 2). This interaction between CD40 on B cells with CD40 ligand (CD40L) on antigen-activated $CD4^+$ T cells[24], triggers either a follicular or an extrafollicular B cell differentiation pathway[25]. In the **extrafollicular pathway**, antigen-activated proliferating B cells differentiate into short-lived plasmablasts (PBs) (Fig. 1).

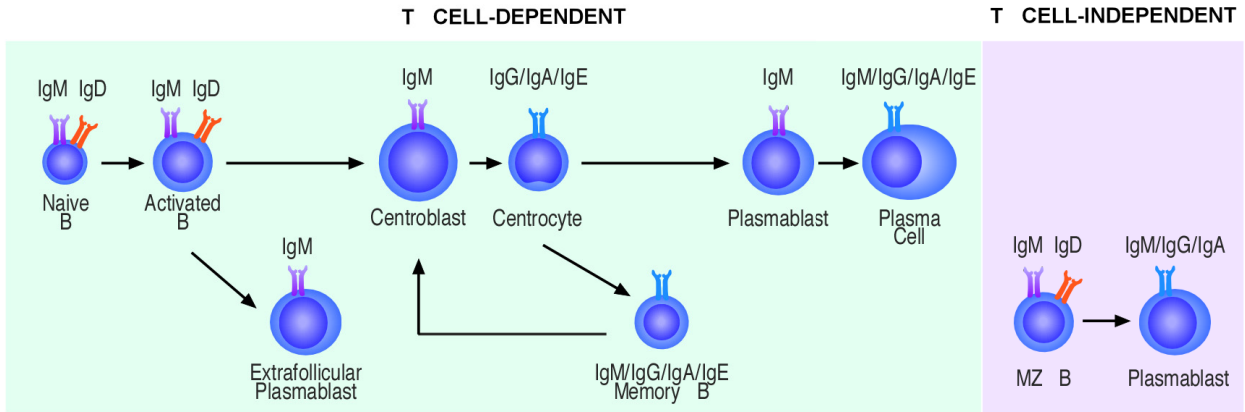

Proliferation	No	Yes	Yes	Yes	No	No	No	No	No	Yes
AID	No	No	No	++	++	No	No	No	No	No
IgV gene mutations	No	No	No/Low	Yes	Yes	Yes	Yes	Yes	Yes	Yes
Phenotype	IgM^+ IgD^{hi} $CD10^-$ $CD19^+$ $CD27^-$ $CD38^-$ $MHC\text{-}II^+$ $Ki67^-$	IgM^+ IgD^+ $CD10^-$ $CD19^+$ $CD27^-$ $CD38^-$ $MHC\text{-}II^+$ $Ki67^+$	IgM^+ IgD^- $CD10^-$ $CD19^+$ $CD27^+$ $CD38^+$ $MHC\text{-}II^+$ $Ki67^+$	IgM^+ IgD^- $CD10^+$ $CD19^+$ $CD27^-$ $CD38^+$ $MHC\text{-}II^+$ $Ki67^+$	$IgG/IgA/IgE$ IgD^- $CD10^+$ $CD19^+$ $CD27^-$ $CD38^+$ $MHC\text{-}II^+$ $Ki67^-$	$IgG/IgA/IgE$ IgD^- $CD10^-$ $CD19^+$ $CD27^+$ $CD38^-$ $MHC\text{-}II^+$ $Ki67^-$	$IgG/IgA/IgE$ IgD^- $CD10^-$ $CD19^+$ $CD27^+$ $CD38^+$ $MHC\text{-}II^+$ $Ki67^+$	$IgG/IgA/IgE$ IgD^- $CD10^-$ $CD19^+$ $CD27^+$ $CD38^+$ $MHC\text{-}II^-$ $Ki67^-$	IgM^+ IgD^{lo} $CD10^-$ $CD19^+$ $CD27^+$ $CD38^-$ $MHC\text{-}II^+$ $Ki67^-$	$IgM/IgG/IgA$ IgD^- $CD10^-$ $CD19^+$ $CD27^{hi}$ $CD38^+$ $MHC\text{-}II^+$ $Ki67^+$
Location	Circulation, 1ary follicle Mantle	Interfollicular area	Interfollicular area	Germinal center (dark zone)	Germinal center (light zone)	Circulation, interfollicular area	Circulation, interfollicular area	BM	MZ	Extrafollicular area

Figure 1. Development of mature B cells in secondary lymphoid organs. After encountering antigen, mature B cells progress along phenotypically and genotypically distinct stages of differentiation. Naïve B cells populate primary follicles in secondary lymphoid organs and predominantly differentiate through a TD pathway that involves a cognate interaction with antigen primed T_{FH} cells. Activated B cells emerging from this interaction either differentiate along an extrafollicular pathway that leads to the formation of short-lived IgM secreting PBs or enter the GC to become highly proliferating centroblasts. These cells express AID, undergo robust IgV gene SHM and can undergo class switching from IgM to IgG, IgA or (very rarely) IgE, before becoming centrocytes. Centrocytes can further differentiate to long-lived memory B cells, which recirculate and can reenter a GC reaction, or antibody secreting PBs that differentiate to long-lived antibody secreting PCs which migrate to the bone marrow. MZ B cells populate the MZ of the spleen and predominantly differentiate through a TI pathway that involves noncognate interactions with innate immune cells. MZ B cells express moderately mutated IgV genes and differentiate to PBs that secrete IgM, IgG or IgA antibodies.

On the other hand, in the **follicular pathway** B cells express the B cell lymphoma-6 (Bcl-6) transcription factor and migrate to the center of the follicle, where they proliferate within a meshwork of follicular dendritic cells (FDCs) to form the germinal center (GC)[26] (Fig. 2).

a. Germinal Center

GCs in secondary lymphoid organs are unique microenvironments where antigen-activated B cells undergo clonal expansion and interact with cognate $CD4^+$ T cells and antigens displayed on the surface of FDCs to generate a large and highly diverse antibody repertoire of different antibody isotypes (Fig. 2).

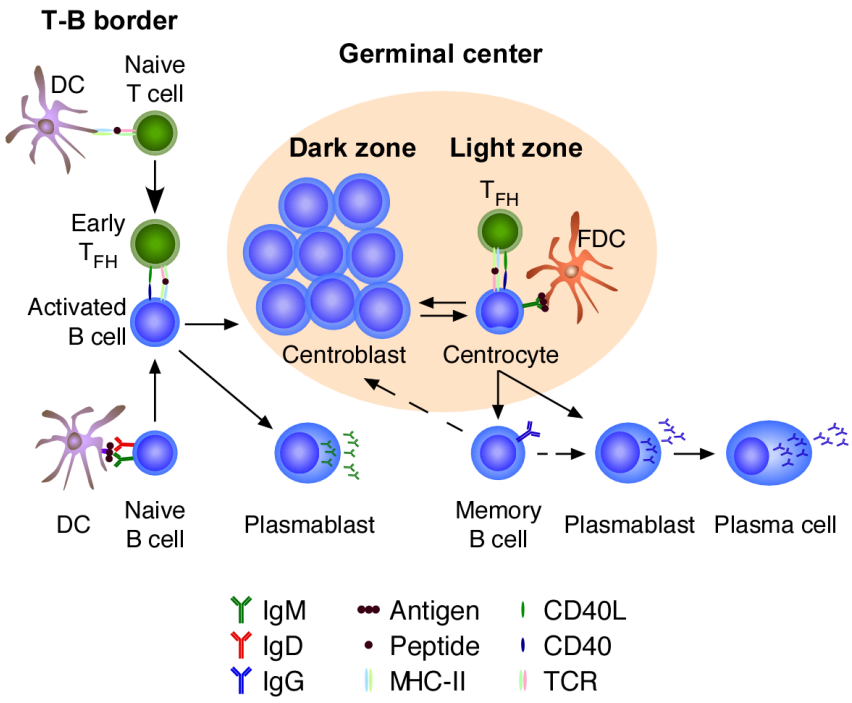

Figure 2. T cell-dependent B cell response. Naïve B cells capture protein antigen through the surface IgM and IgD receptors and subsequently move to the T-B border to interact with antigen activated $CD4^+$ T cells that become early T_{FH} cells. After cognate B cell – T cell interaction, B cells can either follow an extrafollicular pathway to differentiate to IgM^+ short-lived PBs, or a follicular differentiation pathway to become GC centroblasts. In the dark zone of the GC, centroblasts undergo extensive proliferation, express AID, induce SHM and can undergo CSR from IgM to IgG, IgA or IgE (the figure only shows IgG). After exiting the cell cycle, centroblasts move to the light zone where they differentiate to centrocytes and interact with FDCs presenting antigen on their surface and with T_{FH} cells that provide them survival and differentiation signals. Centrocytes bearing low-affinity BCRs die by apoptosis, whereas centrocytes with high affinity for antigen receive survival signals. After undergoing a variable number of cycles of proliferation, SHM and affinity maturation, B cells exit the GC reaction as memory cells that recirculate or as PBs that will home to effector sites and differentiate to PCs.

i. Germinal Center Components

Follicular Dendritic Cells. FDCs are a subset of SCs essential for efficient GC formation and for the production of high-affinity antibodies[27]. They are specialized in the capture and retention of large amounts of antigen on their surface in the form of immune complexes[28,29] and produce abundant C-X-C chemokine ligand (CXCL) 13, which serves as CXCR5 ligand for antigen-activated B and T cells[30]. Importantly, FDCs produce transforming growth factor β (TGF-β) 1, interleukin (IL) 6 and B-cell activating factor of the tumor necrosis factor (TNF) family (BAFF; also known as *TNFSF13B*), which promote B cell survival and contribute to the GC reaction[31-33].

Germinal Center T Cells. The GC contains two major subsets of $CD4^+$ T cells, T follicular helper (T_{FH}) cells and T follicular regulatory (T_{FR}) cells. Both T_{FH} and T_{FR} cells require Bcl-6 for their generation[34-36] and express CXCR5, which allows them to migrate to the B cell follicle in response to CXCL13, released by FDCs[37,38]. More specifically, T_{FH} cells express high levels of CD40L as well as other co-stimulatory molecules such as inducible co-stimulator (ICOS), OX40 and programmed cell death-1 (PD-1), and produce powerful B cell-helper cytokines such as IL-21 and IL-4. Therefore, T_{FH} cells are essential for the maintenance and function of GCs and the generation of memory B cells and plasma cells (PCs)[39].

On the other hand, **T_{FR} cells** express the transcription factors Foxp3, GITR, and CTLA-4, but lack CD40L, and secrete mostly IL-10. Although less abundant than T_{FH} cells, they participate in the regulation of the GC microenvironment by inhibiting T_{FH} expansion and cytokine secretion and by directly suppressing B cells[38].

Germinal Center B Cells. GC B cells were initially described based on their morphological appearance and geographical localization within the GC, which is divided in two compartments known as dark zone and light zone based on their histological appearance. B cells located in the dark zone of the GC are known as centroblasts and appear as large and densely packed proliferating cells that express CXCR4[40,41] within a network of reticular cells expressing CXCL12[42]. On the other hand, GC B cells in the light zone of the GC are referred to as centrocytes, and appear as small non-dividing cells expressing CXCR5[40]. Both centroblasts and centrocytes express IgM, IgG or IgA together with CD19, CD27, CD38 and CD10, but do not express IgD and CD24 (Fig. 1). Two defining characteristics of GC B cells are the expression of the GC-associated transcription factor Bcl-6 and the expression of the enzyme activation-induced cytidine deaminase (AID) that mediates antibody diversification through class switch recombination (CSR) and somatic hypermutation (SHM)[43,44]. Furthermore, unlike naïve B cells from the follicular mantle, centroblasts and centrocytes lack the intracellular anti-apoptotic factor Bcl-2 and instead express intracellular Bcl-2 family members with pro-apoptotic activity[45-47]. These features render GC B cells highly susceptible to apoptosis and allow their elimination in the absence of engagement of BCR by high-affinity antigens.

ii. Germinal Center Reaction

GCs represent the hallmark of **T cell-dependent** (TD) antibody responses arising after antigenic stimulation[48,49]. After increasing the expression of CXCR5, early T_{FH} cells and activated B cells move to the follicle in response to CXCL13 produced by FDCs[50-52] and enter a Bcl-6-dependent genetic program[34,36] essential for the maintenance and development of the GC reaction[53]. In the early GC reaction, B cells grow and differentiate into

B cell blasts that proliferate and populate the network of FDCs in the center of the follicle, thereby displacing the naive IgM^+IgD^+ B cells to the periphery of the follicle to form the mantle zone and thus establishing a **secondary follicle**[53]. The rapid proliferation of the B cell blasts causes an increase in the GC size, and by day 7 after immunization, the GC is already polarized into two different compartments known as the dark zone and the light zone[26] (Fig. 2).

In the dark zone of the GC centroblasts undergo extensive clonal expansion as well as **SHM** and **CSR**, two Ig-diversifying processes that are highly dependent on AID. While CSR diversifies the effector functions of an Ig molecule, SHM provides a structural substrate for the selection of Igs with higher affinity for antigen[44,54-56]. After undergoing proliferation and SHM in the dark zone, centroblasts exit the cell cycle and migrate to the light zone of the GC where they become smaller and non-dividing centrocytes. In the light zone, by using their newly mutated BCR, centrocytes recognize and bind native antigen trapped on the surface of FDCs[57-59], and establish a cognate CD40-CD40L interaction with GC T_{FH} cells[60]. At this point, competition for T cell help from T_{FH} cells that patrol the light zone interacting with many B cells is the major factor determining the selection of B cells based on their affinity for antigen. Centrocytes expressing a low-affinity BCR do not receive survival signals from T_{FH} cells, undergo apoptosis and are finally engulfed by resident phagocytes known as tingible body macrophages[53,61]. On the contrary, GC B cells with higher antigen affinity are selected from the large pool of antigen-specific B cells by receiving survival signals form T_{FH} cells. Moreover, the highly specialized GC microenvironment supports the interaction and rapid movement of various cell types between the different GC compartments. Thus, B cells that receive survival signals in the light zone can either re-enter the dark zone of the GC to undergo

further proliferation and SHM, or can exit the GC as memory B cells or PCs. The GC B cells with the highest antigen affinity are instructed to recirculate to the dark zone to undergo further rounds of division and SHM[62], which results in the production of B cells with increasing affinity for the antigen over time, a process that is known as affinity maturation. T_{FH} cells contribute not only to the maintenance and selection of high-affinity and class-switched centrocytes, but through the production of high levels of IL-21, also contribute to the differentiation of these centrocytes into memory B cells or PCs[63-67].

Class Switch Recombination. CSR is an irreversible DNA recombination event that allows the formation of Igs with identical antigen specificity but different effector functions (Fig. 3). This process replaces the Cμ gene encoding the C_H region of the IgM molecule with the Cγ1, Cγ2, Cγ3, Cγ4, Cα1, Cα2 or Cε gene encoding the C_H region of IgG1, IgG2, IgG3, IgG4, IgA1, IgA2 or IgE, respectively[68,69].

Figure 3. Mechanism underlying antibody class switching. The IgH locus contains a rearranged V_HDJ_H exon encoding the antigen-binding domain of an immunoglobulin. B cells produce IgM and IgD through a transcriptional process driven by a promoter (P) upstream of V_HDJ_H. Production of IgG, IgA or IgE with identical antigen specificity but different effector function occurs through CSR. The diagram shows the mechanism of IgA CSR, but a similar mechanism underlies IgG and IgE CSR. Appropriate stimuli induce germline transcription of the Cμ and Cα genes from a promoter located upstream of V_HDJ_H and through an intronic μ (Iμ) exon and an intronic switch (Sμ) region located upstream of Cμ, and from a promoter of an intronic Iα exon through an intronic Sα region located between Iα and Cα exons. In addition to yielding sterile Iμ-Cμ and Iα-Cα mRNAs, germline transcription renders the Cμ and Cα genes substrate for AID, which deaminates cytosine residues on both DNA strands of the transcribed S regions to generate multiple DNA lesions that are processed into double-stranded DNA breaks. Fusion of these breaks induces excision of the noncoding intervening DNA (switch circle) and rearrangement of the IgH locus by replacement of Cμ with the downstream Cα gene. Post-switch transcription of the IgH locus generates mRNAs for IgA protein.

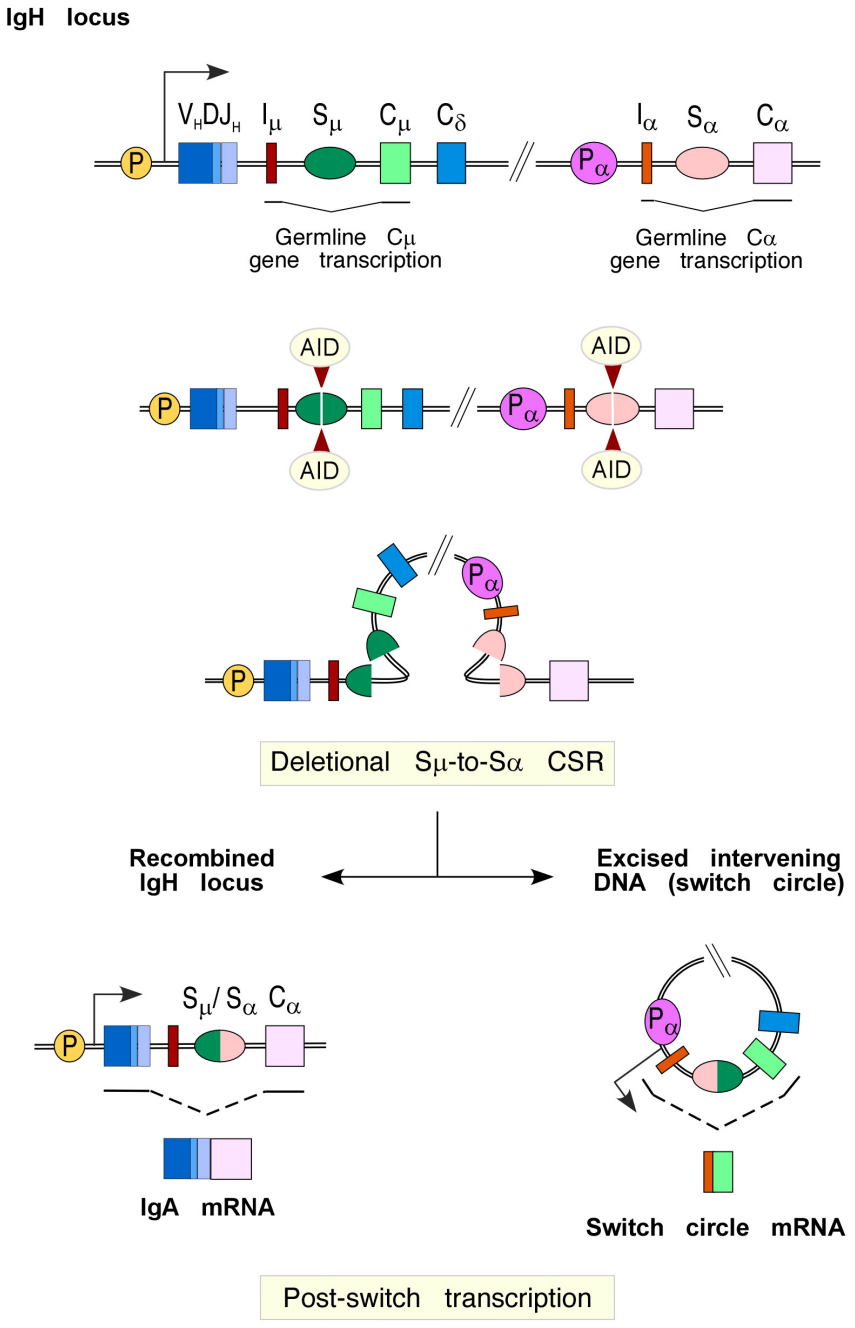
IgH locus
P
VHDJH
Iμ
Sμ
Cμ
Cδ
Pα
Iα
Sα
Cα
Germline Cμ gene transcription
Germline Cα gene transcription
AID
AID
AID
AID
Deletional Sμ-to-Sα CSR
Recombined IgH locus
Excised intervening DNA (switch circle)
Sμ/ Sα
IgA mRNA
Switch circle mRNA
Post-switch transcription

CSR targets intronic DNA sequences termed switch (S) regions located upstream of each of the heavy chain constant (C_H) region genes (Fig. 3). Activation of B cells through the interaction with CD40L and specific cytokine signals[69,70] induces both AID expression and germline transcription of a specific C_H gene. This germline transcription generates a transcript that associates with the template DNA strand of the targeted S region to form a stable DNA–RNA hybrid specifically recognized by AID. AID is a DNA-editing enzyme that deaminates cytosine residues on both DNA strands of the transcribed S region to generate multiple DNA lesions that are processed into double-stranded DNA breaks[69]. Fusion of double-stranded DNA breaks via the non-homologous end-joining pathway induces excision of the noncoding intervening DNA and rearrangement of the IgH locus by replacement of Cμ with a downstream C_H gene. The resulting juxtaposition of the recombined VDJ gene with a Cγ, Cα or Cε gene permits B cells to acquire an Ig with novel effector functions but identical specificity for antigen[69].

Although much debated, it is not clear whether the process of CSR occurs preferentially in the GC or in extrafollicular areas. The fact that CSR requires cell proliferation[71-74] and AID expression, and that class switched B cells are found in the GC, initially pointed towards the dark zone of the GC as the obvious site for antibody class switching[75]. However, AID is also expressed in tonsillar and splenic extrafollicular blasts[76], and mouse studies have shown that class switching can clearly occur as early as 2 days after antigen exposure, prior to GC formation[55,77]. Finally, CSR can also occur independently of T cell help, induced by the production of high levels of BAFF by mucosal epithelial cells and DCs[78-80].

Somatic Hypermutation. SHM is the process by which GC B cells Ig variable (IgV) region genes are diversified to produce a broad spectrum

range of affinities for an immunized antigen[81,82], by introducing point mutations in the recombined V(D)J exons encoding the antigen-binding V region of an antibody[83,84]. These mutations mostly generate aminoacid replacements in complementarity determining regions, which play a key role in the formation of the antigen-binding pocket formed by the V regions of IgH and IgL chains[69,84]. These point mutations provide a structural substrate for the selection of high-affinity B cells by antigen exposed on FDCs, a process known as affinity maturation. SHM includes an initial phase that requires the mutagenic activity of AID, followed by a second phase that involves the error-prone repair of AID-induced mutations[85]. Error-prone DNA repair is performed by members of a family of low-fidelity translesional DNA polymerases that recognize DNA lesions and bypass them by inserting bases opposite to the lesion[86,87]. Amino acid replacements brought about by SHM increase the affinity and fine specificity of an antibody, but do not modify the framework regions, which regulate the structural organization of Ig molecules.

B. T Cell-Independent B Cell Responses

The generation of immune protection in response to a protein antigen via a GC TD pathway is relatively slow and needs to be integrated with a faster T cell-independent (TI) pathway. The TI antibody response is initiated by carbohydrate or lipid antigens captured by macrophages and DCs that activate extrafollicular B cells through CD40L-like factors at mucosal surfaces and in the marginal zone (MZ) of the spleen[88-90]. These CD40L-like factors include BAFF and a proliferation-inducing ligand (APRIL)[91,92], two CD40L-related molecules released by cells of the innate immune system such as macrophages, DCs, granulocytes and epithelial cells after sensing the presence of microbes via TLRs[79,93-96].

While TD immune responses generally involve conventional B2 cells that recognize antigenic epitopes through somatically recombined BCRs, the B cell subsets usually engaged in TI responses are B-1 cells and MZ B cells[97-99]. These 'innate-like' B cell subsets are positioned in areas of continual microbial exposure, such as the skin and mucosal surfaces, and express high levels of TLRs and poorly diversified BCRs molecules that recognize multiple highly conserved microbial determinants[100,101].

In the mouse, **B-1 cells** constitute a distinct lineage of self-renewing B cells that arise during fetal life, home predominantly to the peritoneal cavity, spleen and intestine[97] and express CD5 and high levels of IgM. B-1 cells recognize common bacterial antigens such as phosphorylcoline as well as self-antigens, such as phosphatidylcholine, Ig, DNA, and membrane proteins on erythrocytes and thymocytes. B-1 cells generate innate (or 'natural') adaptive immunity by spontaneously releasing large amounts of polyspecific IgM but also class-switched antibodies that provide a first line of defense against viral and bacterial infections, without previous exposure to any environmental antigens or immunization. However, the existence of a human B-1 cell counterpart has been highly debated but remains uncertain[102].

Similar to B-1 cells, **MZ B cells in mice** express polyspecific antibodies that recognize TI antigens with low affinity[89]. The MZ of the spleen is a unique lymphoid compartment located at the interface between the circulation and the immune system[103], but due to important differences in the splenic anatomy of mice and humans[104], MZ B cells show important differences between the two species. In the **murine spleen**, a fenestrated vessel known as marginal sinus surrounds the B cell follicles and the periarteriolar lymphoid sheath of T cells and separates them from the MZ that is in direct contact with the red pulp. On the other hand, **in humans,**

the MZ surrounds B cell follicles, there is no defined marginal sinus and the blood flow drains in the perifollicular zone, an area of open blood circulation between the MZ and the red pulp, which allows for MZ B cells to rapidly respond against blood-borne TI antigens such as polysaccharides and microbial TLR ligands[101]. Besides its strategic localization, the human splenic MZ is a complex anatomical compartment with multiple types of cells including a specialized subset of neutrophils, stromal cells (SCs) and innate lymphoid cells (ILCs), as well as DCs and macrophages that are able to interact with MZ B cells and participate in TI immune responses to blood-borne pathogens and particulate antigens[101].

After sensing pathogens through BCRs and TLRs, **MZ B cells** receive co-stimulatory signals from myeloid cells from the innate immune system that release B cell-stimulating cytokines such as IL-6 and IL-10 as well as BAFF and APRIL that stimulate the production of low-affinity antibodies by MZ B cells[80,101,105-108]. Although predominantly occurring in the T cell and GC-dependent pathway, CSR and SHM can also occur in extrafollicular B cells engaged in a TI immune response[109,110]. In fact, MZ B cells show elevated expression of the transmembrane activator and calcium-modulating cyclophilin-ligand interactor (TACI), a receptor that triggers CSR and antibody production in response to BAFF and APRIL[89,111]. In particular, **neutrophils** located in the perifollicular zone around the MZ, after receiving reprogramming signals from splenic sinusoidal endothelial cells, including IL-10, are able to induce CSR, SHM and antibody production by MZ B cells through a mechanism involving BAFF, APRIL and IL-21[105]. Moreover, in humans, type 3 ILC (**ILC3**), a recently identified type of ILC, inhabits the MZ and perifollicular zone of the spleen, closely interacting with a specialized type of SC cell known as marginal reticular cell (MRC) that produces mucosal addressin cell adhesion molecule 1 (MAdCAM-1) [112]. Upon

stimulation form lymphotoxin (LT) and TNF from ILC3s, MRCs upregulate the expression of ILC3-targeting survival factors, such as IL-7. ILC3 participate in the differentiation of MZ B cells through the expression of BAFF, CD40L and Delta-like 1, a NOTCH2 ligand, and also release granulocyte macrophage colony-stimulating factor (GM-CSF), which co-opts neutrophils expressing BAFF and APRIL[112].

Human MZ B cells express high levels of surface IgM and low levels of surface IgD ($IgM^{hi}IgD^{low}$) as well as the molecules CD1c, CD21 and CD27, do not express CD23 and show low levels of mutations in the Ig V(D)J genes[105,110,113,114] (Fig. 1). MZ B cells typically produce high levels of low affinity antibodies, but can also follow a TI pathway to produce antibodies specific for microbial polysaccharides[110,115], and are able to participate in TD antibody responses[116-118]. Finally, it is very important to note that while the murine MZ is a sessile B cell compartment, MZ B cells in humans recirculate and are present in the peripheral blood, in the inner wall of the subcapsular sinus of lymph nodes, in the subepithelial areas of the tonsil and in the subepithelial dome (SED) of intestinal Peyer's Patches (PP)[105,119-121].

C. Humoral Memory

The production of specific antibodies towards a secondary antigenic challenge is known as **humoral memory**, and is of central importance to our immune protection. Humoral memory has two layers of defense against reinfection known as constitutive humoral memory and reactive humoral memory[122]. **Constitutive humoral memory** is the first layer of defense against a secondary antigenic challenge and is based on the presence of pre-existing protective antibodies produced by long-lived PCs. If the antibody concentration at the site of antigen entry is not high enough, a second layer of defense or **reactive humoral memory** arises

and pathogen-experienced memory B cells are rapidly reactivated to differentiate to PBs and produce antibodies[123].

a. Memory B Cells

The reactive humoral memory response generated after a secondary antigen encounter is characterized by rapid memory B cell activation, proliferation, differentiation and secretion of high-affinity antibodies, and therefore, it is faster, of greater magnitude and higher affinity than the primary antibody response[124]. Memory B cells express mutated V(D)J genes and IgM, IgG or IgA, as well as CD19, CD24 and CD27, but not IgD or CD38 (Fig. 1), and bear high-affinity BCRs generated during the primary immune response to the antigen[75,81,82,125].

After the first antigen encounter, naive B cells with higher affinity for the antigen, present more peptide-MHC to cognate T_{FH} cells at the T-B border of the follicle forming durable T_{FH} cell – B cell conjugates that increase the amount of T cell help provided to the activated B cell[126]. In addition to CD40 signaling, IL-21 secreted by T_{FH} cells upregulates the expression of Bcl-6 in B cells, which prompts the differentiation into a GC B cell[60,127]. The mechanism by which GC B cells differentiate to memory B cells is still unclear and it has not been possible to find a single deterministic transcription factor associated with memory differentiation[122]. One hypothesis is that memory B cells may differentiate stochastically from GC B cells and the fact that they require lower levels of cytokines for their maintenance compared to GC B cells, confers them a survival advantage[128,129]. Finally, the primary immune response gives rise to memory B cells that enter the circulation and form lymphoid aggregates in draining lymph nodes, which are critical to mount quick secondary humoral responses to recall antigens and respond different upon re-exposure[130]. While some studies suggest the presence of antigen-

independent signals provided by TLRs and others point to antigen-dependent signals provided by T cells and basophils, the factors involved in the long term survival of memory B cells remain unclear[93].

Some studies show that in a secondary immune response, IgG^+ memory B cells preferentially differentiate into PBs, whereas IgM^+ memory B cells tend to proliferate more and enter a GC reaction[6,131]. However, this preferential differentiation may not be determined by the Ig isotype expressed by the memory B cell, but correlate with the expression of other molecules, such as CD80 and programmed cell death 1 ligand 2 (PDL2). In mice, upon secondary antigenic challenge, $CD80^-$ $PDL2^-$ memory B cells enter the GC reaction, whereas $CD80^+$ $PDL2^+$ memory B cells differentiate into PBs[132].

Besides the well-established memory B cell generation pathway involving the GC and producing high affinity antibodies, recent murine studies have explored the existence of different pathways of memory B cell generation, giving rise to the idea of a heterogeneous B cell memory[133-136], but it is not clear yet whether these findings apply to human memory B cells. Some of these works point to the existence of a GC-independent memory B cell generation pathway[134,136] and suggest that the strength and duration of the interaction between antigen-activated B cells and cognate $CD4^+$ T cells is the key factor affecting the B cell fate decision towards the GC-dependent or independent pathway[126]. If the duration of the T_{FH} cell – B cell interaction is rather short, B cells are likely to differentiate into GC-independent memory B cells because CD40 signaling alone can induce activated B cells to differentiate to memory B cells but is not sufficient to induce GC differentiation[6]. Due to the fact that CSR can occur at this early phase of activation but SHM is infrequent, the BCR specificities of the memory B cells generated through this pathway resemble those of the

initial responding B cells, thus adding another layer to the broad range of antigen-specific B cells that may provide protection against pathogens bearing distinct but related antigens.

b. Plasma Cells

Terminal B cell differentiation generates antibody-secreting cells (ASC), which include dividing PBs and non-dividing PCs[137]. As previously discussed, the primary TD response to antigen can generate a follicular or extrafollicular response. In the **extrafollicular pathway**, antigen-activated proliferating B cells can differentiate to memory B cells, or upregulate the B lymphocyte-induced maturation protein 1 (Blimp-1) transcription factor and move to the extrafollicular area to differentiate to short-lived IgM^+ or class-switched PBs. This pathway generates the majority of the early protective antibodies produced after antigenic challenge and due to the fact that in the initial proliferative phase activated B cells may undergo Ig CSR but little SHM, the resulting PBs will secrete antibodies with low affinity for the antigen[88]. The **follicular pathway** involves the engagement in the GC reaction and leads to the formation of high-affinity long-lived PCs that migrate to the bone marrow and sustain the production of high levels of antibodies[138,139], which together with memory B cells[6,77] provide effective protection against a future reinfection.

The transition from an activated B cell into an ASC requires the coordinated silencing of transcription factors that control B cell identity such as paired box 5 (PAX5) or Bcl-6, and the expression of ASC specific regulators including interferon regulatory factor 4 (IRF4), Blimp-1 and X-box-binding protein 1 (XBP1)[140-142]. The maintenance of factors that determine B cell identity or the loss of crucial ASC differentiation factors, fails to complete the B cell to ASC transition and is a major cause of late-stage B cell lymphomas[143-151]. Of note, B1 cells and MZ B cells can

rapidly generate ASCs in a TI manner because they express lower levels of PAX5 and Bcl-6 than follicular B cells and are able to easily induce Blimp-1 expression[152,153].

ASCs accumulate IgM, IgG, IgA or IgE in their cytoplasm and usually express mutated V(D)J genes, CD19, high levels of CD27 and CD38, but not IgD (except some PBs from the upper respiratory tract) or CD24[139,154] (Fig. 1). Short-lived PBs from extrafollicular areas or peripheral blood express the proliferation-associated molecule Ki-67 as well as some levels of surface Ig receptors[88] and low levels of Blimp-1[155-157]. On the other hand, long-lived PCs from the bone marrow usually lack Ki-67 and surface Ig receptors, but typically express higher levels of Blimp-1[155,157] and the syndecan-1 molecule CD138. In the bone marrow SCs, eosinophils and megakaryocytes provide powerful survival signals to PCs[93,158,159], including CXCL12, vascular cell adhesion molecule 1 (VCAM-1), APRIL and IL-6[160], and can be negatively regulated by the antibodies present in the serum, that can induce PC apoptosis by crosslinking the inhibitory Fc receptor FcγIIB on PCs[161].

II. Mucosal Immune Responses

1. Mucosal Immunology

Our body, through the skin and the mucosal membranes, is in constant contact with a high number of microorganisms that shape our microbiota[162]. Whereas the skin isolates and protects us from the exterior, mucosal membranes are dynamic interfaces that regulate the absorption of beneficial substances, such as oxygen and nutrients, while controlling our relationship with the microbiota. To that end, the mucosal immune system has evolved to generate a highly organized immune response, through

different layers of defensive mechanisms with increased specificity. They include the mucus layer, the epithelium and the MALT[163].

These mucosal barriers have evolved to adapt to the different requirements found throughout our anatomy. Thus, we can find changes in the mucus and epithelial composition at different body compartments, as well as specialized MALT, such as the nasopharynx-associated lymphoid tissue (NALT), bronchus-associated lymphoid tissue (BALT) or gut-associated lymphoid tissue (GALT). Through regional specialization and by using physical, mechanical and chemical defensive strategies, as well as sophisticated immunological mechanisms, mucosal membranes are able to repel toxins and control the high microbial load present in our internal environment[163].

2. Anatomy and Histology of the Gut

The gut is the largest mucosa of our body and comprehends the small and large intestines. The small intestine extends from the gastric pylorus to the ileocecal valve, and is divided in three different segments, namely, duodenum, jejunum and ileum with an average length of 6 to 7 meters in the human adult. On the other hand, the large intestine extends from the ileocecal valve to the anus, comprising the terminal 1 to 1.5 meters of the gastrointestinal tract, and it is divided into cecum, ascending colon, transverse colon, descending colon, sigmoid colon and rectum.

From a histological point of view, the intestinal wall is divided into four layers, serosa, muscularis externa, submucosa and mucosa, which are common to the small and large intestine, although with variations along the gut. The **serosa** envelops and protects the intestine and is composed by a single layer of mesothelial cells and a thin band of connective tissue. The **muscularis externa** or muscularis propria has an inner circular and

outer longitudinal muscular layer, with an interspersed neural plexus – the myenteric plexus of Auerback, responsible for intestinal motility. The **submucosa** serves a structural function and is a loose, paucicellular fibrous layer with adipose tissue and a prominent vascular and neural component – the Meissner's plexus. Finally, the **mucosa**, composed by the epithelial cell layer, the lamina propria (LP) and the muscularis mucosa, is the complex anatomical compartment where the majority of the intestinal digestive and immunological processes take place and it contains the largest collection of lymphoid cells in our body[164].

A. Regional Differences along the Gut

Although the previous general histological structure applies to the intestine as a whole, varying proportions and types of cells, as well as anatomical peculiarities of the different intestinal portions confer them distinct physiological functions[165]. The small intestine is characterized by the presence of finger-like projections, termed villi, which further increase the mucosal surface area. The duodenum and jejunum, with long villi and a high proportion of absorptive cells with microvilli, known as 'brush border', are mostly involved in digestion. The ileum, with shorter villi and less proportion of absorptive cells to mucus-producing goblet cells, contributes much less to nutrition, whereas it is of central importance in the generation of immune responses to intestinal microbes due to the presence in this area of a high number of immunological follicular structures[166]. By contrast, the large intestine shows a flat surface without villi and is mainly involved in the reabsorption of water, the elimination of undigested foodstuffs and in acting as a barrier to the commensal microbiota by producing a thick layer of mucus. Of note, within the colon, the caecum is a blind-ended sac that acts as a reservoir for the commensal bacteria involved in the fermentative digestion of complex carbohydrates that cannot be dealt with by small intestinal enzymes[165]. Under the surface

of the luminal epithelium, both small and large intestine have crypts of Lieberkühn, which contain epithelial stem cells, neuroendocrine cells, Paneth cells, goblet cells and absorptive enterocytes involved in absorption, mucus secretion and different immune functions.

3. Immunological Components of the Gut Mucosa

A. Mucosal Barrier: Mucus and Epithelial Cells

The epithelial cell layer and the mucus layer compose the mucosal barrier that separates the gut mucosa from the intestinal contents.

The epithelial cell layer is composed by a single layer of two types of columnar epithelial cells, enterocytes specialized in the absorption of nutrients, and goblet cells specialized in the production of mucus. Moreover, intestinal epithelial cells (IEC) transport immunoglobulins across the epithelium to the lumen in a process known as trancytosis, and are also an important source of antimicrobial peptides such as lysozyme and defensins, and cytokines such as BAFF. Although IECs are the main cell type in the epithelium, there are also intraepithelial lymphocytes that are usually $CD8^+$ T cells, and cells specialized in antigen capture, known as microfold cells or M cells[165].

Classically, mucus has been described to act as a physical barrier that isolates the sterile epithelium from the intestinal lumen, where trillions of bacteria normally reside, but it has been shown that it has additional antimicrobial and immunological functions. Importantly, mucus enhances gut homeostasis and oral tolerance by delivering immunoregulatory signals to DCs and IEC[167]. The proportion of mucus-producing goblet cells progressively increases along the intestine. It is of no surprise then, that the mucus layer that coats the mucosa also changes along the gut. Whereas the small intestine has a single, thin and loose mucous layer, the

large intestine has an outer mucus layer similar to the one found in the ileum, containing discrete amounts of bacteria, and an inner, dense layer attached to the epithelial flat surface that is mostly sterile in normal conditions[168].

B. Gut-Associated Lymphoid Tissue

The GALT includes highly organized follicular structures appearing as PPs, which are follicular B-cell aggregates with GCs and interfollicular T cell zones; and individual B-cell follicles termed isolated lymphoid follicles (ILFs). Both PPs and ILFs are characterized by the presence of an overlying specialized follicular-associated epithelium (FAE).

a. Peyer's Patches

PPs are highly organized lymphoid structures in the small intestine composed by multiple B cell follicles with GCs and associated interfollicular areas containing T cells and DCs. PPs develop during embryonic life in a sterile environment through a highly orchestrated interaction between a specialized type of SC cell known as **lymphoid tissue organizer** (LTo) cell and **lymphoid tissue inducer** (LTi) cells. LTi cells, also known as ILC3s, are bone-marrow derived and express the transcription factor Id2, the retinoic acid-related orphan receptor γt (RORγt) and IL-7R and are responsible for the delivery of signals required for the formation of secondary lymphoid structures during gestation[169-171]. In response to IL-7, fetal LTi cell upregulates the expression of LT and ligates the LTβR expressed on VCAM-1^+ LTo cells, which induces the expression of chemotactic factors that attract B cells and T cells to the PP anlagen[172]. The resulting cellular aggregates mature into recognizable PPs with FDC networks but without GCs[166]. The establishment of the gut microbiota, beginning immediately after birth,

strongly impacts the development of GALT. At this crucial moment trillions of bacteria colonize the sterile gut microenvironment and PPs become larger and form GCs.

The number of macroscopically visible PPs in humans varies with age from 100 to 250, with their number peaking at puberty, and their size and density increases from the jejunum to the ileum, where they are particularly concentrated[166]. B cell follicles in the PPs have an overlying SED and a specialized FAE. The perpetual presence of GCs in these structures is indicative of the continuous immune stimulation received from luminal antigens[173]. The FAE is a specialized area of the epithelial cell layer covering the follicular structures present in the LP, either PPs or ILFs. The FAE contains less goblet cells than the adjacent areas and its major characteristic is the presence of **M cells**. This type of specialized epithelial cell does not contain microvilli like neighboring enterocytes, but instead, its membrane folds into small pockets or microfolds. This special cellular conformation allows M cells to uptake bacteria, viruses and inert particles from the intestinal lumen and transport them to DCs located in the underlying **SED** region, where they can be presented to adaptive immune cells[174]. Similar to PPs in the small intestine, equivalent structures can be found in the appendix and the large intestine, known as cecal patches and colonic patches respectively[175,176].

b. Isolated Lymphoid Follicles

In mice, ILFs are described as clusters of B cells with scant T cells surrounded by a thick rim of DCs and macrophages[177], and in wild-type mice the majority of ILFs lack GCs. In humans, ILFs can either have or lack a GC, but their precise cellular composition and biological function in health and disease states remain unclear. It has been estimated that the human intestine contains up to 30,000 ILFs[178], and that their frequency

increases 10-fold from the jejunum to the ileum[179]. Similarly, in the colon their frequency triples from the ascending colon to the rectum[180].

The fetal gut contains small anlagen structures termed **cryptopatches** (CPs) that are considered ILF precursors[179]. CPs are loosely organized clusters of cells located at the base of the intestinal epithelial crypts. The cellular components of CPs are LTi cells, which represent the majority of cells in the CPs, $CD11c^+$ DCs and $VCAM\text{-}1^+$ LTo cells[181,182]. Mature B or T lymphocytes are a minor or absent population in CPs. In a process parallel to PPs formation during embryonic life, IL-7 produced by IECs induces LTi cells to express membrane-bound LT, which subsequently ligates the LT-β expressed by LTo cells. This interaction results in the production of chemotactic factors recruiting in CCL25-producing DCs, which act to recruit additional LTi cells and results in the formation of a CP[181,182].

ILFs will develop only after birth following bacterial colonization of the gut [177] and the size and cellular composition of ILFs is dependent on the intestinal bacterial load[183,184]. At this point, IECs recognize bacterial peptidoglycans through the innate receptor nucleotide-binding oligomerization domain-containing protein-1, which induces epithelial expression of CCL20 and β-defensin-3, ligands of CCR6 expressed on LTi cells[183]. CCR6 ligation activates LTi cells, which induce LTo cells to express adhesion molecules and chemokines including CCL20 that attract $CCR6^+$ B cells to the ILF[185]. Additionally, DCs and macrophages produce TNF-α upon recognition of bacterial compounds through TLRs, and the ILF further grows in size and cellular numbers.

C. Lamina Propria

The LP consists of loosely packed connective tissue that acts as scaffolding for the mucosa, supports the presence of the vascular,

lymphatic and nervous supply and contains many cells of the innate and adaptive immune systems, such as B cells, T cells, DCs, macrophages, eosinophils, mast cells and ILCs[164].

The most abundant cell type in the LP is the **PC**, especially of the IgA isotype. The IgA producing PCs comprise around 75% of the PC population in the duodenum and up to 90% in the colon. The rest of the PCs secrete mostly IgM[186].

Both $CD4^+$ and $CD8^+$ **T cells** are found in the LP at a ratio of 2/1 and derive from conventional T cells primed in secondary lymphoid organs. The $CD4^+$ T cell compartment in the intestine is highly diverse and it includes different types of effector T cells. After antigen recognition, antigen-specific $CD4^+$ T cells proliferate and under different environmental stimuli differentiate into different effector T_H subsets characterized by a specific profile of cytokine production and effector function[187]. T_H1 cells produce IFN-γ, and IL-2, and react towards intracellular bacteria, fungi and viruses. T_H2 cells produce IL-4, IL-5 and IL-13, react towards parasites and are involved in the etiology of allergies[188]. Moreover, T_H17 cells produce IL-17 and IL-22, cytokines involved in neutrophilia, tissue organization and repair, and production of antimicrobial proteins. Abundant at mucosal surfaces, T_H17 cells react towards extracellular bacteria and fungi[189]. Finally, T regulatory (T_{REG}) cells produce abundant IL-10 to suppress or downregulate the proliferation of effector T cells and are important for immunological tolerance in the intestine[190]. Foxp3 is a transcription factor necessary for the induction and maintenance of T_{REG} cells[191]. The induction of Foxp3 expression requires strong TCR signaling and the consequent acquisition of the regulatory T cell phenotype can occur both in the thymus and the intestine, where it is highly influenced by environmental factors[192]. The

balance between the different effector T cell subsets is necessary to maintain intestinal homeostasis.

ILCs are a recently characterized group of non-T, non-B lymphocytes with important roles in GALT development and early immune responses in the intestinal mucosa[172]. ILCs have lymphoid morphology but lack the expression of somatically rearranged antigen receptors. The ILC family includes classical cytotoxic NK cells involved in protection against viruses and tumors, and non-cytotoxic ILC populations[193]. These non-cytotoxic ILCs include different types of helper-like innate cells that have been classified in three groups according to the expression of T_H1-type, T_H2-type or T_H17-type transcription factors required for their development and the effector cytokines produced[193-196]. Group 1 ILCs (ILC1) resemble T_H1 cells in the expression of the transcription factor T-bet, production of IFN-γ and TNF in response to IL-12, and ability to mediate immunity to intracellular bacteria and parasites[195,197]. ILC2 resemble T_H2 cells in the expression of the transcription factor GATA-3, also require ROR-α for their development and produce the cytokines IL-4, IL-5, and IL-13 in response to IL-25, IL-33 and thymic stromal lymphopoietin (TSLP). ILC2 have the ability to provide immunity to helminthic infection and mediate allergic inflammation[198,199]. Finally, ILC3 resemble T_H17 cells in the expression of (RORγt), production of IL-17A and IL-22 in response to IL-23 and IL-1β and also produce GM-CSF and TNF. ILC3 include LTi cells important in lymphoid organogenesis, and natural cytotoxicity receptor $(NCR)^+$ILC3 and NCR^-ILC3, which promote epithelial integrity through their involvement in tissue repair and immune responses against extracellular bacteria[200-202]. While ILC1s and ILC2s are found in the LP of the small and large intestine[201], ILC3s seem to be more abundant in the terminal ileum and colon, where the bacterial load is higher[203]. Given the ability of ILCs to respond rapidly to stimulation, ILCs represent an early

source of effector cytokines during the innate phase of an immune response, prior to the initiation of an adaptive immune response[204].

Large numbers of **mononuclear phagocytes** – macrophages and DCs – populate the LP and are involved in the uptake and presentation of antigens in the intestine. They share the expression of several molecules, such as CD11c, MHC-II, CD11b and CX3CR1[205,206]. **Macrophages** are the most abundant leukocytes in the LP[207]. They express CD68, CD163 and epidermal growth factor module-containing mucin-like receptor 1 or EMR1 (human equivalent of murine F4/80 molecule). Macrophages' main functions involve phagocytosis and degradation of microorganisms and cellular debris, production of mediators that drive epithelial cell renewal, production of large amounts of IL-10 that block proinflammatory responses, and promotion of the survival of $FOXP3^+$ T_{REG} cells in the mucosa[205,208].

Intestinal DCs can be classified in the intestine based on their expression of CD103 and CX3CR1[209]. $CD103^+$ DCs can uptake antigen via transient antigen-channels generated by goblet cells[210], and following CCR7-dependent migration to the MLN to initiate T and B cell immune responses with intestinal tropism through the induction of the intestinal homing receptors CCR9 and $\alpha4\beta7$[211-213]. Moreover, $CD103^+$ DCs can promote TI IgA CSR by intestinal B cells[214]. On the other hand, $CX3CR1^+$ DCs are thought to be non-migratory[215,216], lie adjacent to the epithelial barrier and by sending transepithelial processes, are able to sample antigen directly from the gut lumen[217,218].

Eosinophils account for up to 30% of myeloid cells in the LP, although they are more abundant in the duodenum and jejunum. They express CCR3 and Siglec-F[219], and seem to be important for tissue repair in the gut, both in homeostasis and during inflammation.

Mast cells are also abundant in the LP, and produce mediators that regulate epithelial barrier integrity, peristalsis, vascular tone and permeability[220]. In the small intestine mast cells are involved in tissue remodeling and can also sense microorganisms through TLRs, while in the colon they have a more proinflammatory function[221].

4. Mesenteric Lymph Nodes

The mesenteric lymph nodes (MLNs) are the regional lymph nodes draining the whole small intestine and the proximal colon. They develop during embryonic life like the rest of the peripheral lymph nodes. In the mouse MLNs form a string of four or five lymph nodes, whereas in humans they are found throughout the intestinal mesentery. MLNs are considered part of the mucosal immune system and induce tolerance to food antigens while acting as a firewall to prevent the invasion of live intestinal bacteria to the systemic immune system[222].

The intestinal mucosa is continuously exposed to vast amounts of food and microbial antigens and while generating protective immune responses against pathogens it has to provide tolerance to harmless intestinal contents. The process by which orally administered antigens suppress subsequent immune responses in the gut and in the systemic immune system is known as **oral tolerance** and plays a central role in immune homeostasis[223].

Many food antigens are absorbed as protein fragments and reach secondary lymphoid structures via lymph and blood, but hypersensitivity to food components is normally avoided[224]. To achieve this tolerance $CD103^+$ DCs in the gut LP uptake antigen and upregulate CCR7 to

migrate to the MLNs, where T cell tolerization is induced[211-213,225]. The subsequent immune hyporesponsiveness can be the result of the generation of T_{REG} cell populations or even direct inactivation of lymphocytes through deletion or anergy when the antigen dose or the number of antigen-specific T cells is low[226]. Due to the migration of T_{REG} cells generated in the MLNs through the lymph and blood, this induced tolerance affects local and systemic immune responses[227].

On the other hand, although only small numbers of live bacteria can be carried to the MLNs by DCs, they are extremely immunogenic. Systemic tolerance to these organisms is not induced because tolerance is not as effective for particulate antigens as it is for soluble proteins. $CD103^+$ DCs do not penetrate further than the MLNs, which in this case act as firewall to prevent commensal organisms reaching the systemic immune system. This scheme allows for the generation of strong local immune responses and prevents unwanted systemic priming reactions from live bacteria so the systemic immune system can still respond to commensals or related pathogens reaching the systemic immune system[222].

5. Gut Microbiota

The number of bacteria present in our body exceeds that of our eukaryotic cells by at least an order of magnitude[162]. In the gastrointestinal tract the amount of bacteria present in the lumen increases downwards. In the stomach it ranges from 100-1000 per ml of intestinal content due to a highly acidic environment. On the other end, the intestine of a human adult contains up to 10^{14} microorganisms of more than 500 different species, and constitutes the major source of commensal microbes[165]. Regarding bacterial load, the upper small intestine, duodenum and jejunum, host about 10^5 bacteria per ml, whereas this number increases up to 10^{12} per ml in the colon. Some studies show that the terminal ileum

may contain even larger numbers of bacteria than the colon[228]. The composition of the intestinal microbiota is highly complex and comprises thousands of bacterial species, with the Firmicutes, Bacteroidetes, Proteobacteria and Actinobacteria being the most prevalent, although their relative numbers vary greatly between individuals[229].

The massive presence of bacteria in our organisms shows how humans have coevolved with microbes developing symbiotic and mutualistic relationships at the mucosal membranes, particularly in the intestine. As commensals, bacteria help our digestion by processing indigestible food components and producing essential metabolites, such as vitamins, biotin or short-chain fatty acids, while they use complex polysaccharides and other components of mucus and undigested fiber as energy sources. Even more important from an immunological point of view, are the constant antigenic stimulation of the mucosal immune system that helps its development and maturation, and the formation of a stable ecological niche that prevents the proliferation of pathogenic species[230].

This mutualistic relationship allows the establishment of a non-inflammatory homeostatic balance characterized by hyporesponsiveness against commensals, but active response against pathogens[231]. On the other hand, alterations in the distribution of the species that shape our microbiota, known as dysbiosis, has been associated with many pathological conditions, including obesity, metabolic diseases, allergy, inflammatory bowel disease and autoimmunity[232].

6. IgA Responses in the Gut

Compared to the spleen or peripheral lymph nodes, mucosal tissues experience a constant antigen exposure and must establish a complex equilibrium between the elimination or exclusion of pathogens and the

maintenance of commensal microbiota. The Ig isotype IgA, predominant in mucosal surfaces, blocks the penetration of invading pathogens to our body through a process known as "immune exclusion" and also modulates the interaction of commensal bacteria with the mucosal immune system by mitigating associated inflammatory immune responses[233].

A. IgA Structure and Function

Immunoglobulin A (IgA) constitutes the most abundant antibody class in the intestine and by extent in our whole body[234]. It accounts for at least 70% of all Ig produced in mammals[235]. Its concentration in the serum compared to IgM or IgG is low because it is mostly secreted across mucous membranes. Thus, although it does not participate in systemic immune responses as much as the other Ig isotypes, IgA is the central piece of the mucosal immune system.

Whereas mice have only one IgA class found as a monomer, humans have two IgA subclasses, namely IgA1 and IgA2[236]. The relative proportions of the two IgA subclasses vary along different tissues, correlating with the presence of IgA1-producing and IgA2-producing PCs[111]. IgA1 is abundant in the serum, bone marrow and upper digestive and respiratory tracts. IgA2 predominates at sites heavily colonized by bacteria, such as the distal digestive tract and the female urogenital tract[234,237]. This phenomenon may be explained by a different sensitivity to bacterial degradation, due to the presence of a shorter hinge region in the structure of the IgA2 molecule that seems to make it more resistant to bacterial proteases[238,239], and gives it a more rigid structure that favors the binging to large particles[240]. IgA appears in the serum mostly as a monomer, while in the mucosal secretions forms dimers held together by a polypeptide, termed joining (J) chain, produced by PCs[241].

In the intestine, the main function of IgA is the confinement of commensal bacteria in the intestinal lumen, and it involves IgA transepithelial release[242,243]. IgA polymers in the LP are transported across the epithelial cell layer in a process known as **transcytosis**, which starts with the J chain binding to a polymeric Ig receptor (pIgR) on the basolateral surface of IECs. After the internalization of the IgA polymer, the pIgR is cleaved into the secretory component, which remains bound to the J chain of polymeric IgA to form a secretory IgA (SIgA) complex[244]. The secretory component increases the stability of SIgA[245], facilitates its localization in the mucosal environment, makes it more resistant to IgA proteases[240], and increases its interaction with antigens[246]. Moreover, it is important to note that polymeric IgM is also actively transcytosed across the intestinal epithelium by pIgR[244].

After being secreted into the gut lumen, SIgA interacts with self-antigens, food components and the intestinal microbiota limiting their access to the LP and by extent to the blood circulation[247]. This process is known as **"immune exclusion"** and includes the reduction of bacterial motility[248] and invasiveness[249], as well as the entrapment of antigens in the mucus, which prevents them from binding receptors on epithelial cells and also plays an important role in the selection and maintenance of a diverse and spatially diversified community of commensal bacteria. Importantly, SIgA also facilitates the controlled uptake of luminal antigens across the intestinal epithelium into underlying lymphoid structures[250,251], therefore dampening pro-inflammatory immune responses and contributing to intestinal **homeostasis**. When either commensal or pathogenic bacteria trespass the epithelial barrier, a second line of defense provided by IgG elicits a robust inflammatory response to control the invasion.

Experimental models of targeted IgA-deficient mice show only a mild phenotype, with compensatory increases of IgM and IgG levels and

mostly normal immune responses[252]. Similarly, **IgA deficiency**, a common immunodeficiency in humans, is usually asymptomatic[253]. These phenotypes can be partly explained by the fact that IgM can substitute IgA by being also secreted across the epithelium[241,244]. However, some patients suffer recurrent infections of the respiratory and gastrointestinal tracts, allergic disorders, and autoimmune manifestations, symptoms that may be due to functional advantages of IgA over IgM, such as resistance towards proteolytic bacteria that cannot be controlled by IgM alone[254], or the fact that IgA specifically targets some bacteria[255].

B. IgA Induction

Two functional compartments known as inductive and effector sites, are classically described regarding IgA induction and function[235]. PPs, ILFs and MLNs are the primary inductive sites where IgA immune responses are generated, while the LP is the effector site where IgA-producing PBs and PCs terminally differentiate and exert their function[256].

After their generation in the intestinal inductive sites, IgA^+ PBs and memory B cells migrate to the MLNs via the draining lymph and through the thoratic duct reach the general blood circulation. In peripheral blood, IgA^+ cells expressing the gut homing receptors α4β7 and CCR9 or CCR10, relocate to the LP via MAdCAM-1^+ high endothelial venules to exert their effector functions.

IgA production is highly dependent on intestinal microbiota, as mucosal IgA and IgA-secreting cells are nearly absent from germ-free mice and neonates before bacterial colonization, and are rapidly induced after colonization by commensal microbiota[257-259]. In the gut, IgA can be generated following follicular or extrafollicular pathways as well as TD or TI pathways[256].

a. T Cell-Dependent IgA Induction

In the gut, the TD follicular pathway induced in the GCs of PPs accounts for about three-quarters of the total IgA production[260,261]. In a classical TD pathway in the PPs, after uptaking luminal antigen from M cells in the SED, DCs relocate to the interfollicular area to present processed antigen and activate naïve T cells that will become T_{FH} cells (Fig. 4). At this initial stage, primed $CD4^+$ T cells interact with antigen-specific follicular B cells at the T-B border. This interaction initiates a B cell clonal expansion and through CD40L, TGF-β and IL-21 from the T cells, may induce B cell CSR form IgM to IgA. Similar to systemic GC responses, after upregulation of CXCR5, mature T_{FH} cells and activated B cells enter the GC reaction in response to CXCL13 produced by FDCs.

In the GC reaction B cells expand, undergo SHM and CSR and later on, affinity maturation through the interaction with FDCs and T_{FH} cells. When compared to their systemic counterparts, GCs in the gut have special characteristics. The most important difference lies in the fact that whereas systemic GC reactions arise after immunization or infection, the gut is under continuous stimulation by commensal microbiota. That is why GCs are always present in PPs and some ILFs while they appear as transient structures in other peripheral lymphoid organs[262]. Another defining characteristic of gut GCs is the predominant Ig isotype produced. Systemic GCs produce mostly memory B cells and PBs of the IgM or IgG isotypes, whereas gut GCs produce mostly IgA due to the presence of specific metabolic and immunologic signals generated by local IECs, DCs, B cells and T cells[263,264]. Amongst these signals skewing the response to the generation of IgA are TGF-β, IL-10 and retinoic acid (RA)[265]. TGF- β, produced by T_{FH} cells in PPs and by DCs and IECs in the SED in response to TLR ligands[266], induces IgA class switching in

cooperation with CD40L and IL-21[64,267-269]. RA is a metabolite of dietary vitamin A produced by DCs, IECs and FDCs in response to TLR ligands, and synergizes with TGF-β and IL-6 to enhance IgA CSR and production, and also induces the expression of gut-homing receptors in B cells emerging from PPs[214,270,271]. Also, IL-10 is an anti-inflammatory cytokine that can be produced by many leukocytes, such as T cells, DCs and macrophages, and augments TGF-β-mediated IgA class switching[272]. Moreover, GC FDCs produce BAFF, APRIL and TGF-β in response to TLR ligands and dietary RA and further enhance the skewing towards IgA class switching. Finally, in response to RA, IgA^+ PBs and memory cells emerging from the GC reaction upregulate the gut homing receptors α4β7 and CCR9 that allow them to migrate to the intestinal LP to exert their functions.

Figure 4. TD IgA induction. Intraluminal antigens are captured by M cells and taken up by DCs located in the SED of PPs. After processing antigen, DCs relocate to interfollicular areas to activate naïve T cells and initiate a transcriptional program that generates T_{FH} cells. In PPs, T_{FH} cells can originate from either $Foxp3^+$ T_{REG} cells or T_H17 precursors. Early T_{FH} cells interact with antigen-specific follicular B cells at the T–B border of the follicle and by expressing CD40L and secreting TGF-β and IL-21, induce B cell clonal expansion and CSR from IgM to IgA. After upregulating CXCR5, both mature T_{FH} cells and IgA class-switched B cells migrate to the GC in response to the CXCR5 ligand CXCL13, which is produced by FDCs. In the dark zone of the GC, follicular B cells complete IgA CSR and undergo SHM. In the light zone of the GC B cells undergo affinity maturation by interacting with FDCs and T_{FH} cells. FDCs expose immune complexes on their surface to select follicular B cells expressing high-affinity BCRs, and enhance IgA CSR by releasing BAFF, APRIL, and TGF-β in response to dietary RA and microbiota-derived TLR ligands. T_{FR} cells regulate GC B cell responses by inhibiting T_{FH} cell expansion and cytokine secretion and directly suppressing B cells. Class-switched IgA^+ PBs emerging from the GC reaction upregulate the gut homing receptors α4β7 and CCR9 in response to RA from TLR-stimulated DCs, which permits the migration of PBs to the LP, where they become long-lived PCs.

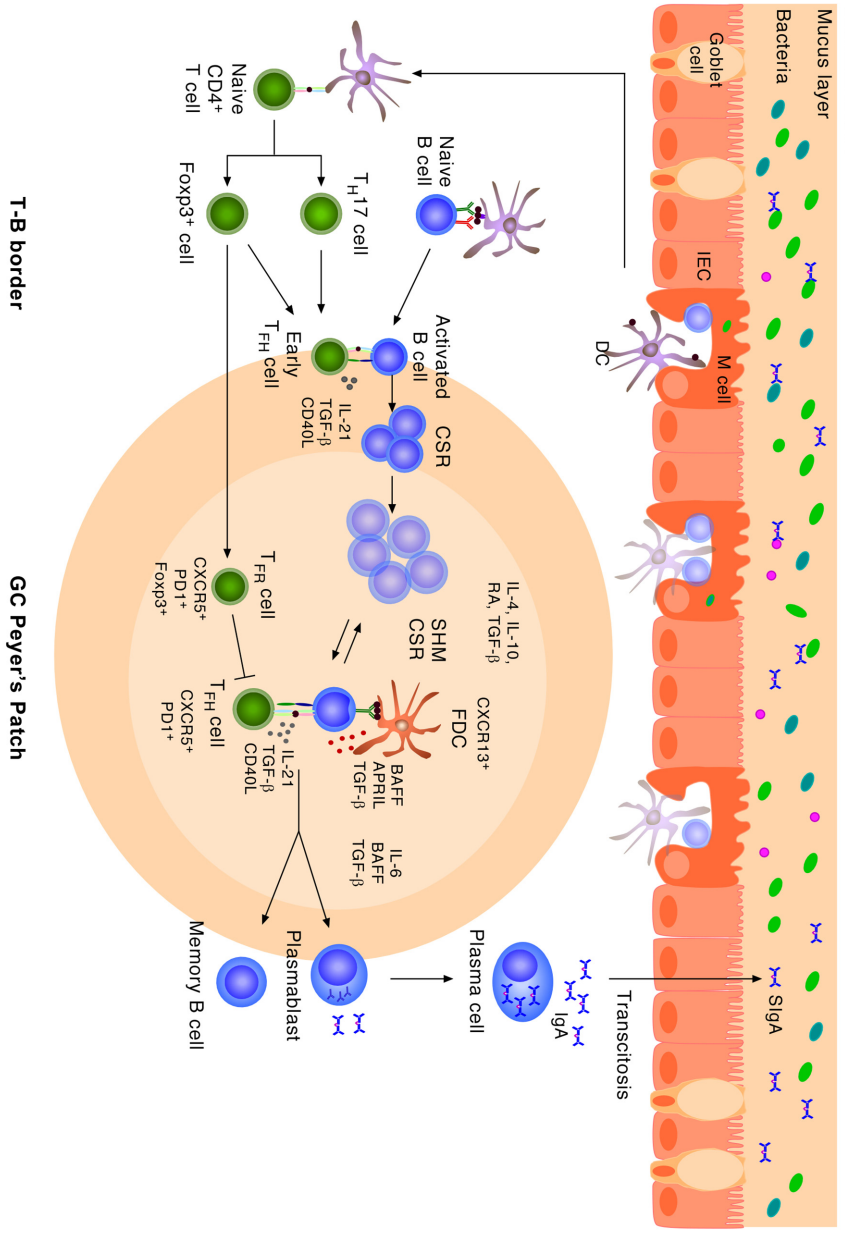
Intestinal lumen
Mucus layer
Bacteria
Goblet cell
IEC
M cell
DC
Transcitosis
SIgA
IgA
Plasma cell
Memory B cell
Plasmablast
Naive CD4+ T cell
Foxp3+ cell
TH17 cell
Naive B cell
Activated B cell
CSR
Early TFH cell
IL-21
TGF-β
CD40L
IL-4, IL-10, RA, TGF-β
SHM CSR
CXCR13+ FDC
BAFF APRIL TGF-β
IL-6 BAFF TGF-β
TFR cell
CXCR5+ PD1+ Foxp3+
TFH cell
CXCR5+ PD1+
T-B border
GC Peyer's Patch

Of note, recent evidence in mice suggests that PPs lead to the induction of IgA producing PCs that preferentially migrate to the small intestine, whereas IgA producing PCs generated in the cecal patches migrate to the colon in response to the local microbiota[273].

b. T Cell-Independent IgA Induction

Intestinal B cells can produce IgA in a TI manner. Indeed, murine studies have shown that mice lacking T cells are still able to produce small amounts of IgA in the gut[185,274]. These IgA responses usually take place within ILFs[185] but can also occur in PPs, MLNs and the LP. In humans, patients with genetic defects in the CD40 or CD40L genes, who cannot form GCs, still have IgA^+ PCs in the gut and IgM^+ and IgA^+ memory B cells in blood[96,275,276]. Moreover, CD40L-deficient patients have $CD27^-$ IgA^+ memory B cells that show limited proliferation and bear poorly mutated polyreactive antibodies generated through a TI induction pathway[125,277].

In murine ILFs, that lack GCs under homeostatic conditions, bacteria-activated DCs and ILC-activated SCs produce BAFF, APRIL, and TGF-β (Fig. 5). Furthermore, ILCs stimulate macrophage-DCs to release the active form of TGF-β, and macrophages-DCs and SCs also secrete BAFF and APRIL. These soluble factors cooperate with bacterial TLR ligands to induce IgA CSR and antibody production in B cells independently of cognate T cell help[94,107,185,274,278].

Moreover, TI IgA induction can occur in MLNs and PPs through a pathway involving plasmacytoid DCs, which have a similar morphology to PCs and show little or none antigen presentation activity[274]. In response to TLR signals, SCs in MLNs and PPs produce type I interferon and stimulate plasmacytoid DCs to release BAFF and APRIL. Moreover, in response to RA and TLR ligands, FDCs also produce BAFF, APRIL and

TGF-β, further enhancing the induction of IgA CSR and production.

In the intestinal LP, multiple subsets of conventional myeloid DCs contribute to IgA synthesis upon receiving TLR signals from bacteria. DCs present near the epithelium can sample antigen through different mechanisms. $CX3CR1^+$ DCs are able to send transepithelial projections to sample antigen directly from the gut lumen and transfer it $CX3CR1^-$ DCs with IgA inducing functions. On the other hand, $CD103^+$ DCs can uptake antigen via transient antigen-channels generated by goblet cells (Fig. 5)[210,217]. Moreover, DCs located in a follicular area can also uptake antigen from M cells located in the FAE[279]. These DC subsets produce the IgA inducing factors BAFF and APRIL that after engaging TACI on B cells[94,107,280-282], cooperate with TLR ligands, TGF-β, and IL-10 to induce IgA class switching and PC differentiation[96,185,283].

ILC3s and $Foxp3^+$ T_{REG} cells also contribute to IgA induction in the LP. $ROR\gamma t^+$ ILCs in the LP expressing membrane-bound $LT\alpha1\beta2$ induce nitric oxide secretion by $CD11c^+$ DCs[284]. In the presence of TLR ligands, nitric oxide stimulates DC secretion of BAFF and APRIL, therefore enhancing IgA responses in the LP[278]. Moreover, $Foxp3^+$ T_{REG} cells produce TFG-β and IL-10, further enhancing IgA CSR. Lastly, IECs produce high amounts of BAFF and APRIL, as well as TSLP, that stimulates DC production of BAFF, APRIL, and IL-10, further inducing IgA CSR and PC survival in the gut[79,80,285].

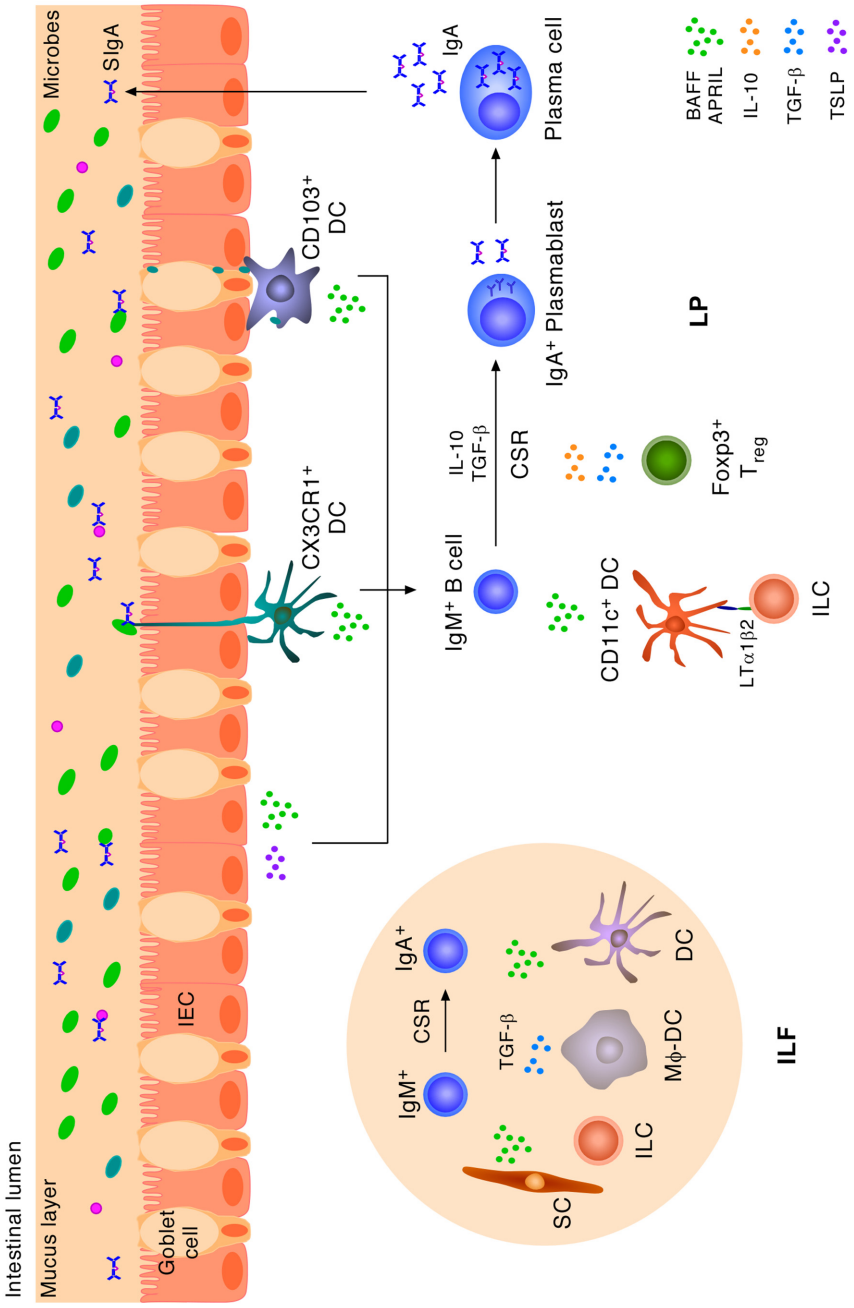
Intestinal lumen
Mucus layer
Microbes
SIgA
Goblet cell
IEC
CD103+ DC
CX3CR1+ DC
IgM+ B cell
IL-10
TGF-β
CSR
IgA+ Plasmablast
IgA
Plasma cell
CD11c+ DC
Foxp3+ Treg
LP
LTα1β2
ILC
BAFF
APRIL
IL-10
TGF-β
TSLP
IgM+
CSR
IgA+
TGF-β
DC
Mϕ-DC
ILC
SC
ILF

Figure 5. TI IgA induction. B cells in ILFs and in the LP can produce IgA even in the absence of T cell help. In ILFs, soluble factors such as BAFF, APRIL and TGF-β produced by bacteria-activated DCs and ILC-activated SCs stimulate B cells to undergo preferential CSR from IgM to IgA. ILCs further enhance IgA CSR by inducing nitric oxide secretion by extrafollicular iNOS-expressing DCs through a mechanism involving membrane-bound LTα1β2. In the intestinal LP, multiple subsets of conventional myeloid DCs contribute to IgA synthesis upon receiving TLR signals from bacteria. Intraluminal bacteria are sampled by $CX3CR1^{+}$ DCs through transepithelial projections and thereafter can transfer antigen to $CX3CR1^{-}$ DCs with IgA-inducing function. $CD103^{+}$ DCs uptake antigen via transient antigen-channels generated by goblet cells. IgA-inducing cytokines such as BAFF, APRIL, RA, and TGF-β are also produced by IECs and help PC survival and possibly differentiation in addition to IgA CSR and production. IECs may further enhance IgA responses by stimulating DC production of APRIL via TSLP. Similarly, $Foxp3^{+}$ T_{REG} cells further enhance IgA CSR via TGF-β and IL-10.

7. Clinical Relevance

IgA recognizes commensal bacteria, pathogens and self-antigens in the gut and regulates their interaction with the mucosal immune system[286]. By doing so, IgA neutralizes intestinal pathogens and toxins while preventing associated inflammatory responses in the gut[287]. Therefore, it is not surprising that some patients with primary antibody disorders eventually develop gastrointestinal infections, inflammatory bowel disease and autoimmune disorders[288-291].

Selective IgA deficiency (SIgAD) is the most common primary immunodeficiency in humans, causes an isolated defect of IgA and is defined as a level of 0.07 g/l of IgA in serum after the age of four years in the absence of IgG and IgM deficiencies. The majority of patients are asymptomatic and in many cases the diagnosis is an unexpected finding. This is probably due to an overproduction of IgM and IgG that compensates for the lack of IgA[292]. Yet, some patients develop symptoms

and suffer from frequent respiratory and gastrointestinal infections, allergy, autoimmunity and lymphoproliferative disorders[288,290,292,293].

SIgAD has been reported to be associated with certain IgG subclass deficiencies, especially IgG2 and IgG4 deficiencies, and can even progress to **combined variable immunodeficiency** (CVID), which impairs IgM, IgG and IgA production[294,295]. CVID comprises a heterogeneous group of rare diseases in which antibody production is impaired. These patients suffer from frequent respiratory and gastrointestinal infections[288,290,292,293] and in addition, some CVID patients develop celiac disease, inflammatory bowel disease and nodular lymphoid hyperplasia[296]. This last disorder corresponds to a benign lymphoproliferative disorder that consists of multiple nodular lesions made up of lymphoid aggregates in the LP of the small intestine[291,296], probably originating from clonal expansions of LP B cells induced by commensal bacteria[297]. Moreover, both SIgAD and CVID patients develop small bowel bacteria overgrowth syndrome, which leads to malabsorption[288,289,291]. The molecular basis of impaired mucosal IgA responses in SIgAD and CVID remains largely unknown, but some patients have defective TACI signaling[298-301].

On the other hand, **hyper-IgM syndrome** (HIGM) also comprises a group of rare inherited immune deficiency disorders characterized by the impairment of CSR, resulting from defects in the CD40L/CD40 signaling pathway. These defects can occur at multiple levels of the signaling pathway and have different clinical implications. In HIGM caused by CD40 deficiency, follicles cannot form GCs, and yet the LP from both intestinal and upper respiratory tracts contains B cells that express some AID and IgA[80,94], which is most probably generated through a TI IgA

induction pathway. However, the result is the presence of elevated levels of IgM and reduced levels of IgA and IgG.

Over time, bacterial overgrowth, dysbiosis and lymphoid hyperplasia may lead to the aberrant expansion of allergen-reactive, autoreactive, and clonal B cells, which could contribute to the increased frequency of allergy, autoimmunity (including hemolytic anemia and immune thrombocytopenic purpura), and B cell tumors (mostly non-Hodgkin lymphoma) in patients with SIgAD, CVID, and HIGM.

CHAPTER 2
AIMS

The overall goal of this project was to characterize the geography, nature and function of IgM^+IgD^- memory (ME-M) B cells, an enigmatic population of IgM^+ memory lymphocytes thought to emerge from TD systemic immune responses, as well as their relationships with intestinal effector cells and microbes.

AIM 1: To determine the topography, phenotype, transcriptome and function of human intestinal ME-M B cells.

AIM 2: To elucidate the clonal architecture of intestinal ME-M B cells and their relationship with antibody secreting cells in ileum and colon.

AIM 3: To evaluate the BCR reactivity of intestinal ME-M B cells and IgM^+ plasma cells towards prokaryotic and eukaryotic consortia inhabiting the gut mucosa.

CHAPTER 3
MATERIALS AND METHODS

Human tissue samples

Histologically normal tissue samples from terminal ileum and ascending colon were obtained from patients undergoing right hemicolectomy due to colonic tumors, unresectable polyps or angiodysplasia. Peripheral mononuclear cells were isolated from buffy coats and histologically normal spleens were obtained from deceased organ donors or individuals undergoing post-traumatic splenectomy. Tonsils were from people with follicular hyperplasia. The use of tissue samples was approved by the Ethical Committee for Clinical Investigation of the Institut Hospital del Mar d'Investigacions Mèdiques (CEIC-IMIM 2011/4494/I). Fresh tissue samples and formalin-fixed and paraffin-embedded tissue sections were collected from the Mar Biobanc tissue repository with patient signed informed consent. All tissue samples were assigned coded identifiers and relevant clinical information remained concealed.

Mice

Female C57BL/6 mice were housed in specific pathogen–free conditions and used at 8–12 weeks of age unless specified otherwise in the text. All experiments involving mice were in accordance with approved protocols from the Institutional Animal Care at PRBB.

Sample processing

For the isolation of mononuclear cells from human intestinal samples, mucosa and submucosa were dissected from muscularis externa and cut into 2- to 3-mm pieces. These pieces were first washed in calcium and magnesium-free Hanks' balanced salt solution (HBSS) before incubation at 37°C for 20 min in HBSS containing 5mM Dithiothreitol (DTT) and 1 mM Ethylenediaminetetraacetic acid (EDTA). The tissue pieces were

transferred into a falcon tube with 30ml of HBSS and shaken vigorously for 10 seconds twice. The supernatant, containing the intra-epithelial lymphocytes fraction, was discarded. The remaining fraction was digested by incubation for 40 min at 37°C with stirring in a solution of HBSS containing 1 mg/ml collagenase IV (Invitrogen), 50ng/ml DNAse (NewEnglandBiolabs) and 0.5% human serum (Sigma). LP suspensions were passed through a 70-µm filter, washed, and resuspended in RPMI 1640 medium (Lonza) with 10% fetal bovine serum (FBS). Human splenocytes, tonsillar mononuclear cells and peripheral blood mononuclear cells were obtained from fresh samples as reported in published studies[105,112]. For the isolation of mononuclear cells from murine lymphoid tissues, spleen, peripheral and MLN were harvested, crushed and filtered to obtain a cell suspension. PPs were mechanically excised from small intestines, incubated in HBSS containing 5mM DTT and 1 mM EDTA for 20 min at 37ºc and then crushed and filtered. To isolate LP lymphocytes, intestinal pieces were opened longitudinally and cut into 5mm pieces. Murine mucosal tissues were then processed following the same procedure used for human intestinal samples.

Cell sorting

Human intestinal and splenic N ($CD45^+CD19^+CD38^-CD10^-IgD^{++}IgM^+CD27^-$), splenic MZ ($CD45^+CD19^+CD38^-CD10^-IgD^+IgM^{++}CD27^+$), ME-M ($CD45^+CD19^+CD38^-CD10^-IgD^-IgM^+CD27^+$), ME-SW ($CD45^+CD19^+CD38^-CD10^-IgD^-IgM^-$) B cells, PC-M ($CD45^+CD19^+CD38^{++}CD10^-IgD^-IgM^+$ $CD27^{++}$), PC-SW ($CD45^+CD19^+CD38^{++}CD10^-IgD^-IgM^+$ $CD27^{++}$) were stained with the appropriate 'cocktails' of fluorochrome-labeled mAbs (Table 1) and were sorted with a FACSAria II (BD Biosciences) after exclusion of dead cells

through 4′-6-diamidine-2′-phenylindole (DAPI) staining. The purity of cells sorted this way was consistently >95%.

Flow cytometry

Cells were incubated at 4°C with Fc-blocking reagent (Miltenyi Biotec) before the addition of the appropriate 'cocktails' of fluorochrome-labeled mAbs (Table 1, 2). Dead cells were excluded through the use of DAPI. Cells were acquired with LSRFortessa (BD Biosciences) and data were further analyzed with FlowJo V10 software (TreeStar).

Cultures

Human sorted intestinal naïve, ME-M and ME-SW B cells (1 x 10^5 per well) were plated in 96-well U-bottomed plates and cultured for 6-7 days in complete RPMI medium supplemented with 10% FBS, penicillin and streptomycin (10 U/ml), with or without 200ng/ml megaCD40L (Enzo Life science), 50ng/ml IL-10 (Peprotech) , 30ng/ml IL-21 (Peprotech), 1ug/ml CpG ODN-2006 (Invivogen), 500ng/ml BAFF (Alexis), 100ng/ml Mega APRIL (Alexis).

Proliferation assays

Cell proliferation was assessed by staining with CFSE (carboxyfluorescein diacetate succinimidyl ester) through the use of a CellTrace CFSE Cell Proliferation Kit (Invitrogen).

Generation of Epstein-Barr virus immortalized B cell lines

Sorted B cells were seeded at 5x10^4 cells per well in 96 U-bottom microplates in complete medium containing 2.5 μg/ml CpG ODN-2006, in the presence of Epstein-Barr virus (EBV) (30% supernatant from the

EBV-producing marmoset B-cell line (B95-8)). Proliferating cells were maintained in culture for 2-3 weeks and then frozen. Culture supernatants containing polyclonal immunoglobulins were stored at -80ºC.

ELISA

Total IgM, IgG and IgA from culture supernatants were detected as reported[112]. To measure Ab-reactivity, ELISA plates were coated with specific antigens (Table 3) and supernatants were used at 20ug/ml antibodies concentrations and three 1:10 dilution in PBS. All ELISAs were developed with horseradish peroxidase-labeled goat anti-human IgM or IgA Fc Ab (Jackson ImmunoReseach) and TMB substrate reagent set (BD Bioscience). OD450 was measured and Ab-reactivity was calculated after subtraction of background (OD450 of culture supernatants on PBS coated plates). Self-reactivity screens were performed using QUANTA Lite™ ANA ELISA plates (INOVA Diagnostics, Inc.), following the manufacturer's instructions.

Immunofluorescence analysis

Formalin-fixed paraffin-embedded (FFPE) human tissue sections 3 μm in thickness were treated in xylene, a decreasing alcohol gradient and distilled water for dewaxing and rehydration of the tissue. Heat induced epitope retrieval was performed for 15 minutes in Citrate buffer (pH 6) or Tris-EDTA buffer (pH 9). After epitope retrieval, tissue sections were permeabilized with 0.2% Triton X-100 in PBS, blocked with 5% bovine serum albumin and 5% Fc receptor blocking and stained with various combinations of antibodies to specific antigens (Table 1). Biotinylated antibodies were detected with streptavidin–Alexa Fluor conjugates. Nuclear DNA was visualized with DAPI and coverslips applied with FluorSave reagent (Merck Millipore). Images were acquired either with a

Leica TCS SP5 Upright confocal microscope or a Nikon Eclipse Ni-E microscope and were further analyzed with ImageJ software.

GIEMSA staining

Cytospins were performed from sorted intestinal population at 800rpm for 5 minutes on the Cytospin 4 (Thermo Scientific, Waltham, MA). Approximately 5,000 cells per subset were dried overnight on albumin coated slides and stained with Giemsa Stain Kit (Jenner-Wright) (Dako).

RNA extraction and Reverse Transcription

Total cellular RNA was isolated with the RNeasy Micro kit (Qiagen) by following the manufacturer's protocol. Approximately 2 ng of RNA with were reversed transcribed into cDNA using TaqMan® Reverse Transcription Reagents and Random hexamers (Thermo).

Conventional and Quantitative Real-Time RT-PCR

For the quantification of human gene products, quantitative RT-PCR was done in 384-well plates with Power Sybr green PCR master mix (Thermo) and specific primer pairs (Table 4). Gene expression was normalized to that of the gene encoding β-actin (ACTB) for each sample. For the analysis of Iμ-Cμ, Iα-Cα_1 and Iα-Cα_2 germline transcripts, conventional PCR was carried out using specific primers (Table 5) in a PCR volume of 50μl with AmpliTaq Gold PCR mastermix (Invitrogen). Nested PCR analysis of Iα-Cμ circle transcript was carried out using two pairs of specific primers (external and internal) and cycling conditions as follows. In the first round, the external primers were used at 95°C for 9 min in the denaturing step, 94°C for 30 sec, 60°C for 1 min for 30 cycles and 72ºC for 10min. In the second round, the internal primers were used at 95°C for

9 min in the denaturing step, 94°C for 30 sec, 60°C for 1 min for 25 cycles and 72ºC for 10min.

Microarray

RNA samples were processed according to the manuals NuGEN Ovation® Pico WTA System V2 (M01224 v2) and Encore™ Biotin Module (M01111 v6) (NuGEN, San Carlos, CA, USA), and Affymetrix Expression Wash, Stain and Scan User Manual (P/N 702731 Rev. 3) (Affymetrix Inc., Santa Clara, CA, USA). Whole transcriptome analysis was performed by using Affymetrix GeneChip Human Gene 2.0 ST Arrays (Affymetrix) in a GeneChip hybridization oven 640. Correction for multiple comparisons was performed using false discovery rate (FDR) (Benjamini & Hochberg 1995), by adjusting the p-value. Genes with an adjusted p-value less than 0.05 and with an absolute fold change (FC) value above 1.5 were selected as significant. All analyses were performed in R (v 3.1.1, ref4) with packages aroma affymetrix, limma, Biobase, Vennerable and XLConnect.

Next generation Sequencing (NGS) of the Immunoglobulin repertoire

For the amplification of Ig gene, aliquots of the resulting single-stranded cDNA products were mixed with HPLC-purified primers specific for VH1-VH6 framework region 1 (50 nM) and primers specific for constant regions Cα, Cμ and Cγ (250 nM) containing respectively the respective Illumina Nextera sequencing tags (Table 6) in a PCR volume of 25 μl (4 μl template cDNA) with High Fidelity Platinum PCR Supermix (Invitrogen). Amplification was performed with the following conditions: after an initial step of 95 °C for 5 min, 35 cycles of 95 °C for 30 s, 58 °C for 30 s, and 72 °C for 30 s, ending with a final extension step of 72 °C for 5 min. Products were purified with miniElute PCR purification Kit

(Qiagen) and Nextera indices were added via PCR with the following conditions: 72 °C for 3 min, 98 °C for 30 s, 5 cycles of 98 °C for 10 s, 63 °C for 30 s, and 72 °C for 3 min. Ampure XP beads (Beckman Coulter Genomics) were used for purification of the products, which were subsequently pooled and denatured. Single-strand products were paired-end sequenced on a MiSeq (Illumina) with the 500 cycle v2 kit (2 x 250 bp).

Analysis of Next Generation Sequencing data

Paired-end raw sequencing reads were processed into donor-specific Ig-sequences and grouped in clonal families using a bioinformatic pipeline based on pRESTO[302], IgBLAST[303] and Change-O[304]. First, raw reads with a Phred score lower than 20 were filter out, and C-region and VH gene primers were masked. Next, corresponding paired-end reads were aligned and merged together (minimum overlap of 6 nucleotides) and annotated with donor, cell type and isotype origin. Finally, donor-specific Ig subsets were combined (prior to VDJ annotation) to estimate donor-specific clonal families. VDJ calling and assignment was performed using the default parameters for IgBLAST and querying the latest downloaded human IGH IMGT database (Feb 2016). Donor-specific clonal groups were inferred using a distance-based clustering method implemented in Change-O: sequences with the same VH and JH annotation, having the same CDR3 region length, and with Hamming distance higher than 85%, were considered to belong to the same clonal group or family[304]. Finally, germline sequence for each clone was reconstructed using the annotated VDJ information as implemented in Change-O. Donor-specific clonal groups were represented through Circos plots[305] to visualize the relationships between B-cell subsets at clonal level. VH and JH gene usage was estimated for each donor and B-cell subset, with bars

representing average values among donors. SHM levels were estimated by averaging the number of mutations (compared to the inferred germline sequence) of each clone belonging to a given B-cell subset and donor. Donor-specific clonally related B-cell lineage trees were estimated and plotted using IgTree software[306].

Kappa-deleting recombination excision circle assay

Genomic DNA was isolated from each sorted B-cell subset with QIAamp DNA Mini Kit (Qiagen). The replication history of each B cell subset was determined using the κ-deleting recombination excision circle (KREC) assay, which is based on a quantification of coding joints and signal joints of an Igκ-deleting rearrangement (intron RSS-Kde) by real-time quantitative PCR (RT-PCR) as previously described[307]. The ΔCT between the signal joint and the coding joint exactly represents the number of cell divisions a B cell has undergone. The previously established control cell line U698 DB01 (InVivoScribe) contains 1 coding and 1 signal joint per genome and was used to correct for minor differences in efficiency of both real-time quantitative-PCR assays.

Mucus collection

Microbial samples were obtained by collecting mucus samples from intestinal surgical specimens. Mucus was obtained by scrapping of the epithelial surface of macroscopically unaffected fresh tissue samples from terminal ileum and ascending colon from patients undergoing right hemicolectomy due to colonic tumors, unresectable polyps or angiodysplasia. All patients signed informed consent for the collection of biological samples before the procedure. Intestinal contents from murine small and large intestine were collected and stored at −80 °C until further processing.

FlowMicrobiome

Aliquots of intestinal mucus samples were weighed and resuspended at 0.1 mg/μL in PBS with protease inhibitors (SIGMAFAST Protease Inhibitor Tablets). Samples were homogenized by vigorously vortexing for 5 minutes and then centrifuged at 400g for 5min to pellet large debris. The supernatant was filtered through a sterile 70μm cell strainer and centrifuged at 8000g for 5 minutes to pellet microbes. At this point, supernatant was saved and frozen at -80ºC for the analysis of free Ig.

To measure endogenous bound Ig microbial pellets were resuspended in MACS 5% FBS and incubated for 30 minutes on ice with a combination of anti IgM and IgA labeled antibodies. Finally the samples were washed and resuspended in PBS with SYTO BC (life technologies) for 15 minutes on ice for flow cytometry analysis. For the analysis of Ig bound to fungi, microbial pellets were stained for 1 hour with anti IgM and IgA labeled antibodies in combination with FITC-conjugated rabbit anti-Candida polyclonal antibody (Meridian Life Science). .This Ab is cross-reactive with a wide variety of fungal species including *C. tropicalis*, *C. albicans*, *S. cerevisiae*, *S. fibuligera* and *A. fumigatus*, but did not stain bacteria[308].

To measure Ab-reactivity against intestinal microbiota, we first stripped endogenous bound immunoglobulins by incubation for 3 min in an acidic sodium citrate buffer (40 mM sodium citrate and 140 mM NaCl, pH 3.0). Then, microbes were quickly spun down for the removal of the acidic buffer and PBS was added to the cells for pH neutralization. Microbiota were incubated with supernatants from EBV immortalized B cell lines for 30min in ice. After washing, microbial pellets were resuspended in MACS 5% FBS and incubated for 30 minutes on ice with a combination of anti

IgM and IgA labeled antibodies. Finally the samples were washed and resuspended in PBS with SYTO BC (life technologies) for 15 minutes on ice for flow cytometry analysis.

Flow cytometry was performed on a FORTESA Cytometer (Becton Dickinson) with a low FSC and SSC threshold to allow bacterial detection. FSC and SSC were set to a Log scale and samples were gated $FSC^{+}SSC^{+}DAPI^{-}SYTO\ BC^{+}$ and then assessed for IgA and IgM staining.

Table 1. Antibodies to human antigens

Antigen	Label	Isotype	Clone	Manufacturer	Use
Candida Albicans	FITC‡	Rabbit, N/A	B65411F*	Meridian	FC#
CD1c	PE∫	Mouse, IgG1, κ	L161	Biolegend	FC
CD1d	PE	Mouse, IgG1, κ	51.1	Biolegend	FC
CD10	PE	Mouse, IgG1, κ	HI10a	Biolegend	FC
CD10	APC-Cy7^	Mouse, IgG1, κ	HI10a	Biolegend	FC
CD11c	PE	Mouse, IgG1, κ	X2	BD	FC
CD19	PE-Cy7	Mouse, IgG1, κ	HIB19	Biolegend	FC
CD20	FITC	Mouse, IgG2b, κ	2H7	BD	FC
CD21	PE	Mouse, IgG1	B-ly4	BD	FC
CD24	PE	Mouse, IgG2a, κ	ML5	BD	FC
CD27	PE	Mouse, IgG1, κ	O323	eBioscience	FC
CD27	PerCP-Cy5.5º	Mouse, IgG1, κ	M-T271	BD	FC
CD35	PE	Mouse, IgG1, κ	E11	Biolegend	FC
CD38	APC	Mouse, IgG1, κ	HIT2	BD	FC
CD38	APC-Cy7	Mouse, IgG1, κ	HIT2	Biolegend	FC
CD43	PE	Mouse, IgG1, κ	1G10	BD	FC
CD45	AF700	Mouse, IgG1, κ	HI30	Biolegend	FC
CD62L	PE	Mouse, IgG1	LT-TD180	EuroBio Science	FC
CD66 a/c/e	PE	Mouse, IgG2b, κ	ASL-32	Biolegend	FC
CD84	PE	Mouse, IgG2a, κ	CD84.1.21	Biolegend	FC
CD138	APC	Mouse, IgG1, κ	DL-101	Biolegend	FC
CD138	PerCp-Cy5.5	Mouse, IgG1, κ	DL-101	Biolegend	FC
CD148	PE	Mouse, IgG1, κ	143-41	R&D	FC
CCR10	PE	Arm. Hamster, IgG	6588-5	Biolegend	FC
CCR7	PE	Mouse IgG2a, κ	G043H7	Biolegend	FC
CCR9	PE	Mouse IgG2a, κ	L053E8	Biolegend	FC
CXCR4	PE	Mouse, IgG2a, κ	12G5	Biolegend	FC
CXCR4	APC	Mouse, IgG1, κ	L291H4	Biolegend	FC
FcRL2	PE	Mouse, IgG1	296902	R&D	FC
FcRL4	APC	Mouse, IgG2b, κ	413D12	Biolegend	FC
FcRL4	PE	Mouse, IgG2b, κ	413D12	Biolegend	FC
HLA-DR	AF700	Mouse, IgG2a, κ	L243	Biolegend	FC
HLA-	BV605	Mouse, IgG2a, κ	L243	Biolegend	FC

DR					
Ig light chain λ	PE	Mouse, IgG2a, κ	MHL-38	Attendbio	FC
IgA	APC	Mouse, IgG1	IS118E10	MACS	FC
IgA	Biotin	Goat, IgG	2052-08*	Southern	IFA¶
IgA	FITC	Mouse, IgG1, κ	IS118E10	Invitrogen	FC
IgA	PE	Mouse, IgG1	IS11-8E10	MACS	FC
IgA2	PE	Mouse, IgG1	A9604D2	Southern	FC
IgD		Rabbit, IgG	IR517*	Dako	IFA
IgD	APC	Mouse, IgG2a	IAG-2	BD	FC
IgD	PerCP-Cy5,5	Mouse, IgG2a	IAG-2	Biolegend	FC
IgD	FITC	Goat, IgG	2032-02*	Southern	FC
IgM		Goat, IgG	H15000*	Invitrogen	IFA
IgM	APC	Mouse, IgG1	SA-DA4	Southern	FC
IgM	BV605	Mouse, IgG1, κ	MHM-88	Biolegend	FC
IgM	PE	Mouse, IgG1	SA-DA4	Southern	FC
Integrin β7	FITC	Rat, IgG2, κ	FIB504	Biolegend	FC

‡FITC, fluorescein
*Catalogue number
#FC, flow cytometry
∫PE, phycoerythrin
^APC and Cy, allophycocyanin and cyanin
ºPerCP, peridin chlorophill
¶IF, immunofluorescence

Table 2. Antibodies to mouse antigens

Antigen	**Label**	**Isotype**	**Clone**	**Manufacturer**	**Use**
IgD	FITC	Rat, IgG2a, κ	11-26c.2a	BD	FC
CD45	AF700	Rat, IgG2b, κ	30-F11	Biolegend	FC
CD45R/ B220	PE-Cy7	Rat, IgG2a, κ	RA3-6B2	BD Pharmingen	FC
CD73	AF647	Rat ,IgG1, κ	TY/11,8	Biolegend	FC
CD80	PE	Rat, IgG	16-10A1	eBioscience	FC
CD138	Biotin	Rat, IgG	281-2	Biolegend	FC
GL7	PerCP-Cy5,5	Rat, IgM, κ	GL7	Biolegend	FC
IgA	PE	Rat, IgG1	KLH/G1-2-2	Southern	FC
IgD	BV605	Rat, IgG2a, κ	11-26c.2a	Biolegend	FC

IgM	APC	Rat, IgG2a, κ	II/41	BD	FC
IgM	FITC	Rat, IgG2a, κ	RMM-1	Biolegend	FC
PD-L2	PE	Rat, IgG2a, κ	TY25	eBioscience	FC

Table 3. Coating strategy for ELISA

Purified Antigens	**Source**	**Company**	**Antigen concentration**
β-D-Glucan	*Barley*	Sigma	50µg/ml
CPS (serotypes 9N, 14, 19F, 23F)	*Pneumococcus*	American Type Culture Collection	10ng/ml
Galα1-3Gal-HSA (3 atom spacer)		Dextra	10µg/ml
Laminarin	*Laminaria digitata*	Sigma	50ug/ml
Phosporylcoline		Bioresearch Technologies	0,5µg/ml

Table 4. Primers for human gene products

Target gene		**Primer sequence**
ACTB	S	GGATGCAGAAGGAGATCACT
	AS	CGATCCACACGGAGTACTTG
AHR	S	AATACAAAGCCATTCAGAGCC
	AS	CAGAAAACAGTAAAGCCAATCC
AICDA	S	AGAGGCGTGACAGTGCTACA
	AS	TGTAGCGGAGGAAGAGCAAT
BCL2	S	CCTCCCTGGCCTGAAGAAGA
	AS	TGTCCTTCGGCGTGGAAATC
BCL6	S	TTCCGCTACAAGGGCAAC
	AS	TGCAACGATAGGGTTTCTCA
CD70	S	TACGTATCCATCGTGATG
	AS	GTTGGTGCAGAGTGTGTC
FCRL4	S	TCAGCTGGGAGAAGAAGAGGAA
	AS	GAGTTATCTGGGTGTTGTGTCTTTACC
GPR15	S	TTACTATGCTACGAGCCCAAACT
	AS	CTCCCATGAGAACAAGGTTCC
GPR34	S	GAAAGGTTGCGACTATTACCAAA
	AS	GTGAAAGTGCTAAATGACATATTCCTC

IL10	S	ACCTGCCTAACATGCTTCGAG
	AS	TGTCCAGCTGATCCTTCATTTG
IL21R	S	CCCGACCTCGTCTGCTACA
	AS	TGGTCTTGCCAGGTAAGGGT
IRF4	S	GCCAAGATTCCAGGTGACTC
	AS	ATCGTAGCCCCTCAGGAAAT
PRDM1	S	GTGGTATTGTCGGGACTTTGCAG
	AS	TCGGTTGCTTTAGACTGCTCTGTG
RANKL	S	GTGCAAAAGGAATTACAACA
	AS	CGGTGGCATTAATAGTGAG
RUNX2	S	CCAACCCACGAATGCACTATC
	AS	TAGTGAGTGGTGGCGGACATAC
SIGLEC6	S	AAGGGGCTGATGTTCCAGTG
	AS	ATGCAGCATTGTCCCTCCTC
TNFRSF13B	S	CAGACAACTCGGGAAGGTACC
	AS	GCCACCTGATCTGCACTCAGCTTC
TNFRSF17	S	GCTTGCATACCTTGTCAACTTCGATG
	AS	GAATCGCATTCGTTCCTTTCACTG
XBP1	S	AGGAGTTAAGACAGCGCTTGG
	AS	AGAGGTGCACGTAGTCTGAGTGCTG

Table 5. Primers for CSR

Target gene		**Primer sequence**
Iμ	S	GTGATTAAGGAGAAACACTTTGAT
Cμ 243	AS	CACACCACGTGTTCGTCTG
Cμ 268	AS	GTTGCCGTTGGGGTGCTGGAC
Iα 1/2	S	CAGCAGCCCTCTTGGCAGGCAGCCAG
Iα internal	S	CTCAGCACTGCG GGCCCTCCA
Cα1	AS	GGGTGGCGGTTAGCGGGGTCTTGG
Cα2	AS	TGTTGGCGGTTAGTGGGGTCTTCA

Table 6. Primers for NGS

Target gene		Primer sequence
VH1a	S	TCGTCGGCAGCGTCAGATGTGTATAAGAGACAG CAGGTKCAGCTGGTGCAG
VH1b	S	TCGTCGGCAGCGTCAGATGTGTATAAGAGACAG SAGGTCCAGCTGGTACAG
VH1c	S	TCGTCGGCAGCGTCAGATGTGTATAAGAGACAG CARATGCAGCTGGTGCAG
VH2	S	TCGTCGGCAGCGTCAGATGTGTATAAGAGACAG CAGGTCACCTTGARGGAG
VH3	S	TCGTCGGCAGCGTCAGATGTGTATAAGAGACAG GGTCCCTGAGACTCTCCTGT
VH4	S	TCGTCGGCAGCGTCAGATGTGTATAAGAGACAG ACCCTGTCCCTCACCTGC
VH5	S	TCGTCGGCAGCGTCAGATGTGTATAAGAGACAG GCAGCTGGTGCAGTCTGGAG
VH6	S	TCGTCGGCAGCGTCAGATGTGTATAAGAGACAG CAGGACTGGTGAAGCCCTCG
VH7	S	TCGTCGGCAGCGTCAGATGTGTATAAGAGACAG CAGGTGCAGCTGGTGCAA
Cμ	AS	GTCTCGTGGGCTCGGAGATGTGTATAAGAGACA GCAGGAGACGAGGGGGAAAAGG
Cα	AS	GTCTCGTGGGCTCGGAGATGTGTATAAGAGACA GGAAGACCTTGGGGCTGGTCG

CHAPTER 4
RESULTS

ME-M B cells are enriched in the human gut

Continuous TD diversification of IgA class-switched memory (ME-A) B cells in GCs from PPs generates clonally related IgA-secreting PCs (PC-A)[309] that colonize the intestinal LP via the expression of gut-homing receptors, such as the integrins α4β7 and the chemokine receptor CCR9[310,311]. However, the role of non-switched memory B cells in gut homeostasis remains unknown.

Flow cytometry of peripheral blood lymphocytes from a cohort of healthy donors (Fig. 1A) showed that a large fraction of human circulating $IgM^{+}IgD^{-}$ memory (ME-M) B cells co-express integrin β7 and CCR9, (Fig. 1B, C), thus indicating a selective recruitment of ME-M B cells to the gut.

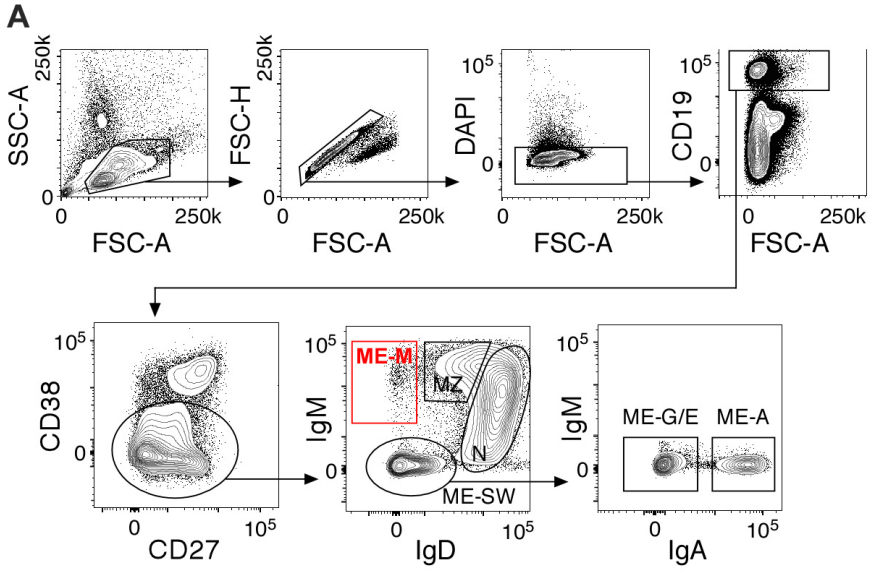

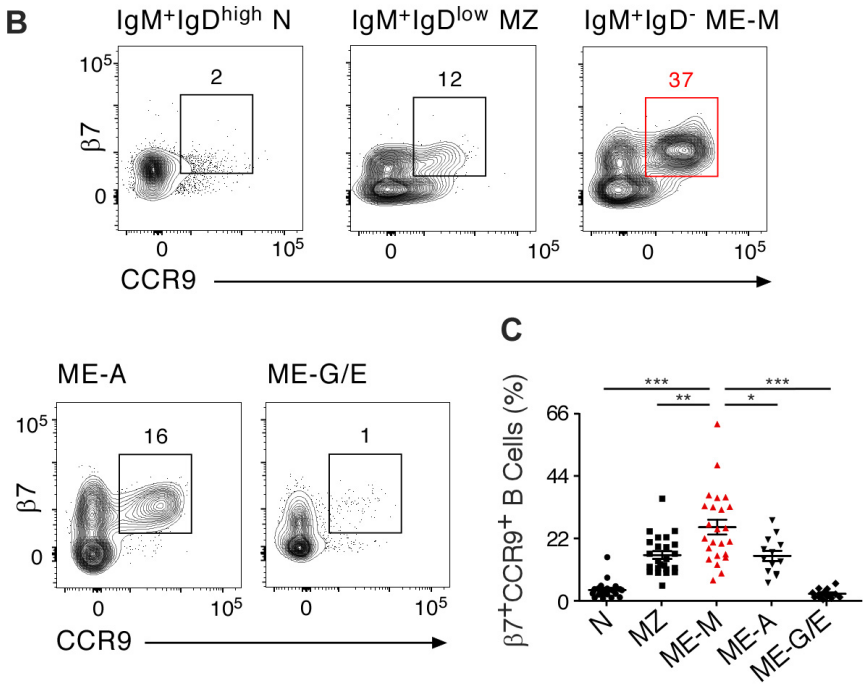

Figure 1. A large fraction of human circulating IgM$^+$IgD$^-$ ME-M B cells express integrin β7 and CCR9. (A) Flow cytometry of viable (DAPI$^-$) peripheral blood lymphocytes stained for CD19, CD38, CD27, IgM, IgD and IgA. (B) Expression of integrin β7 and CCR9 on freshly isolated circulating IgM$^+$IgD^{high}CD27$^-$ N, IgM$^+$IgD^{low}CD27$^+$ MZ, IgM$^+$IgD$^-$CD27$^+$ ME-M, ME-A and ME-G/E B cells, assessed by flow cytometry. Numbers above outlined areas indicate percentage of β7, CCR9 double positive lymphocytes. (C) Frequency of circulating β7$^+$CCR9$^+$ B cells in N, MZ, ME-M, ME-A and ME-G/E B cell subsets. SSC-A, side scatter area; FSC-A, forward scatter area; FSC-H, forward scatter height. N, naïve; MZ, marginal zone; ME-M, IgM$^+$ memory; ME-A, IgA$^+$ memory; ME-G/E, IgG$^+$/IgE$^+$ memory; ME-SW, switched memory B cells. Small horizontal lines indicate the mean (± s.e.m.); *P <0.05, **P<0.01, ***P<0.001 (two-tailed unpaired Student's *t*-test). Data show one representative (A, B) of 24 experiments (C).

Similar to ME-M, circulating IgM$^+$IgD^{low} MZ and ME-A B cells expressed β7 and CCR9. In contrast, naïve and IgG/IgE memory (ME-G/E) B cells showed very low frequencies of double positive cells.

To confirm this hypothesis, we analyzed the distribution of mature B cell populations in different human tissues (Fig. 2A, B). Compared to MZ B cells, which were present in blood and accumulated in spleen, and switched memory (ME-SW) B cells that were similarly distributed in different lymphoid tissues, ME-M B cells were rare in blood, spleen and tonsillar mucosa, but accounted for a large fraction of B-lymphocytes in the intestinal mucosa of the terminal ileum and proximal colon (Fig. 2B, C).

Murine studies have demonstrated the induction of ME-M B cells after immunization with different protein antigens, thus indicating a systemic TD response[6,131]. Additionally, in humans, ME-M B cells have been described as a small B cell population accounting for a small fraction of circulating B cells[117]. Surprisingly, their mean frequency in the terminal ileum was around 12% of total B lymphocytes, with some patients going up to 20 or even 25%. In the proximal colon, ME-M B cells had a mean frequency of 5% of total lymphocytes with some patients going up to 10% (Fig. 2B, C).

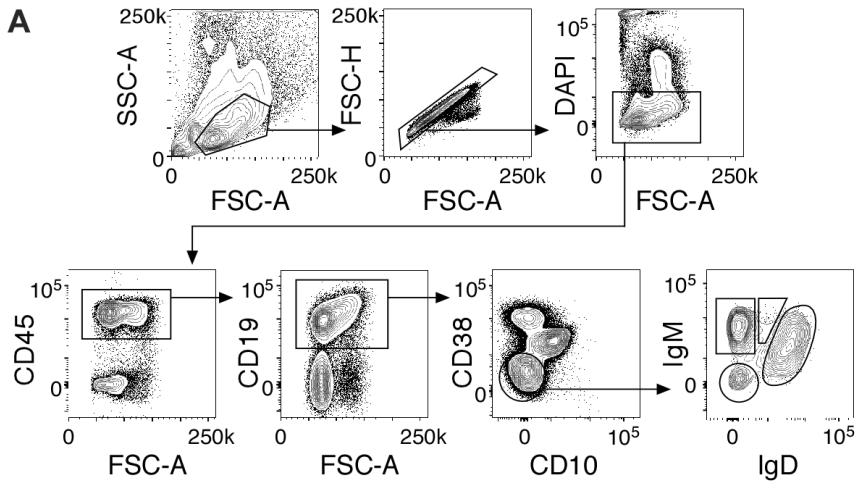

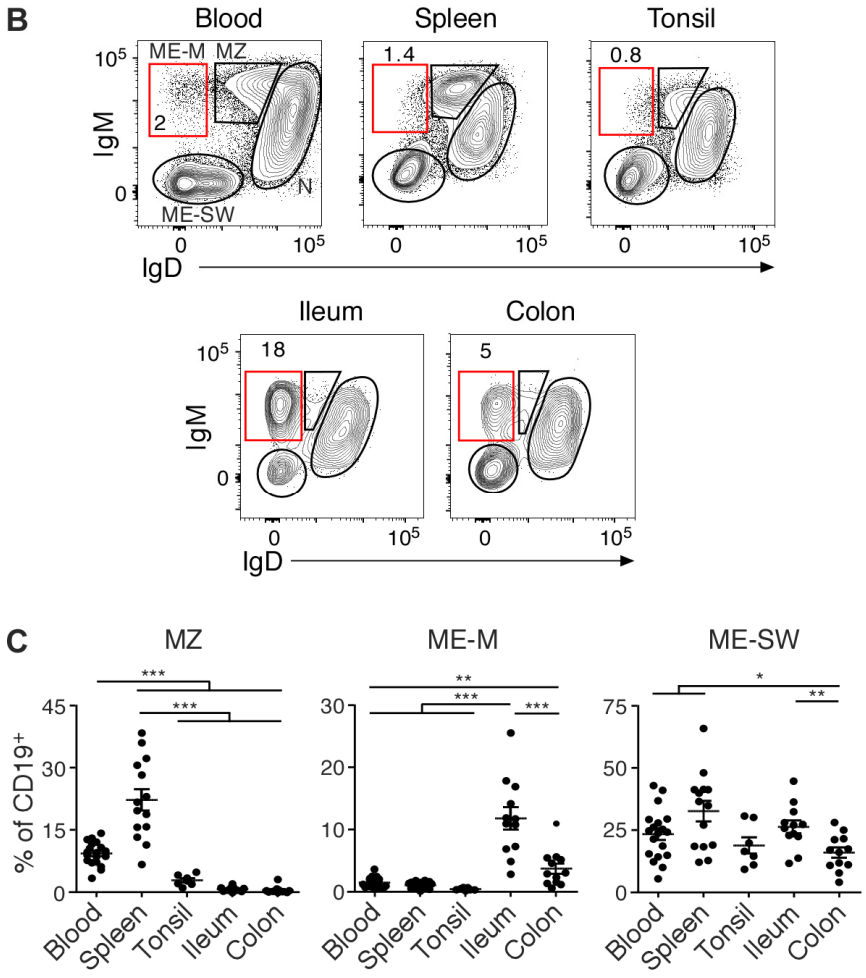

Figure 2. Human ME-M B cells express gut homing receptors and are enriched in the gut mucosa. (A) Flow cytometry of viable ($DAPI^-$) intestinal lymphocytes stained for CD45, CD19, CD38, CD10, IgM and IgD. (B) Flow cytometry of N, MZ, ME-M and ME-SW B cells in human blood, spleen, tonsil, terminal ileum and proximal colon stained as in A. Numbers adjacent to red outlined areas indicate frequency of $CD45^+CD19^+CD38^-CD10^-CD27^+IgM^+IgD^-$ ME-M B cells in the different tissues (calculated from total $CD19^+$ B cells). (C) Frequency of MZ (left), ME-M (center) and ME-SW (right) B cells in human blood, spleen, tonsil, terminal ileum and proximal colon (calculated from total $CD19^+$ B cells). N, naïve; MZ, marginal zone; ME-M, IgM^+ memory; ME-SW, switched memory B cells. Small horizontal lines indicate the mean (± s.e.m.); *P <0.05, **P<0.01, ***P<0.001 (two-tailed unpaired Student's *t*-test). Data are one

representative (A, B) of 64 experiments (19 peripheral blood, 14 spleens, 7 tonsils, 12 ileums and 12 colons; C). Each symbol represents an individual sample (C).

On the other hand, when assessing the distribution and frequency of murine $B220^{+}IgM^{+}IgD^{-}$ ME-M B cells in specific pathogen free (SPF) mice, compared to other mature B cell subsets in murine lymphoid tissues by flow cytometry, we found that ME-M B cells were present in the gut, albeit at very low frequencies (Fig. 3A, B). To confirm this result, we performed an in depth study of the classical murine memory phenotype, which indicated that murine ME-M B cells, expressing B220 and lacking the GC associated marker GL7, expressed CD73 and CD80, but revealed similar results regarding frequency in the small and large intestines, with mean frequencies around 1.7% and 0.5% respectively (Fig. 4A, B).

Thus, human circulating ME-M B cells express gut homing receptors and preferentially accumulate in small and large intestines, where they account for an important fraction of B lymphocytes, whereas murine ME-M B cells do not represent an abundant fraction of lymphocytes in the mouse.

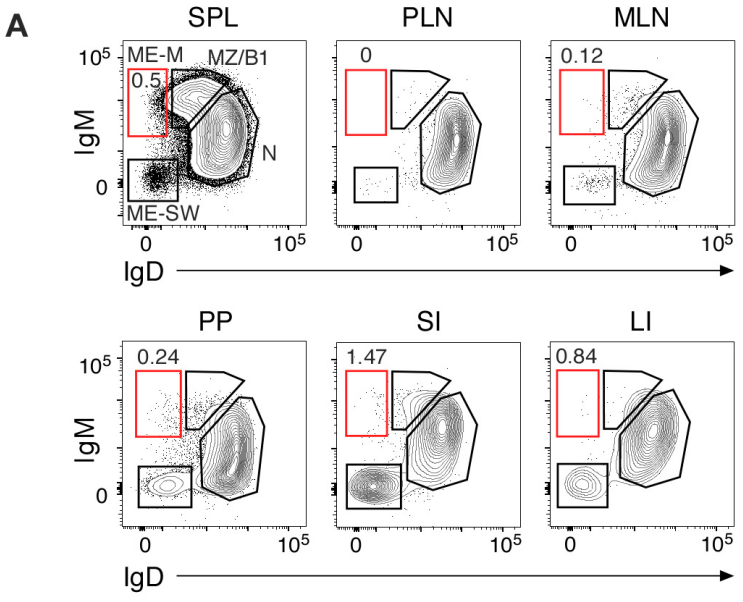

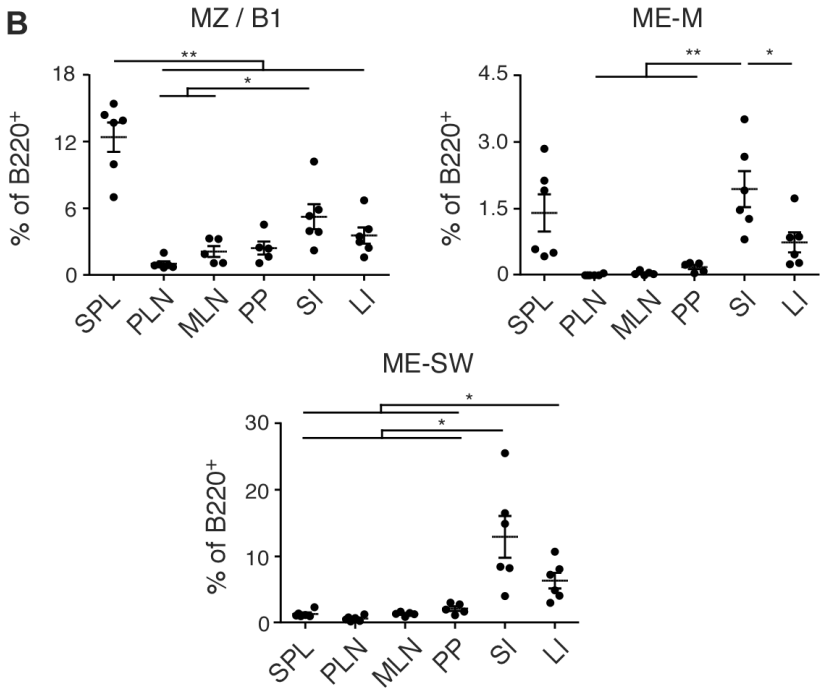

Figure 3. Murine ME-M B cells can be detected in the gut, albeit at very low frequencies. (A) Flow cytometry of viable ($DAPI^-$) N, MZ/B1, ME-M and ME-SW B cells in murine SPL, PLN, MLN, PP, SI and LI stained for CD45, B220, GL-7, IgM and IgD. Numbers adjacent to red outlined areas indicate the frequency of $CD45^+B220^+GL7^-IgM^+IgD^-$ ME-M B cells in the different tissues (calculated from total $B220^+$ B cells). (B) Frequency of MZ/B1 (upper left), ME-M (upper right) and ME-SW (bottom) B cells in murine SPL, PLN, MLN, PP, SI and LI (calculated from total $B220^+$ B cells). N, naïve; MZ/B1, marginal zone and B1; ME-M, IgM^+ memory; ME-SW, switched memory B cells; SPL, spleen; PLN, peripheral lymph nodes; MLN, mesenteric lymph nodes; PP, Peyer's patches; SI, small intestine; LI, large intestine. Small horizontal lines indicate the mean (± s.e.m.); *P <0.05, **P<0.01 (two-tailed unpaired Student's *t*-test). Data are from one experiment (A) of six experiments with similar results (SPL, PLN, SI and LI from 6 mice, and MLN and PP from 5 mice; B). Each symbol represents an individual sample (B).

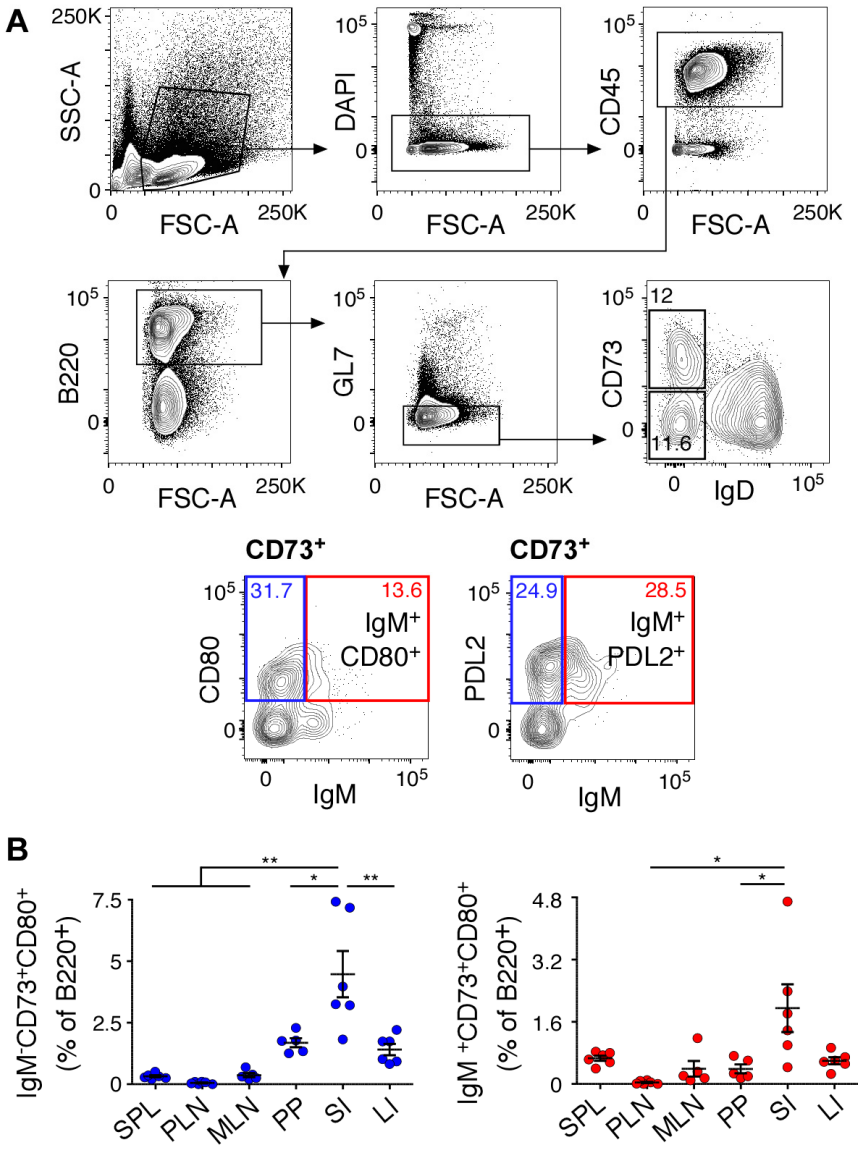

Figure 4. CD73$^+$CD80$^+$ classical memory ME-M B cells account for a small proportion of B lymphocytes in SPF mice. (A) Flow cytometry of viable (DAPI$^-$) murine intestinal lymphocytes stained for CD45, B220, GL7, CD73, IgD, CD80, PDL2 and IgM. Outlined blue areas indicate either CD80$^+$ (left) or PDL2$^+$ (right) ME-SW B cells. Outlined red areas indicate either CD80$^+$ or PDL2$^+$ unswitched ME-M B cells. (B) Frequency of switched IgM$^-$CD73$^+$CD80$^+$ (left) and unswitched IgM$^+$CD73$^+$CD80$^+$ (right) memory B cells in murine SPL, PLN, MLN, PP, SI and LI (calculated from total B220$^+$ B cells). SSC-A, side

scatter area; FSC-A, forward scatter area. ME-SW, switched memory; ME-M, IgM^+ memory B cells; SPL, spleen; PLN, peripheral lymph nodes; MLN, mesenteric lymph nodes; PP, Peyer's patches; SI, small intestine; LI, large intestine. Numbers next to or inside outlined areas indicate percentage of cells. Small horizontal lines indicate the mean (± s.e.m.); *P <0.05, **P<0.01 (two-tailed unpaired Student's *t*-test). Data show representatives (A) of 34 experiments (SPL, PLN, SI and LI from 6 mice, and MLN and PP from 5 mice; B). Each symbol represents an individual sample (B).

Human ME-M B cells inhabit ILFs and PPs

To assess the localization of ME-M B cells we performed flow cytometric analysis of different chemokine receptors. ME-M B cells isolated from terminal ileum and proximal colon expressed CCR7 and CXCR4, which guide B cell homing to follicles[312]. Of note, the expression levels of CCR7 and CXCR4 were comparable in naive, as well as ME-SW B cells (Fig. 5).

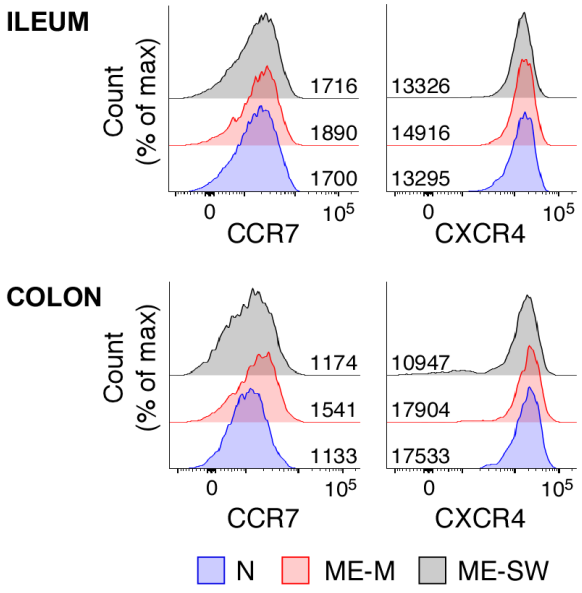

Figure 5. Human intestinal ME B cells show a chemokine receptor profile consistent with follicular localization. Expression CCR7 and CXCR4 on N, ME-M and ME-SW B cells from human terminal ileum and proximal colon assessed by flow cytometry. Numbers in plots indicate mean fluorescence intensity (MFI). N, naïve; ME-M, IgM^+ memory; ME-SW, switched memory B cells. Data show one representative of three experiments with similar results.

Indeed, tissue IFA confirmed that ME-M B cells inhabited ILFs containing or not GC as well as PPs, and were absent or rare in the LP (Fig. 6).

As ILFs are follicular structures emerging after birth in response to gut colonization by the microbiota[177], we wanted to assess the presence of ME-M B cells at early ages. To address that, we performed IFA of formalin-fixed and paraffin-embedded (FFPE) tissue sections from samples of small intestine or cecal appendix from patients ranging from 1.5 months old to 10 years old, and demonstrated that human ME-M B cells are present in the intestine early in life (Fig. 7).

These experiments showed that intestinal ME-M B cells inhabit ILFs and PPs and are rare in the LP, are already present early in life, and persist throughout adulthood.

Figure 6. Human ME-M B cells inhabit ILFs and PPs and are rare in the LP. IFA of intestinal tissue sections including ILF without GC (top), ILF with GC (center) and LP (bottom) stained for IgM (green), IgD (red) and DNA (with the DNA-binding dye DAPI; blue). Dashed lines indicate GC and mantle perimeters; outlined areas correspond to enlargements directly on the right. ILF, isolated lymphoid follicle; PPs, Peyer's Patches; GC, germinal center; M, mantle; LP, lamina propria; N, naïve B cell; ME-M, IgM^+ memory B cell; PC-M, IgM^+ plasma cell; IFA, immunofluorescence analysis. Original magnification, 20X (main images) or 60X (enlargements).

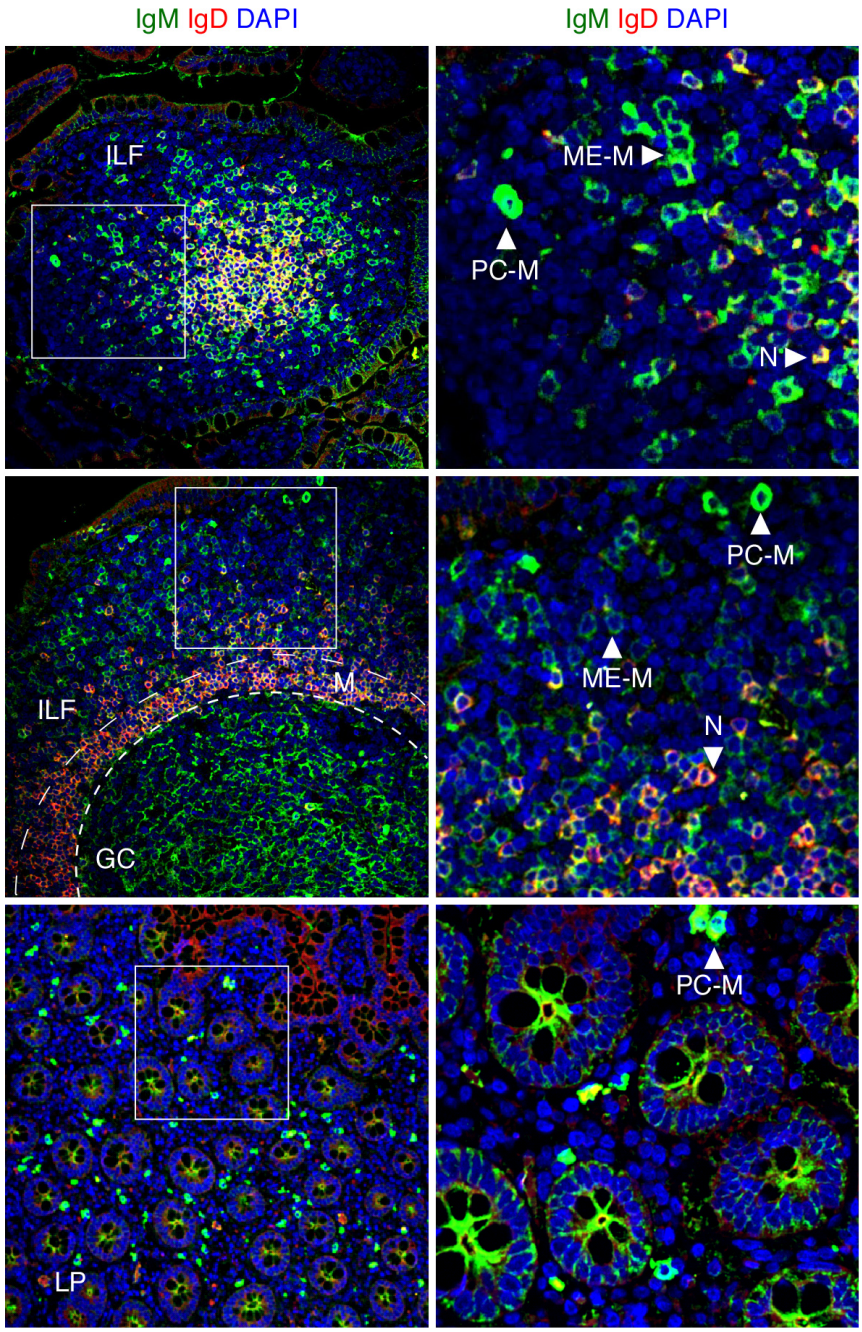
IgM IgD DAPI
IgM IgD DAPI
ILF
ME-M
PC-M
N
ILF
M
GC
PC-M
ME-M
N
LP
PC-M

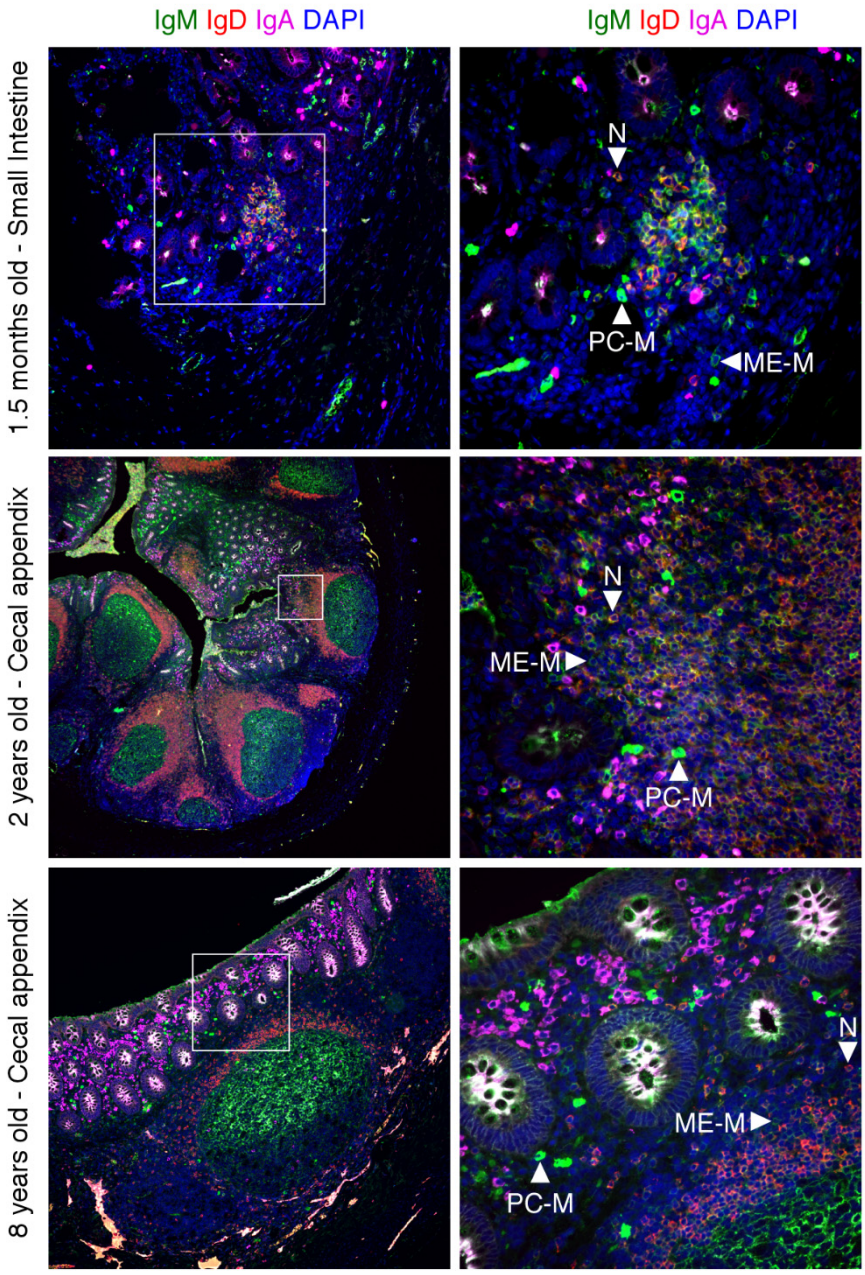

Figure 7. Human ME-M B cells are present in the intestine early in life. IFA of intestinal tissue sections including ILF from one and a half months old child (top), and cecal patches from 2 years old (center) and 8 years old (bottom) children, stained for IgM (green), IgD (red), IgA (magenta) and DNA (with the DNA-binding dye DAPI; blue). Outlined areas correspond to enlargements

directly on the right. ILF, isolated lymphoid follicle; N, naïve B cell; ME-M, IgM^+ memory B cell; PC-M, IgM^+ plasma cell; IFA, immunofluorescence analysis. Original magnification, 10X and 20X (top), 4X and 40X (center) and 10X and 40X (bottom).

ME-M B cells express a common memory gene signature, mucosal phenotype and signs of activation

The murine memory B cell compartment comprises an early GC-independent, unmutated IgM^+ B cell subset[134,135,313], and post-GC affinity matured IgM^+ or switched memory B cells[131]. Upon secondary challenge, IgM^+ memory B cells tend to reenter GC reactions, whereas IgG^+ memory B cells efficiently differentiate into PCs[131]. Of note, IgM^+ memory B cells have been shown to participate in immune responses against TI antigens, although these B cells where short lived and poorly mutated[314]. Importantly, the murine MZ B cell compartment is clearly defined as a sessile population of unmutated B cells residing in the MZ of the spleen, which participates in TI responses to blood borne antigens[315].

On the other hand, the human memory B cell compartment is less well understood. Human MZ B cells are a recirculating spleen-based IgM^+IgD^{low} memory B cell subset involved in systemic TI responses[110]. However, circulating IgM^+IgD^- ME-M B cells are thought to emerge from systemic TD responses due to the fact that this population is not present in HIGM patients carrying mutations of the CD40L gene, who do not possess normally developed GCs nor switched memory B cells[316,317].

To address the possibility of whether intestinal ME-M B cells could be the intestinal counterpart, or share some characteristics with splenic IgM^+IgD^{low} MZ B cells, we performed global gene expression analysis of sorted naive, ME-M and ME-SW B cells from terminal ileum and naive,

MZ and ME-SW B cells from spleen. Unsupervised and supervised hierarchical clustering analysis of global gene expression profiles of the sorted populations showed that whereas naive B cells from both tissues clustered together, splenic and ileal memory B cells clustered by tissue origin (Fig. 8).

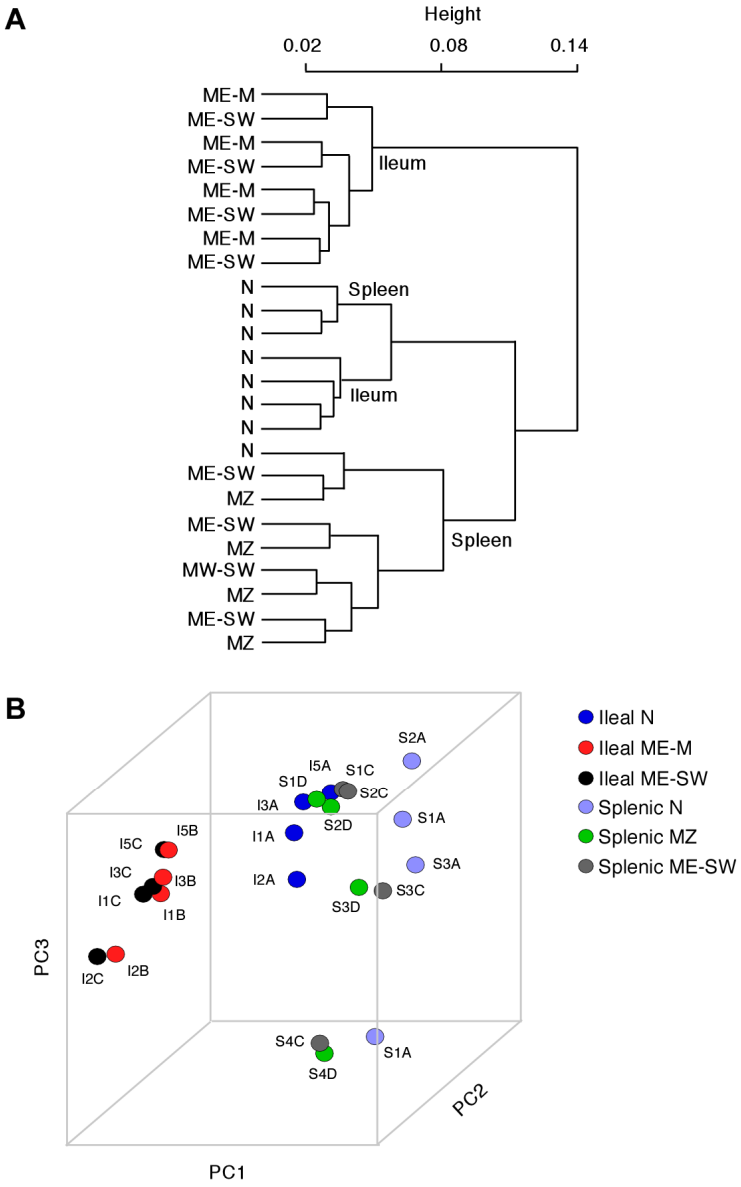

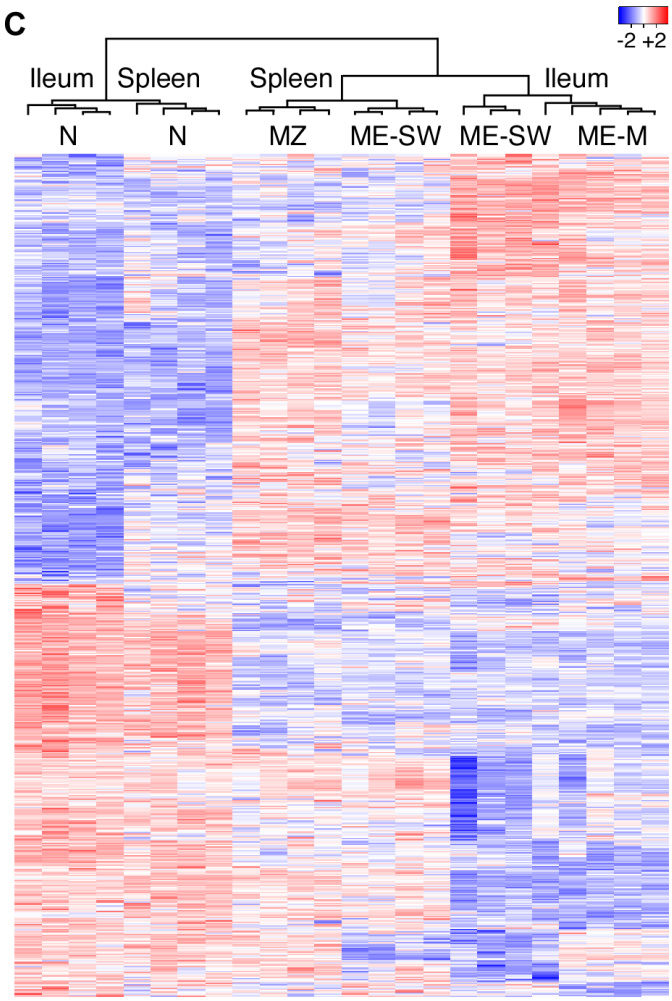

Figure 8. Splenic and ileal ME B cells cluster by tissue origin. (A) Unsupervised hierarchical clustering analysis of global gene expression profiles of sorted N, ME-M and ME-SW B cells from terminal ileum (n=4) and spleen samples (n=4) using correlation distance and the Ward's linkage method. Dendrogram height parameter indicates dissimilarity between clusters. (B) Principal component analysis (PCA) of global gene expression profile of sorted N, ME-M and ME-SW B cells from terminal ileum (n=4) and spleen samples (n=4). (C) Heat map diagram displaying differentially expressed genes (adjusted P value <0.05) between intestinal ME and N ($|\log_2 FC|>0.58$) in intestinal N, ME-M and ME-SW B cells and splenic N, MZ and ME-SW B cells. The color bar depicts normalized intensity values performed on a row basis. From left to right, the x-axis of the heat map depicts N B cells from 4 intestinal samples (terminal ileum) and 4 spleens, MZ and ME-SW B cells from 4 spleens and ME-SW and

ME-M B cells from 4 intestinal samples. The y-axis depicts genes with higher fold decrease (top half of the heat map) and genes with higher fold increase (bottom half of the heat map) in N compared to ME B cells. N, naïve; MZ, marginal zone; ME, memory; ME-M, IgM^+ memory; ME-SW, switched memory B cells.

Moreover, analysis of Robust Multi-Array Average (RMA) expression of ME-M versus N and ME-SW B cells, indicated stronger affiliation of ME-M B cells to ME-SW than to naive B cells (Fig. 9A).

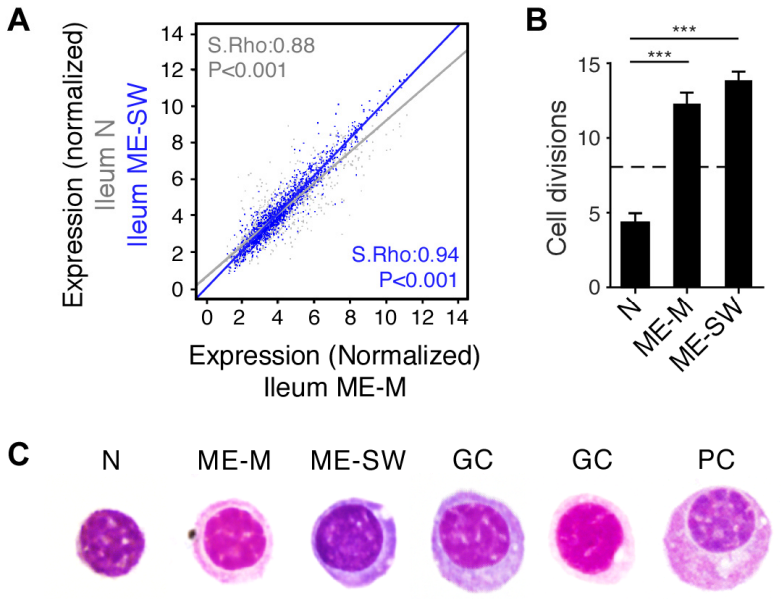

Figure 9. Intestinal ME-M B cells show a gene expression profile, proliferation history and morphology of canonical memory B cells. (A) Scatter plot depicting RMA normalized expression of comparisons from ileum N versus ME-M (grey) and ileum ME-SW versus ME-M (blue) with corresponding regression lines. Spearman's Rho correlation is computed for each scatter point cloud. P value <0.001. (B) Analysis of the replication history of sorted intestinal N, ME-M and ME-SW B cell subsets as measured with the KREC assay. (C) May Grünwald-Giemsa staining of sorted intestinal N, ME-M, ME-SW, GC and PC. Original magnification 100X. RMA, Robust Multi-array Average; N, naïve; ME-M, IgM^+ memory; ME-SW, switched memory; GC, germinal center B cells; PC,

plasma cells; KREC, kappa-deleting recombination excision circles. Dashed line represents values for tonsil-derived centrocytes. Error bars represent s.e.m.; ***P<0.001 (two-tailed unpaired Student's *t*-test).

Additionally, analysis of the replication history of sorted intestinal naive, ME-M and ME-SW B cell subsets as measured with the kappa-deleting recombination excision circles (KREC) assay, showed that ME-M B cells have a similar proliferation history than intestinal ME-SW B cells (Fig. 9B). Taking into account previously described proliferation values of tonsillar centroblasts and centrocytes[307], the obtained proliferation history for ME-M as well as ME-SW B cells is consistent with a GC origin of these cellular subsets.

In line with these results, May Grünwald-Giemsa staining of different sorted intestinal B cell populations showed that ME-M B cells present a morphology typical of memory B cells, with central nucleus and scant cytoplasm (Fig. 9C).

From the analysis of the commonly differentially expressed genes in all memory B cell subsets studied compared to either intestinal or splenic naive B cells we identified a common memory B cell gene signature (Fig. 10A), including genes belonging to different functional categories of the immune response, such as lymphocyte signaling, cytokine production, transcriptional regulators, chemokine activity and others (Fig. 10B, C).

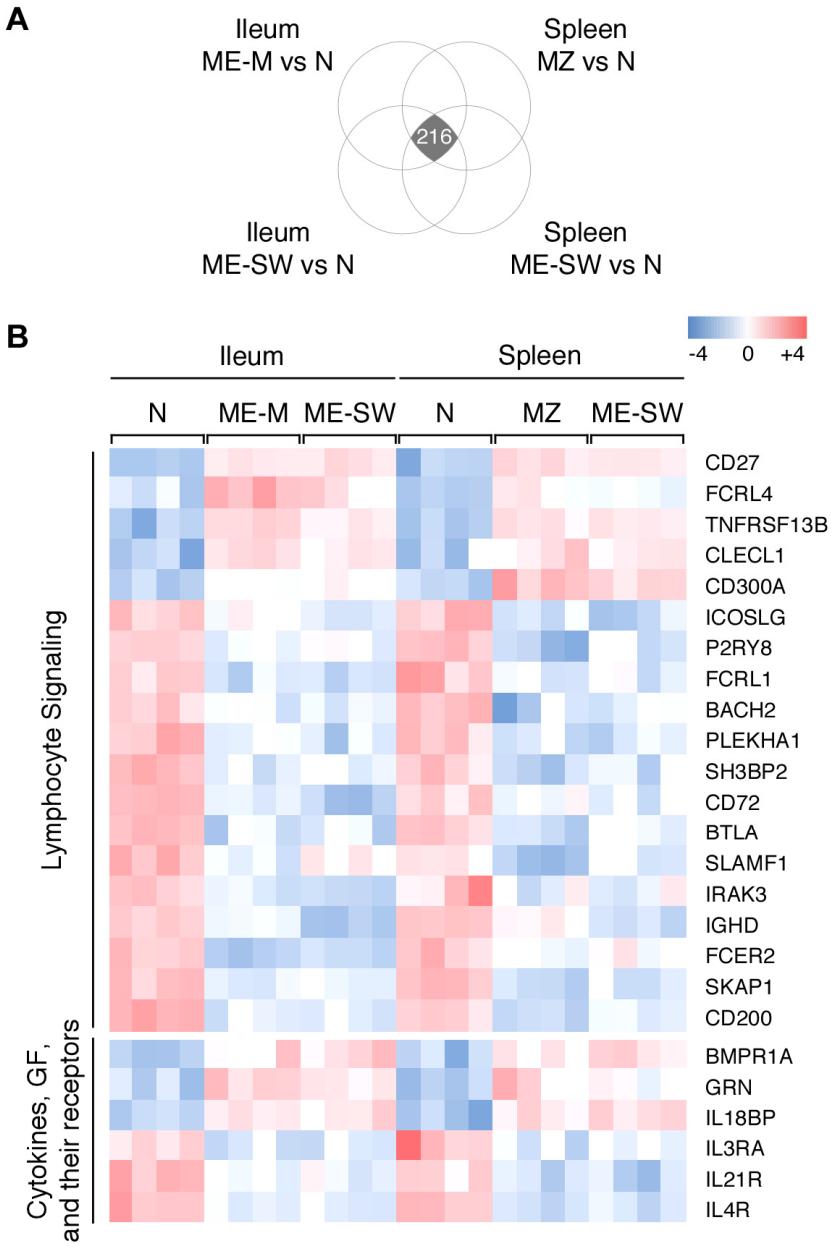
A
Ileum
ME-M vs N
Spleen
MZ vs N
216
Ileum
ME-SW vs N
Spleen
ME-SW vs N
B
-4
0
+4
Ileum
Spleen
N
ME-M
ME-SW
N
MZ
ME-SW
Lymphocyte Signaling
Cytokines, GF, and their receptors
CD27
FCRL4
TNFRSF13B
CLECL1
CD300A
ICOSLG
P2RY8
FCRL1
BACH2
PLEKHA1
SH3BP2
CD72
BTLA
SLAMF1
IRAK3
IGHD
FCER2
SKAP1
CD200
BMPR1A
GRN
IL18BP
IL3RA
IL21R
IL4R

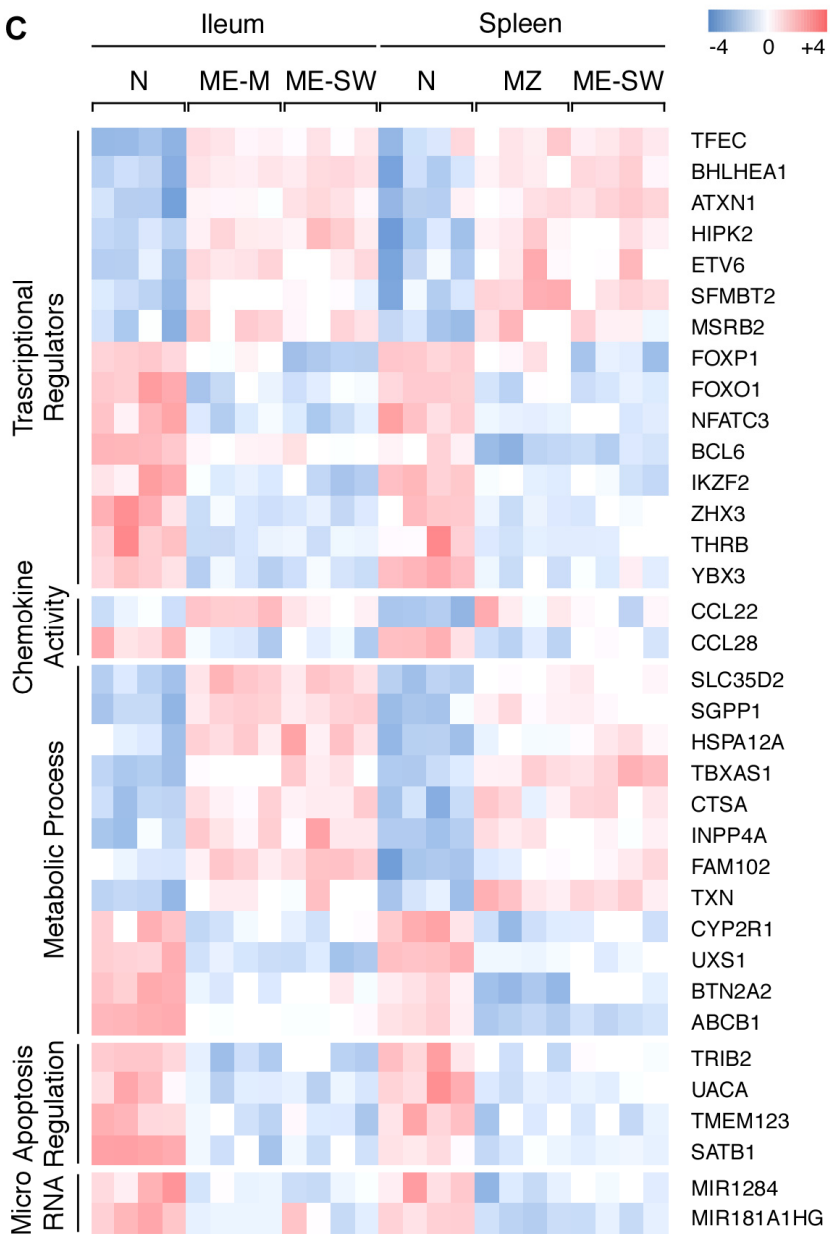

Figure 10. ME-M B cells express a common memory B cell transcriptome. (A) Venn diagram representing commonly differentially expressed genes in all memory B cell subsets studied (number in grey area) compared to either intestinal or splenic N B cells. $|\log_2 FC|>0.58$, adjusted P value <0.05. (B, C) Heat map

diagrams showing a selection of 180 genes from the memory B cell signature grouped by functional categories of immune response genes. Functional categories and genes are listed on the left and right sides of the heat maps, respectively. The color bar depicts normalized intensity values. N, naïve; MZ, marginal zone; ME-M, IgM^+ memory; ME-SW, switched memory B cells.

Flow cytometric analysis of human intestinal ME-M B cells confirmed that ME-M B cells show a classical memory phenotype both in ileum and colon, lacking the expression of IgD and expressing the co-stimulatory molecules CD24 and CD27 on their surface (Fig. 11A). Moreover, analysis of gene expression by quantitative RT-PCR showed that ME-M B cells expressed the anti-apoptotic gene Bcl-2 (*BCL2*), and the TNF receptor family member TACI (*TNFRSF13B*), as well as low levels of IL-21 receptor (*IL-21R*), the GC-related gene Bcl-6 (*BCL6*) and the CSR/SHM inducing enzyme AID (*AICDA*), similar to the levels of ME-SW B cells (Fig. 11B).

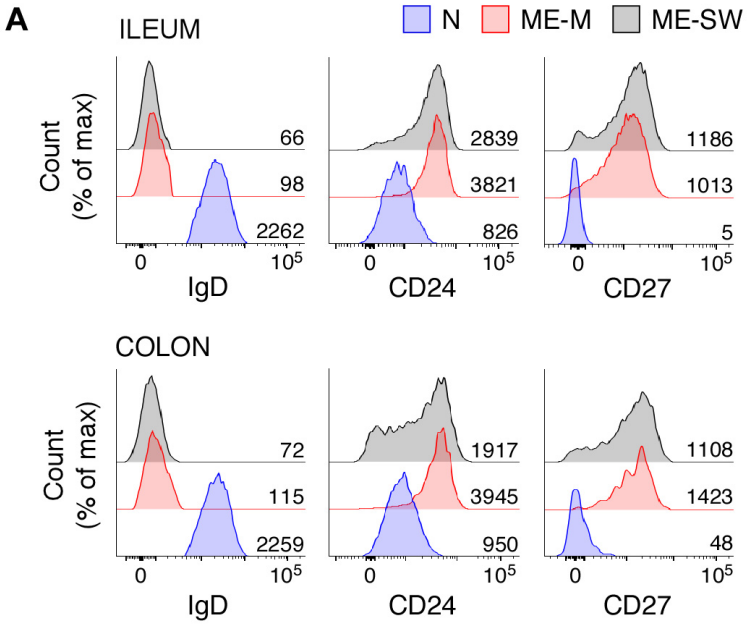

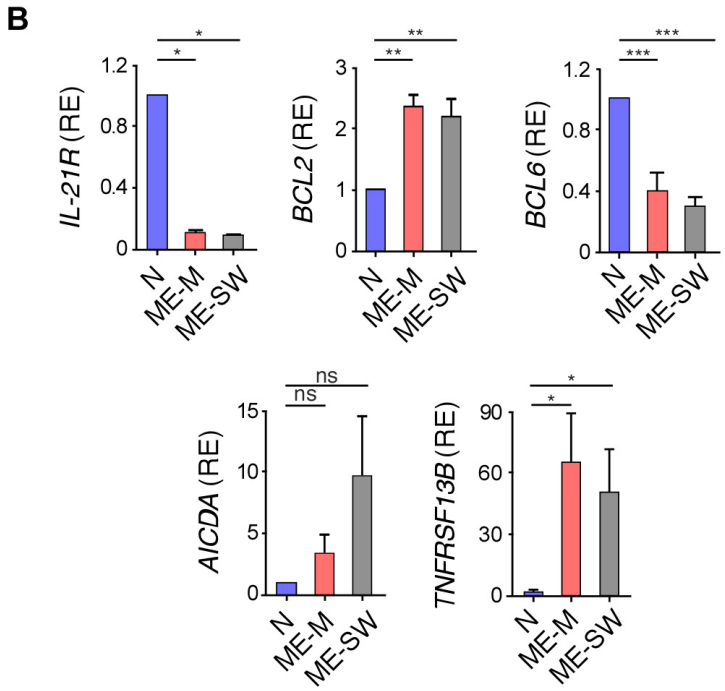

Figure 11. Human intestinal ME-M B cells show a classical memory phenotype. (A) Expression of IgD, CD24 and CD27 on human intestinal N, ME-M and ME-SW B cells from ileum and colon, assessed by flow cytometry. Numbers in plots indicate mean fluorescence intensity (MFI). (B) Quantitative RT-PCR analysis of mRNA encoding IL-21R (*IL21R*), Bcl-2 (*BCL2*), Bcl-6 (*BCL6*), AID (*AICDA*) and TACI (*TNFRSF13B*), in sorted intestinal N, ME-M and ME-SW B cells; results are normalized to those of mRNA encoding β-actin (*ACTB*) and are presented as relative expression (RE) compared with that of N B cells, set as 1. N, naïve; ME-M, IgM^+ memory; ME-SW, switched memory B cells. Error bars represent s.e.m.; *P <0.05, **P<0.01; ***P<0.001 (two-tailed unpaired Student's *t*-test). Data are from one of three experiments with similar results (A), or include at least three different experiments (B).

Additionally, analysis of the correlation of the gene expression profiles of these B cell subsets, revealed that intestinal ME-M B cells show a stronger affiliation to intestinal ME-SW B cells than to splenic MZ B cells (Fig. 12A). Indeed, from the analysis of the commonly differentially expressed genes in intestinal ME-M and ME-SW B cells we identified a

common gut memory B cell gene signature (Fig. 12B), that included genes belonging to different functional categories of the immune response (Figure 13).

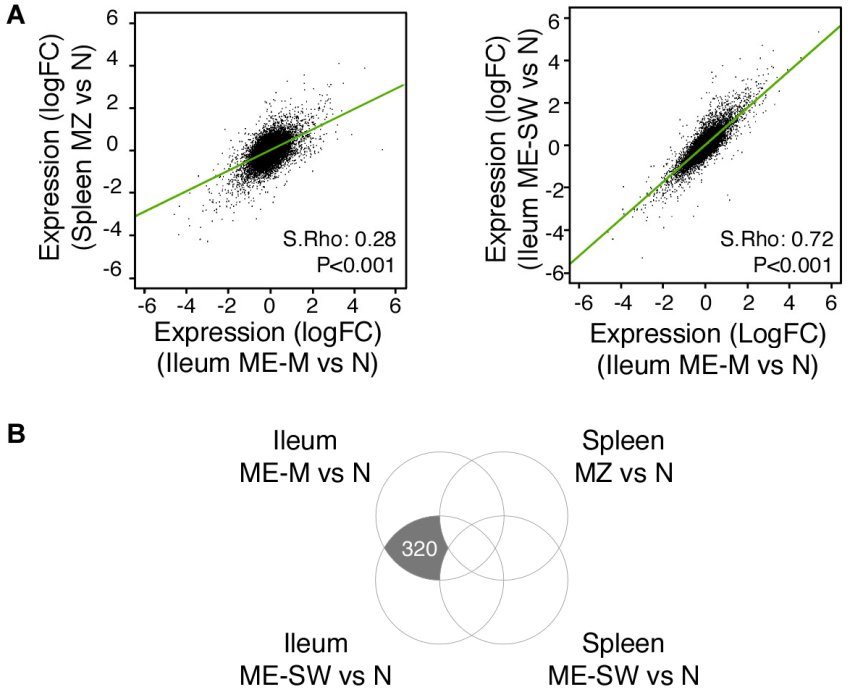

Figure 12. Intestinal ME-M B cells show a stronger correlation with intestinal ME-SW B cells than to splenic MZ B cells. (A) Scatter plot depicting RMA normalized expression of comparison from ileal ME-M versus N B cells and splenic MZ versus N B cells (left), and comparison from ileal ME-M versus N B cells and ileal ME-SW versus N B cells (right). Spearman's Rho correlation is computed for each scatter point cloud. P values <0.001. (B) Venn diagram representing commonly differentially expressed genes in intestinal ME-M and ME-SW B cells (number in grey area) compared to intestinal N B cells. $|\log_2 FC|>0.58$, adjusted P value <0.05. RMA, Robust Multi-array Average; N, naïve; MZ, marginal zone; ME-M, IgM^+ memory; ME-SW, switched memory B cells.

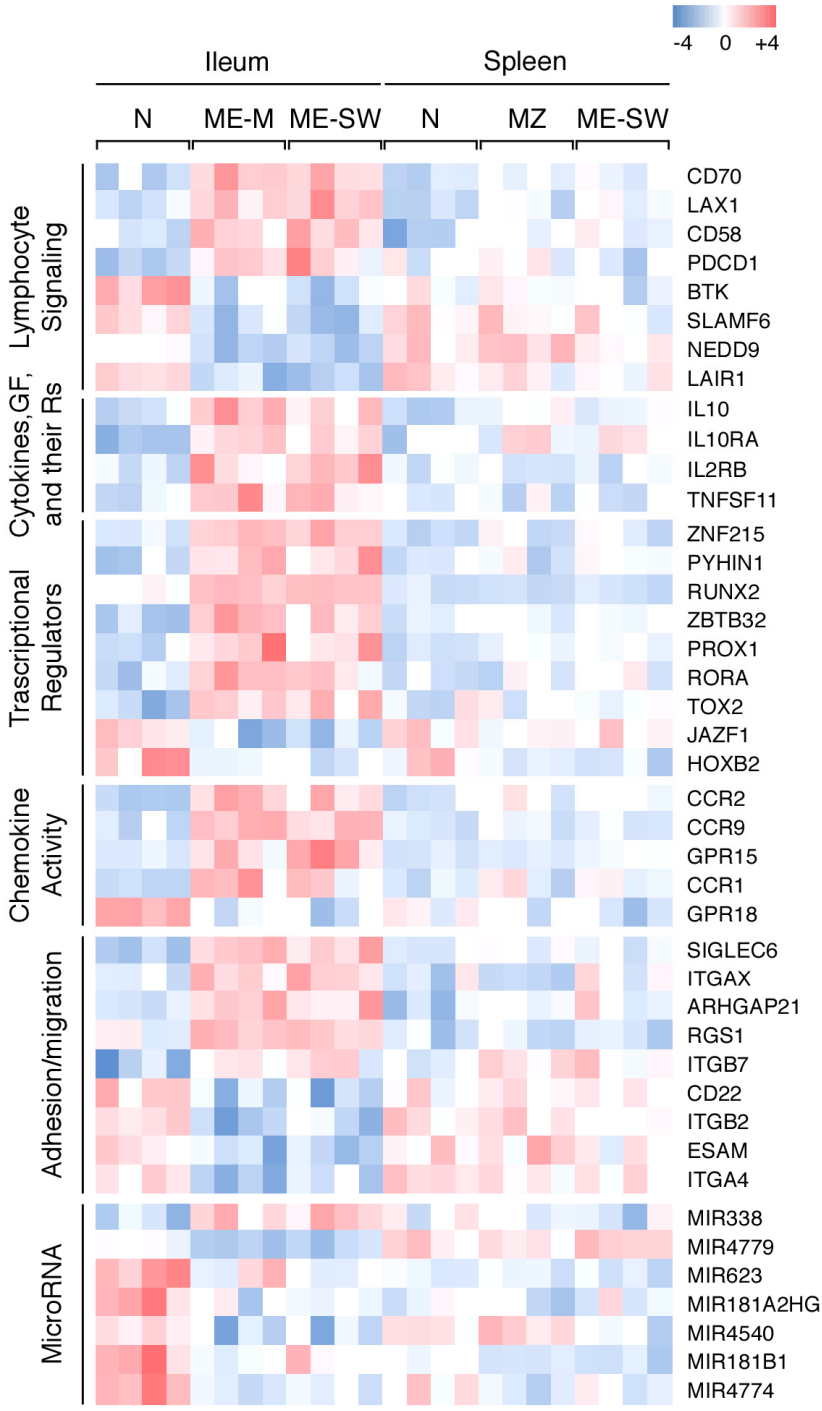
-4
0
+4
Ileum
Spleen
N
ME-M
ME-SW
N
MZ
ME-SW
Lymphocyte Signaling
Cytokines,GF, and their Rs
Trascriptional Regulators
Chemokine Activity
Adhesion/migration
MicroRNA
CD70
LAX1
CD58
PDCD1
BTK
SLAMF6
NEDD9
LAIR1
IL10
IL10RA
IL2RB
TNFSF11
ZNF215
PYHIN1
RUNX2
ZBTB32
PROX1
RORA
TOX2
JAZF1
HOXB2
CCR2
CCR9
GPR15
CCR1
GPR18
SIGLEC6
ITGAX
ARHGAP21
RGS1
ITGB7
CD22
ITGB2
ESAM
ITGA4
MIR338
MIR4779
MIR623
MIR181A2HG
MIR4540
MIR181B1
MIR4774

Figure 13. ME-M B cells share a common gene expression profile with intestinal ME-SW B cells. Heat map diagram showing a selection of genes from the intestinal memory B cell signature grouped by functional categories of immune response genes. Each row represents an individual gene and each column a different sample. Functional categories and genes are listed on the left and right sides of the heat maps, respectively. The color bar depicts normalized intensity values. $|\log_2 FC|>0.58$, adjusted P value <0.05. N, naïve; MZ, marginal zone; ME-M, IgM^+ memory; ME-SW, switched memory B cells.

Consistent with these results, analysis of gene expression by quantitative RT-PCR showed that ME-M B cells show an abundant expression of the immune-regulatory cytokine IL-10 (*IL-10*), the transcription factor RUNX2 (*RUNX2*), the inhibitory receptor Fc receptor–like 4 (*FCRL4*), CD70 (*CD70*) a receptor for CD27 expressed on activated B cells[318], the G protein-coupled receptors GPR34 (*GPR34*) and GPR15 (*GPR15*), aryl hydrocarbon receptor (*AHR*), sialic acid binding Ig-like lectin 6 (*SIGLEC6*) and the receptor activator of nuclear factor kappa-B ligand or RANKL (*RANKL*), at a similar levels than intestinal ME-SW B cells, thus showing a mucosal memory B cell phenotype. Indeed, naive, MZ and ME-SW B cells from spleen expressed these molecules at lower levels than intestinal memory B cells (Fig. 14A).

IL-10 is an important mediator of immune regulation and identifies a subset of regulatory B cells that suppresses pathological immune responses that can result in uncontrolled inflammation[319-321]. To further explore the possibility of ME-M B cells having regulatory properties, we tested the capacity of intestinal ME-M B cells to produce IL-10. After 48h of CpG stimulation, ME-M B cells, as well as ME-SW B cells, showed elevated production of IL-10 compared to naive B cells (Fig. 14B).

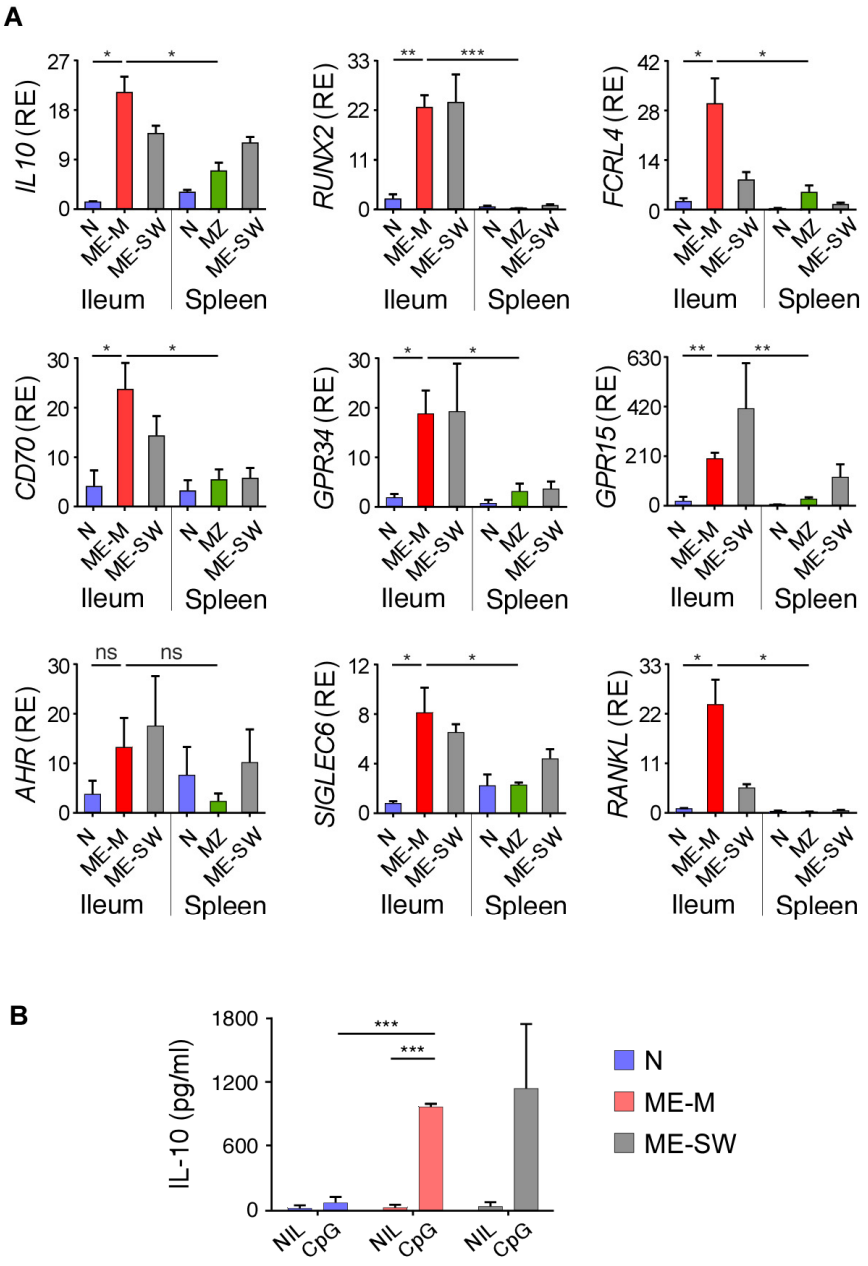
A
IL10 (RE)
RUNX2 (RE)
FCRL4 (RE)
CD70 (RE)
GPR34 (RE)
GPR15 (RE)
AHR (RE)
SIGLEC6 (RE)
RANKL (RE)
N
ME-M
ME-SW
MZ
Ileum
Spleen
ns
B
IL-10 (pg/ml)
NIL
CpG
N
ME-M
ME-SW

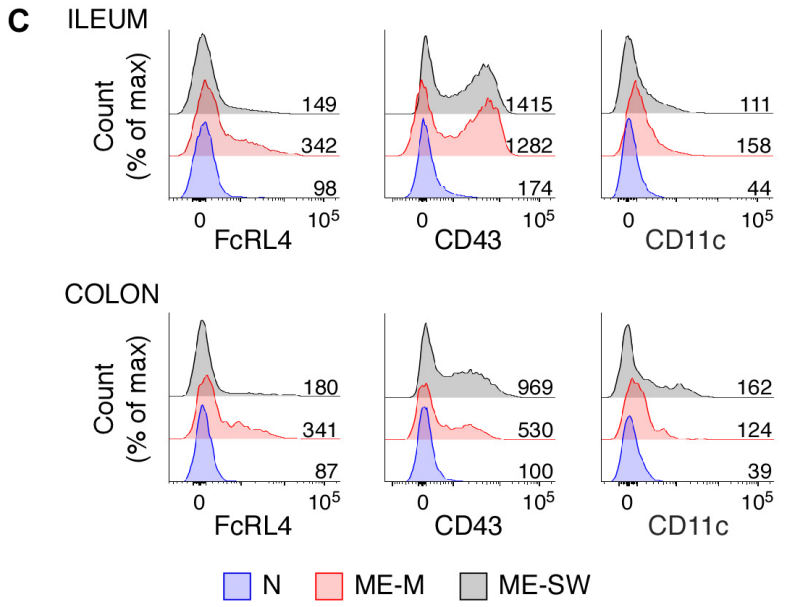

Figure 14. Human intestinal ME-M B cells express a mucosal memory B cell phenotype and show signs of activation. (A) Quantitative RT-PCR analysis of mRNA encoding IL-10 (*IL10*), RUNX2 (*RUNX2*), FcRL4 (*FCRL4*), CD70 (*CD70*), GPR34 (*GPR34*), GPR15 (*GPR15*), AhR (*AHR*), Siglec-6 (*SIGLEC6*) and RANKL (*RANKL*) in sorted intestinal N, ME-M and ME-SW B cells, and splenic N, MZ and ME-SW B cells; results are normalized to those of mRNA encoding β-actin (*ACTB*) and are presented as relative expression (RE) compared with that on N B cells. (B) ELISA of IL-10 from supernatants of intestinal N, ME-M and ME-SW B cells cultured for 48h with medium alone (NIL) or CpG. (C) Expression of FcRL4, CD43 and CD11c on intestinal N, ME-M and ME-SW B cells from ileum and colon, assessed by flow cytometry. Numbers in plots indicate mean fluorescence intensity (MFI). N, naïve; MZ, marginal zone; ME-M, IgM^+ memory; ME-SW, switched memory B cells. Error bars, s.e.m.; *P<0.05; **P<0.01; ***P<0.001 (two-tailed unpaired Student's *t*-test). Data include at least three different experiments (A, B) or are from one of three experiments with similar results (C).

Importantly, a fraction of ME-M B cells showed signs of activation, such as the expression of FcRL4, expressed on a fraction of activated memory B cells[322-324], the activation molecule CD43[325], and the integrin CD11c,

expressed by B cells located at the T-B border of the follicle, an area where B cells interact with T cells and become activated[326] (Fig. 14C).

Overall, these data indicate that human intestinal ME-M B cells have a transcriptional signature reflecting affiliation to gut memory B cells, express phenotypic hallmarks of mucosal memory B cells and show signs of activation.

Intestinal ME-M B cells share some characteristics with splenic MZ B cells

Besides the clear affiliation to gut ME-SW B cells, intestinal ME-M B cells shared the expression of a reduced number of genes with splenic MZ B cells, therefore defining an IgM^+ memory gene signature (Fig. 15A, B). Accordingly, flow cytometric analysis confirmed that intestinal ME-M B cells share phenotypic traits with splenic MZ B cells, such as the expression of the transmembrane protein with immunomodulatory function FcRL2[327]; CD148, a protein tyrosine phosphatase involved in signal transduction in leucocytes thought to contribute to mechanisms of cellular differentiation[328]; the adhesion and signaling molecule CD66a, also known as carcinoembryonic antigen-related cell adhesion molecule 1 (CEACAM1); and the complement receptors CD21 (CR2) and CD35 (CR1) (Fig. 16).

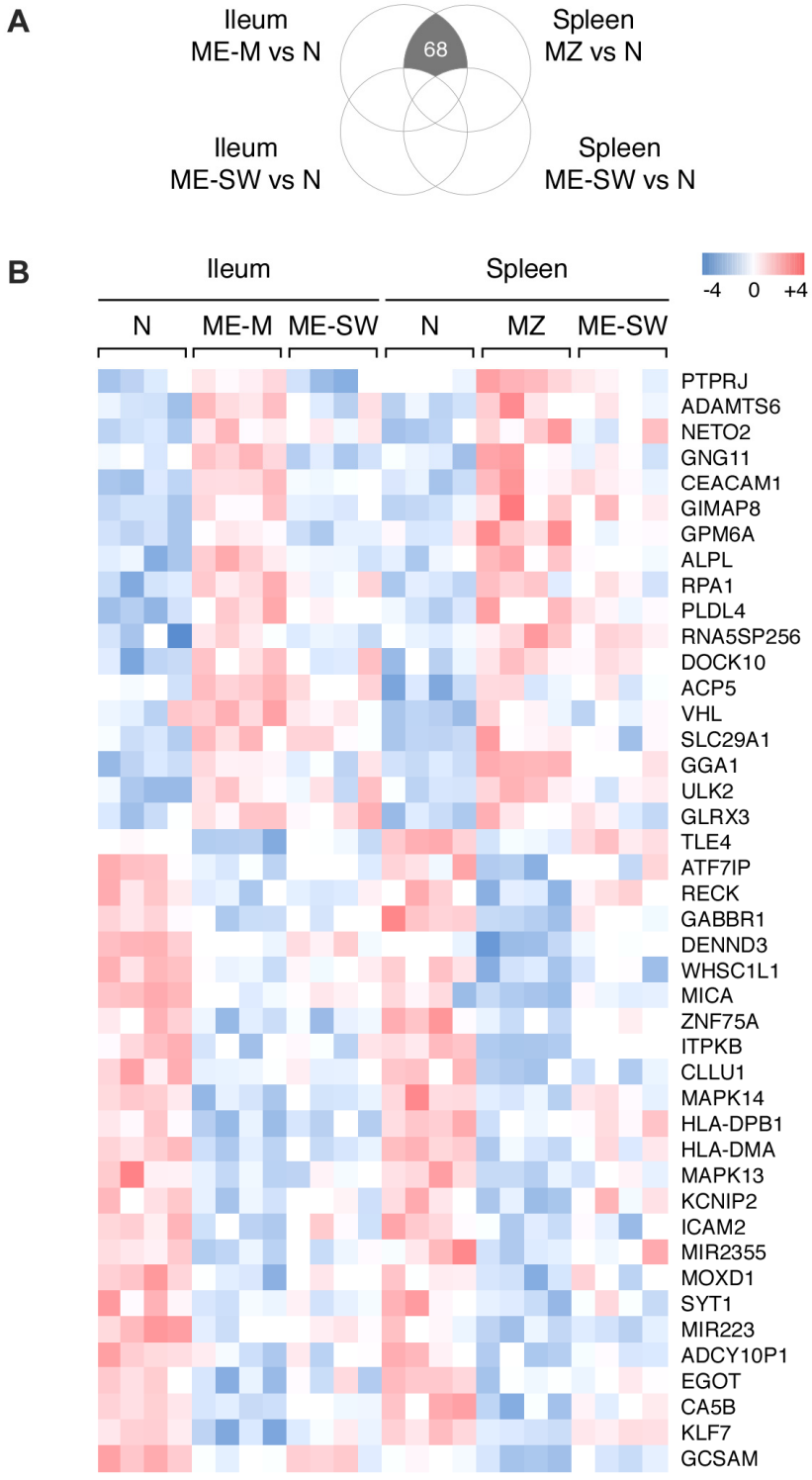
A
Ileum
ME-M vs N
68
Spleen
MZ vs N
Ileum
ME-SW vs N
Spleen
ME-SW vs N
B
Ileum
Spleen
-4 0 +4
N
ME-M
ME-SW
N
MZ
ME-SW
PTPRJ
ADAMTS6
NETO2
GNG11
CEACAM1
GIMAP8
GPM6A
ALPL
RPA1
PLDL4
RNA5SP256
DOCK10
ACP5
VHL
SLC29A1
GGA1
ULK2
GLRX3
TLE4
ATF7IP
RECK
GABBR1
DENND3
WHSC1L1
MICA
ZNF75A
ITPKB
CLLU1
MAPK14
HLA-DPB1
HLA-DMA
MAPK13
KCNIP2
ICAM2
MIR2355
MOXD1
SYT1
MIR223
ADCY10P1
EGOT
CA5B
KLF7
GCSAM

Figure 15. Intestinal ME-M B cells share the expression of a significant number of genes with splenic MZ B cells. (A) Venn diagram representing differentially expressed genes in intestinal ME-M and splenic MZ B cells (number in grey area) compared to intestinal N and splenic N B cells respectively. $|\log_2 FC|>0.58$, adjusted P value <0.05. (B) Heat map diagram showing the differentially expressed genes in intestinal ME-M compared to intestinal ME-SW and in splenic MZ compared to splenic ME-SW B cells. Each row represents an individual gene and each column a different sample. The color bar depicts normalized intensity values. $|\log_2 FC|>0.58$, adjusted P value <0.05; all genes are showed. N, naïve; MZ, marginal zone; ME-M, IgM^+ memory; ME-SW, switched memory B cells.

Figure 16. Intestinal ME-M B cells share phenotypic traits with splenic MZ B cells. Analysis of the expression of IgD, IgM, FcRL2, CD84, CD148, CD66a, CD35, CD21, CD1d and CD1c on intestinal N, ME-M and ME-SW B cells and splenic N, MZ and ME-SW B cells, assessed by flow cytometry. Numbers in plots indicate mean fluorescence intensity (MFI). Data are representative of at least three different experiments for each molecule.

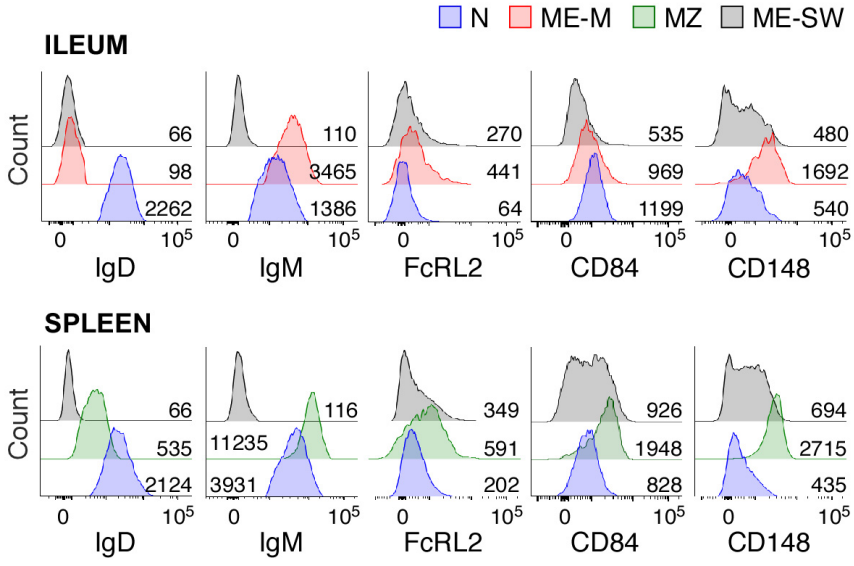

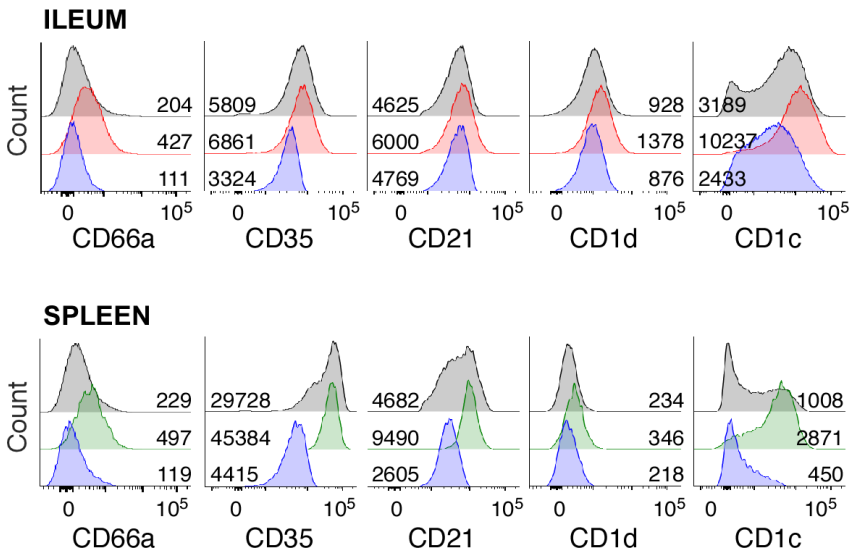

Due to the common gene signature and phenotypic similarities between MZ B cells and ME-M B cells, we wanted to further explore possible ontogenetic relathioships between the two populations. With this aim, we performed high-throughput Ig repertoire analysis of sorted splenic N and MZ B cells as well as ME-M, ME-A, PC-M and PC-A subsets from ileum and colon. This analysis revealed that intestinal ME-M B cells share a common IgH variable region (IGHV) gene usage with splenic MZ B cells (Fig. 17), indicating a possible common progenitor for these two cellular subsets. On the other hand, the IgH joining region 6 (IGHJ6) gene usage appeared negatively selected in intestinal memory B cells compared to splenic N or MZ B cells as well as intestinal PCs (Fig. 18), pointing to a GC selection process for intestinal memory B cell populations that reduces J6 gene usage.

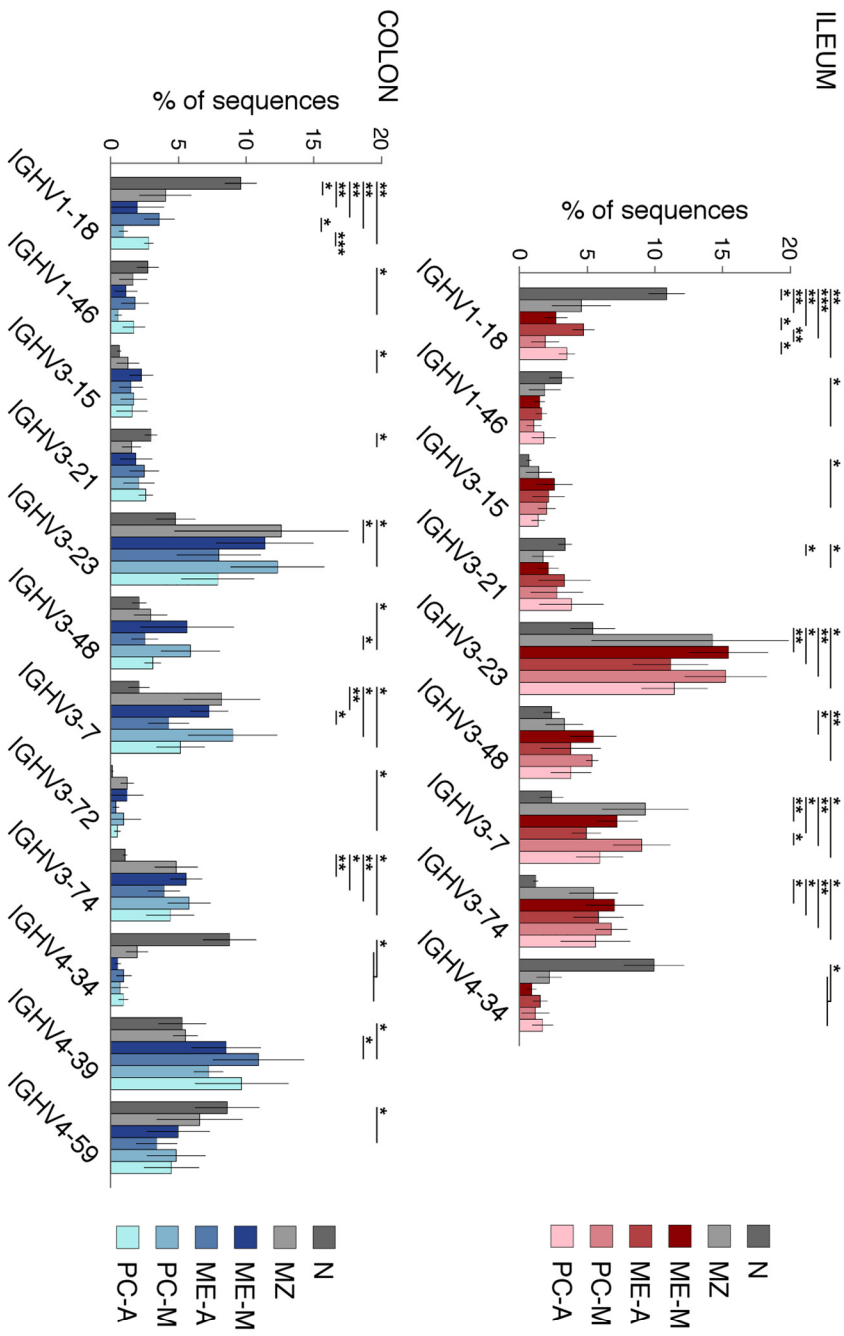

Fig 17. Intestinal ME-M B cells share a common IGHV gene usage with splenic MZ B cells. IGHV gene usage (expressed as relative frequency) within sorted splenic N and MZ B cells and intestinal ME-M, ME-A, PC-M and PC-A in ileum (top) and colon (bottom). The graph shows those IGHV genes that are

significantly differentially used by any of the populations studied. IGHV, Ig heavy chain variable gene; N, naïve; MZ, marginal zone; ME-M, IgM^+ memory; ME-A, IgA^+ memory B cells; PC-M, IgM^+ plasma cells; PC-A, IgA^+ plasma cells. Error bars represent S.D.; *P <0.05, **P<0.01, ***P<0.001 (two-tailed unpaired Student's *t*-test). Data includes 4 samples from terminal ileum, 4 samples from terminal colon (same donors) and 3 samples from spleen.

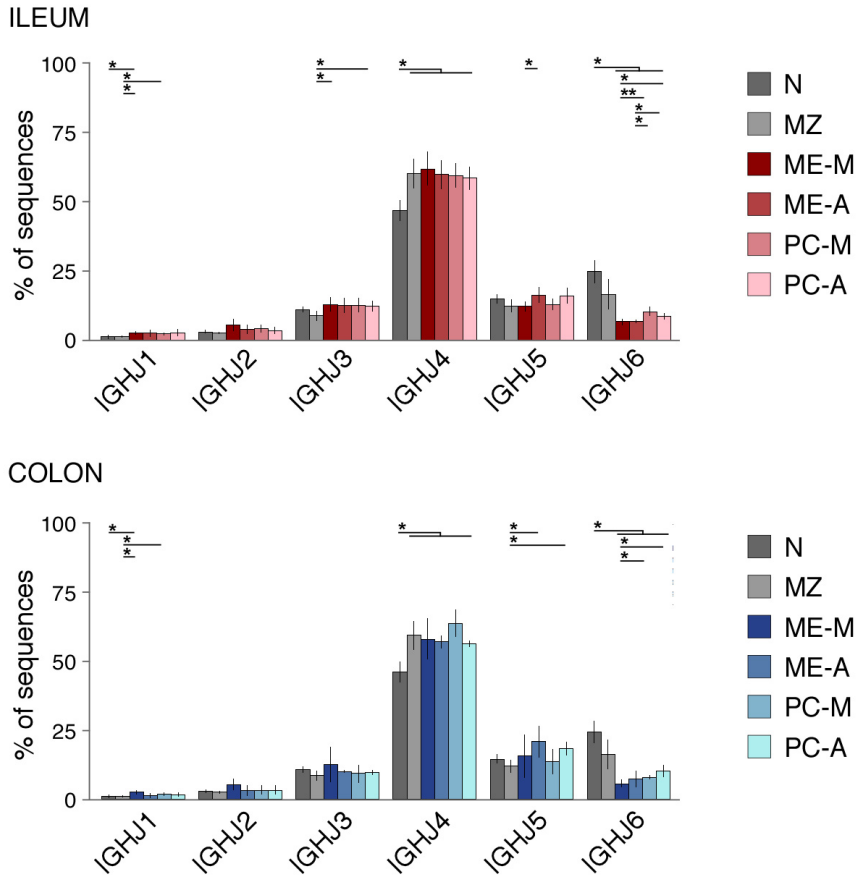

Fig 18. IGHJ6 gene is negatively selected in intestinal ME B cells, but not in MZ B cells. IGHJ gene usage within sorted splenic N and MZ B cells and intestinal ME-M, ME-A, PC-M and PC-A in ileum (top) and colon (bottom). IGHJ, Ig heavy chain joining gene; N, naïve; MZ, marginal zone; ME-M, IgM^+ memory; ME-A, IgA^+ memory B cells; PC-M, IgM^+ plasma cells; PC-A, IgA^+ plasma cells. Error bars represent S.D.; *P <0.05, **P<0.01, ***P<0.001 (two-tailed unpaired Student's *t*-test). Data includes 4 samples from terminal ileum, 4 samples from terminal colon (same donors) and 3 samples from spleen.

Intestinal ME-M B cells were mutated albeit at a lower frequency than ME-SW B cells. In addition, ME-M B cells had a higher proportion of unmutated frequencies than ME-SW B cells. As expected, MZ B cells showed lower levels of mutation and higher proportion of unmutated sequences (Fig. 19A, B).

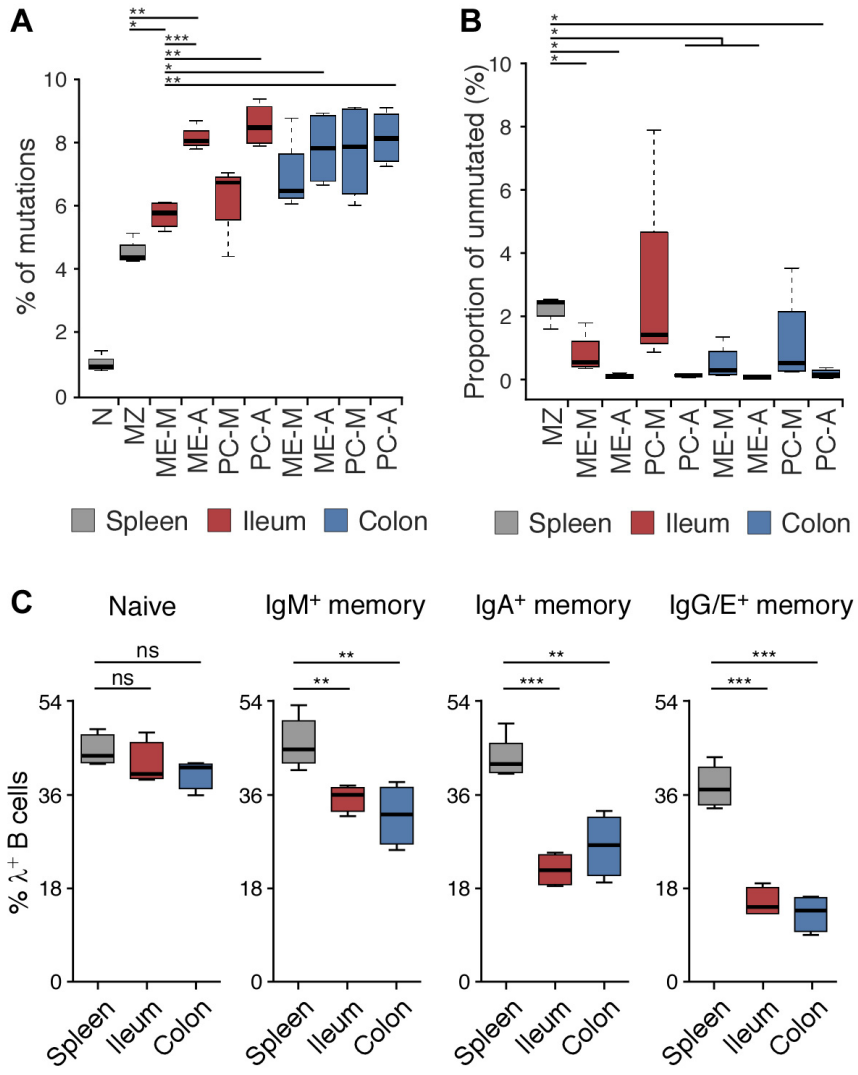

Fig 19. Intestinal ME-M B cells show a GC-derived Ig gene mutation profile and a reduced Igλ usage compared to their splenic counterparts. (A) Mean number of mutations per sequence and donor (expressed as mutations / 100bp) in splenic N and MZ B cells (grey) and intestinal ME-M, ME-A, PC-M and PC-A in ileum (red) and colon (blue). (B) Proportion of unmutated sequences in splenic MZ B cells (grey) and intestinal ME-M, ME-A, PC-M and PC-A in ileum (red) and colon (blue). Unmutated sequences are defined as having zero mutations when compared to its germline sequence. **(C)** Frequency of N, ME-M, ME-A and ME-G/E B cells expressing Igλ chain in their surface in spleen, ileum and colon, analyzed by flow cytometry. N, naïve; MZ, marginal zone; ME-M, IgM^+ memory; ME-A, IgA^+ memory B cells; PC-M, IgM^+ plasma cells; PC-A, IgA^+ plasma cells. Whiskers, minimum to maximum, thick line indicates the median. *P <0.05, **P<0.01 (two-tailed unpaired Student's *t*-test). Data include 4 samples from terminal ileum, 4 samples from terminal colon (same donors) and 3 samples from spleen (A, B) and 13 different experiments (5 spleens, 4 ileums, 4 colons).

These results sugggest that intestinal ME-M B cells emerge from an antigen-driven TD follicular pathway distinct from the TI extrafollicular pathway usually followed by splenic MZ B cells. Interestingly, intestinal memory B cell populations showed a reduced Igλ usage compared to their splenic counterparts (Fig. 19C), suggesting the existence of distinctive features in the selection process followed by memory B cells in intestinal GCs.

Given the described similarities between ME-M and MZ B cells and their common IGHV gene usage, we next wanted to compare their BCR reactivity towards different antigens. We sorted and EBV transformed intestinal and splenic naive, MZ and ME-M B cells. After recovering the Ig enriched supernatants we tested their antibody reactivity by ELISA (Fig. 20). In these assays we found that, similar to naive B cells, Igs from ME-M B cells showed some degree of autoreactivity, as determined by the reactivity towards Hep-2 antigen. In addition, ME-M B cells showed a pronounced carbohydrate and phospholypid reactivity, as determined by the reactivity towards phosphorilcoline, capsular polysacharydes, α-

galactosidase, β-glucan and laminarin similiar to splenic MZ B cells (Fig. 21).

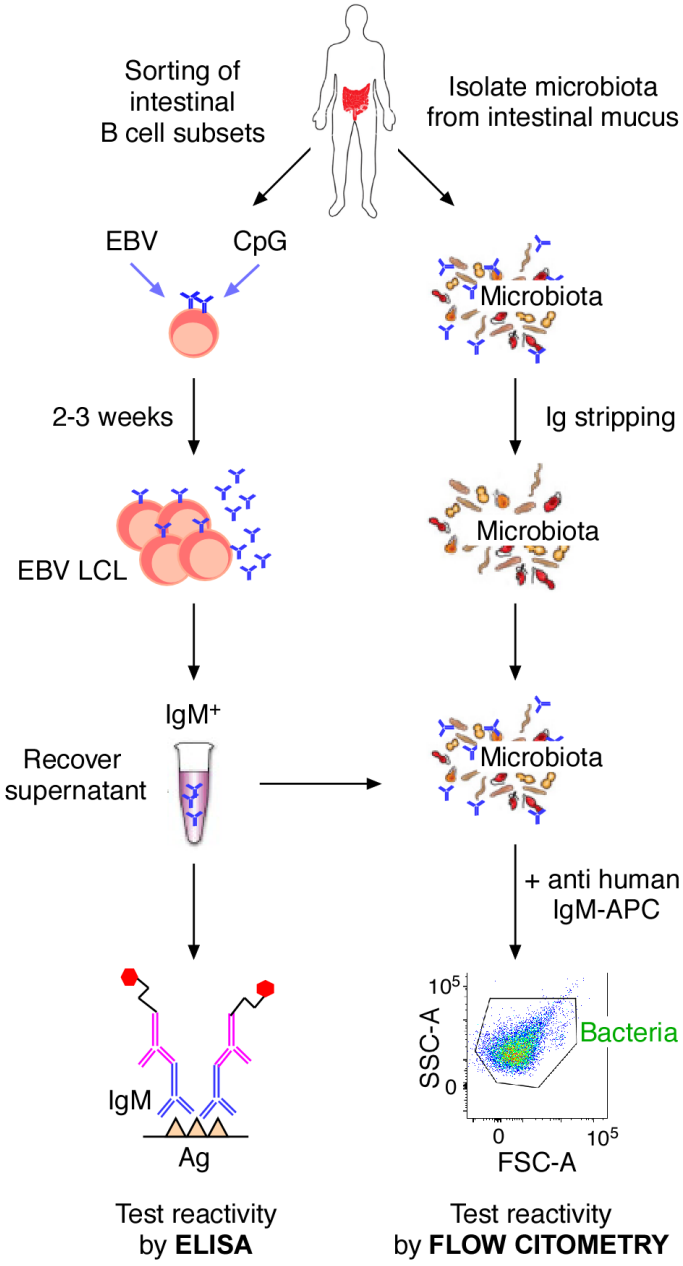

Figure 20. Experimental design used to test reactivity of IgM antibodies from intestinal ME-M B cells. EBV, Epstein-Barr virus; LCL, lymphoblastoid cell

line; Ag, antigen; APC, allophycocyanin; SSC-A, side scatter area; FSC-A, forward scatter area.

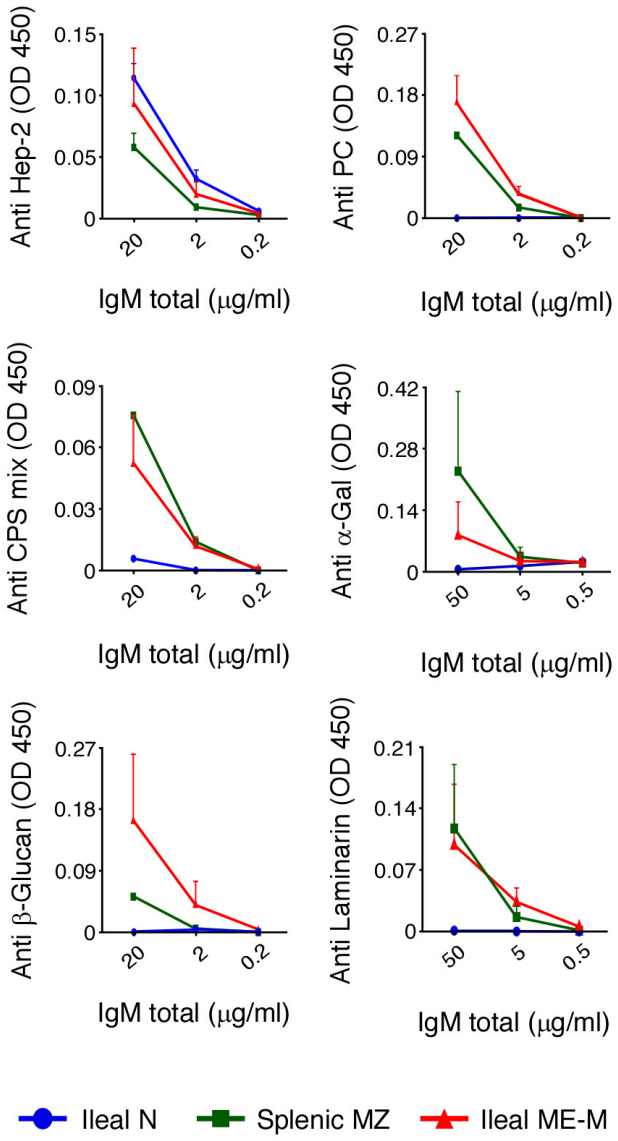

Figure 21. Antibodies from intestinal ME-M B cells have a pronounced carbohydrate and phospholipid reactivity. Reactivity of IgM antibodies from EBV transformed intestinal N and ME-M B cells and splenic MZ B cells towards antigens Hep-2, PC, CPS mix, α-Gal, β-Glucan and laminarin tested by ELISA.

EBV, Epstein-Barr virus; OD, optical density; PC, phosphorylcholine; CPS, capsular polysaccharides; α-Gal, α-Galactosidase; N, naïve; ME-M, IgM^+ memory; MZ, marginal zone B cells. Error bars represent s.e.m. from three independent experiments.

In parallel, to further test the reactivity of Igs from ME-M B cells, we recovered microbiota from human intestinal mucus samples. After stripping endogenous Ig bound to the microbiota (Fig. 20), we tested the reactivity of the Ig enriched SN from the EBV transformed intestinal N and ME-M B cells by flow citometry. This analysis showed that Igs from intestinal ME-M B cells, but not from naive B cells, specifically recognize microbes from human intestinal mucus (Fig. 22).

Altogether, these data indicate that intestinal ME-M B cells exhibit some phenotypic traits and antibody reactivity similar to those of splenic MZ B cells, with whom they share the expression of a reduced number of genes. On the other hand, intestinal ME-M B cells show a GC-like Ig gene mutation profile and a transcriptional signature reflecting affiliation to gut but not splenic memory B cells, and specifically recognize microbiota from human intestinal mucus.

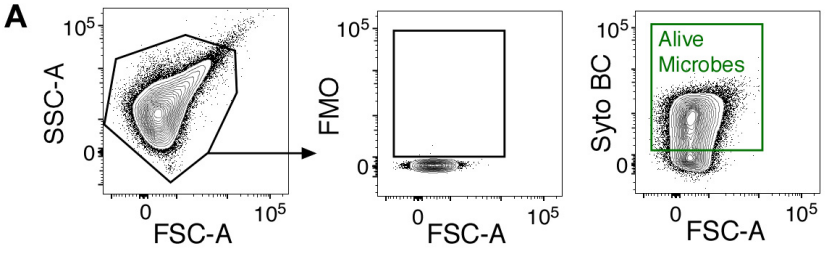

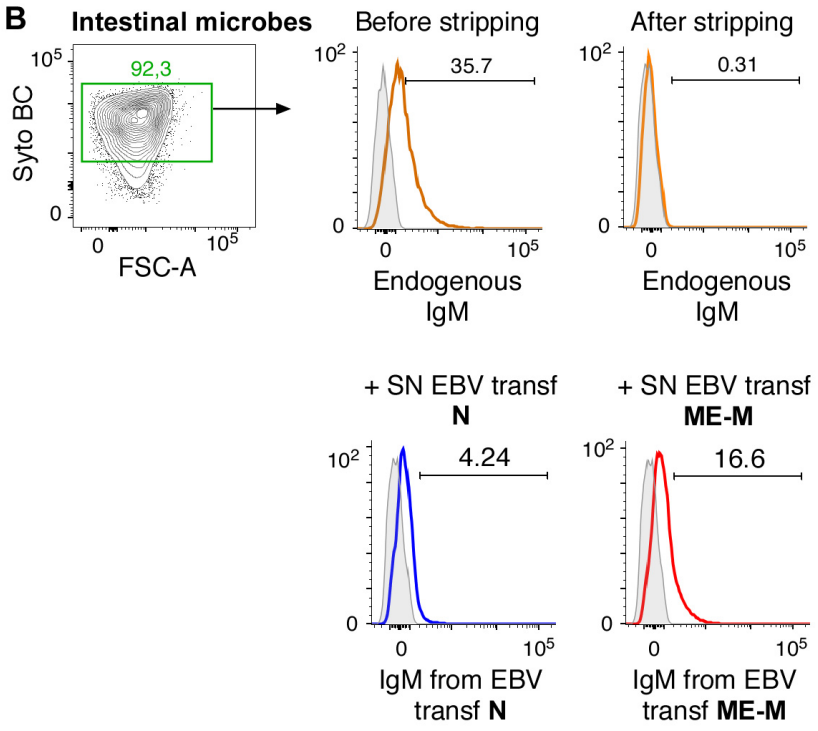

Figure 22. Antibodies from intestinal ME-M B cells specifically recognize microbes from human intestinal mucus. (A) Flow cytometry of intestinal microbes stained for the nucleic acid stain SytoBC. (B) Flow cytometry of intestinal microbes stained for SytoBC and IgM, before (upper center) and after (upper right) performing an endogenous Ig stripping protocol, and incubation with the Ig enriched SN of EBV transformed intestinal N (bottom left), and ME-M (bottom right) B cells. Green numbers and highlighted areas refer to viable microbes. Numbers in overlay graphs indicate percentages. SSC-A, side scatter area; FSC-A, forward scatter area; FMO, fluorescence minus one; EBV, Epstein-Barr virus; SN, supernatant; N, naïve; ME-M, IgM^+ memory B cells.

ME-M B cells respond to TD and TI stimuli *in vitro* by proliferating and generating preferentially IgM^+ but also IgA^+/IgG^+ PBs

By definition, memory B cells are quiescent cells that upon reencounter with cognate antigen and activation though TD or TI mechanisms are able to proliferate and differentiate into antibody secreting PBs[329,330].

Stimuli involved in TD activation of B cells include CD40L, IL-21 and IL-10. The engagement of CD40L on T cells with CD40 on B cells induces proliferation, CSR and antibody secretion, and is involved in the development of GCs and the survival of memory B cells[331,332]. IL-21 is considered a growth and differentiation factor for CD40-stimulated human B cells, by inducing robust B cell proliferation, AID expression and CSR as well as PC differentiation and antibody production[268]. Finally, IL-10 stimulates replication of B cells activated through either CD40 or the BCR, and promotes survival, CSR and Ig secretion[272].

On the other hand, some of the stimuli involved in TI activation of B cells include CpG, IL-10, BAFF and APRIL. Unmethylated CpG oligodeoxynucleotides are equivalent to microbial hypomethylated DNA. CpG interacts with TLR9 expressed on human B cells, and induces proliferation of memory B cells and Ig production[333,334]. Additionally, BAFF and APRIL are released by cells of the innate immune system in response to microbial signals from TLRs, and are the ligands for B cell maturation antigen (BCMA) and TNF receptor homolog TACI, expressed on B cells. BAFF and APRIL promote proliferation, differentiation, Ig production and survival of B cells[335,336].

In order to test the responsiveness of intestinal ME-M B cells and their ability to respond to TD and TI stimuli, we performed a functional in vitro

assay with sorted and CFSE labeled intestinal N and ME-M B cells upon culture without stimuli (NIL) or upon TD (CD40L + IL-21 + IL-10) or TI (CpG + IL-10 or CpG + IL-10 + BAFF + APRIL) stimuli. After 5 days of culture, TD stimuli induced strong proliferation both in N and ME-M B cells, whereas TI stimuli induced proliferation mostly in ME-M B cells, specially with the condition including BAFF and APRIL, which most probably provided survival signals (Fig. 23 A, B).

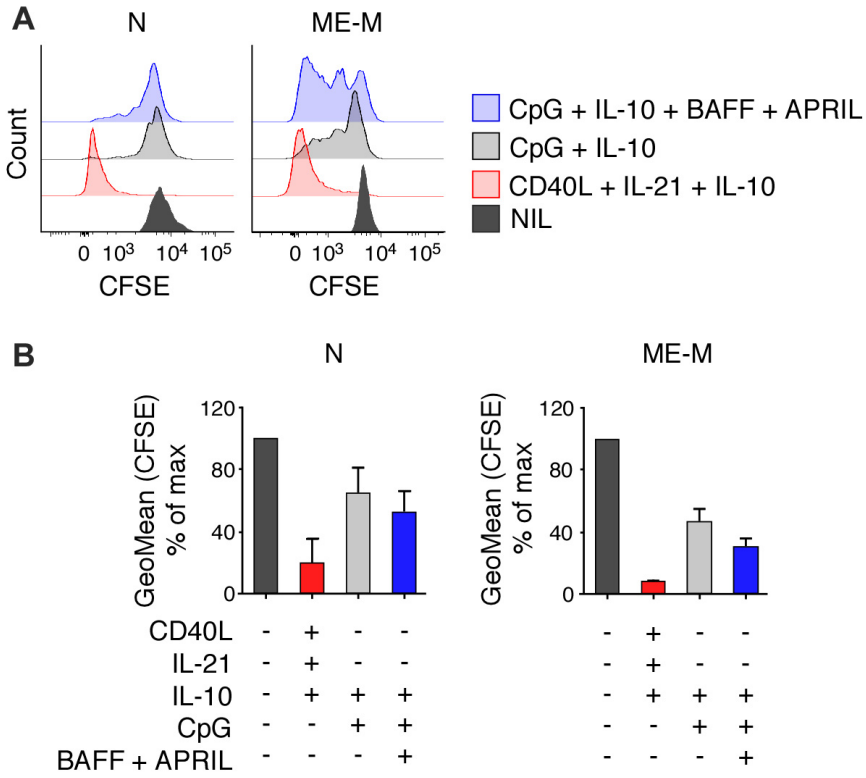

Figure 23. Intestinal ME-M B cells proliferate in response to TD and TI stimuli *in vitro*. (A) Flow cytometric analysis of the CFSE proliferation profile of sorted intestinal N and ME-M B cells cultured for 5 days with medium alone (black), CD40L, IL-21 and IL-10 (red), CpG and IL-10 (grey) or CpG, IL-10, BAFF and APRIL (blue). (B) Profile of CFSE dilution in sorted intestinal N and ME-M B cells cultured for 5 days with medium alone (black), CD40L, IL-21 and IL-10 (red), CpG and IL-10 (grey) or CpG, IL-10, BAFF and APRIL (blue). CFSE, carboxyfluorescein succinimidyl ester; N, naïve; ME-M, IgM^+ memory B

cells; BAFF, B-cell activating factor; APRIL, A proliferation-inducing ligand; CD40L, CD40 ligand. Data shows one representative of two experiments with similar results (A) or includes two separate experiments (B), error bars represent s.e.m.

Additionally, naive B cells differentiated into $CD38^{high}CFSE^{low}$ PBs only upon TD stimuli, whereas ME-M B cells differentiated to PBs more robustly and upon both TD and TI stimuli (Fig. 24A). Importantly, a small fraction of the PBs emerging from ME-M B cells, but not from naive B cells, were identified as IgA^{+} class switched PBs (Fig. 24B).

Then, the capacity of ME-M B cells to undergo CSR in vitro upon TD and TI stimuli was confirmed through the detection by ELISA of large amounts of IgM, but also IgA and IgG in culture supernatans (Fig. 25).

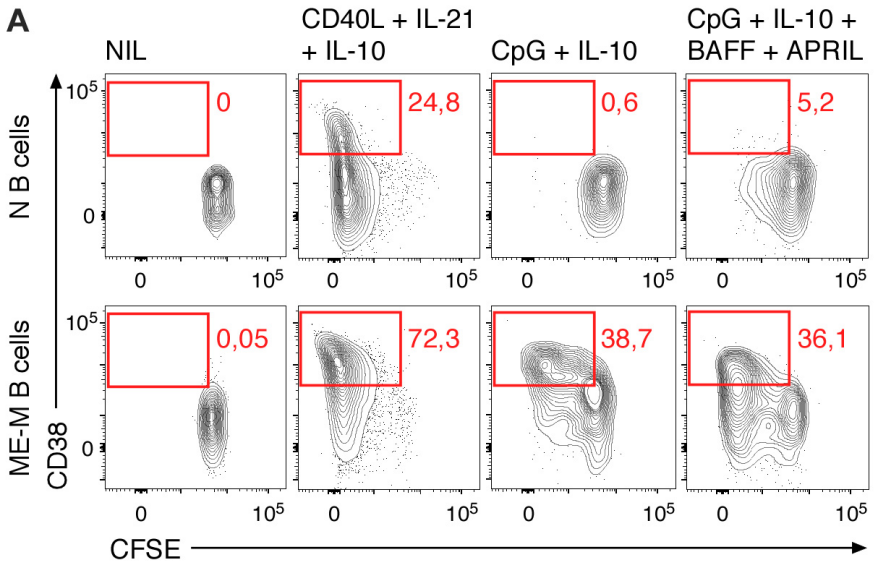

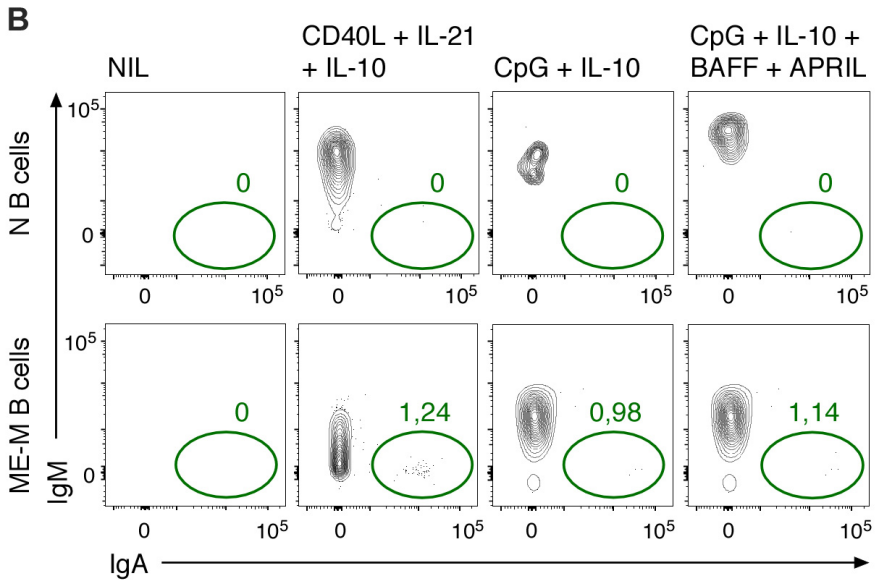

Figure 24. Human intestinal ME-M B cells differentiate to PBs in vitro upon TD and TI stimulation and have the capacity to undergo CSR *in vitro*. (A) Flow cytometric analysis of CFSE and CD38 on intestinal N and ME-M B cells cultured for 5 days with medium alone (NIL), CD40L, IL-21 and IL-10, CpG and IL-10 or CpG, IL-10, BAFF and APRIL (above plots). Numbers next to outlined red areas indicate percentage of $CD38^{hi}CFSE^{low}$ PBs. (B) Flow cytometric analysis of the expression of IgM and IgA on the surface of newly formed $CD38^{hi}CFSE^{low}$ PBs from intestinal N and ME-M B cells cultured for 5 days with medium alone (NIL), CD40L, IL-21 and IL-10, CpG and IL-10 or CpG, IL-10, BAFF and APRIL (above plots). Numbers next to outlined green areas indicate percentage of IgA^+ PBs. CSR, class switch recombination; N, naïve; ME-M, IgM^+ memory B cells; PB, plasmablast; BAFF, B-cell activating factor; APRIL, A proliferation-inducing ligand; CD40L, CD40 ligand. Data shows representatives of two experiments with similar results (A, B).

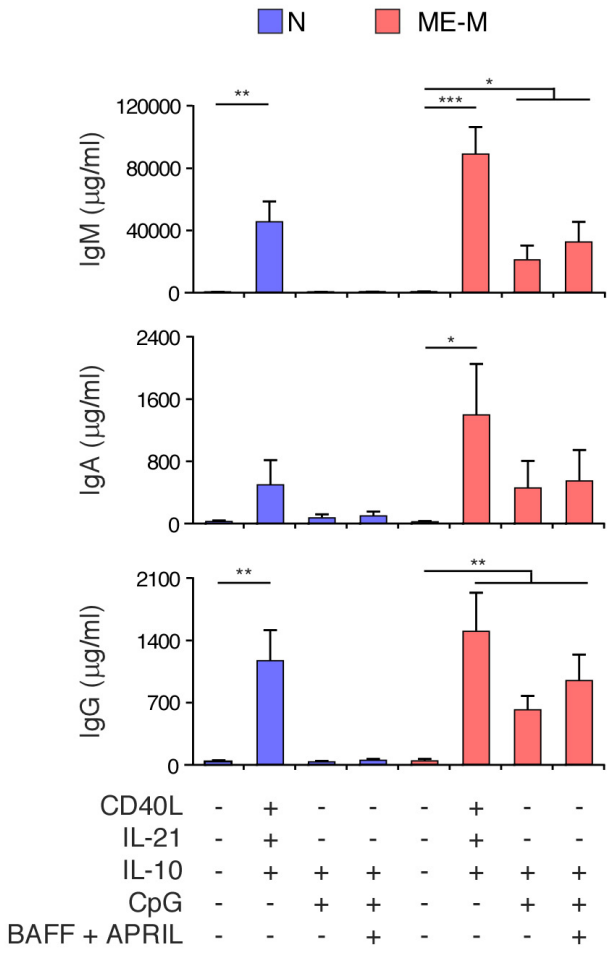

Figure 25. PBs generated from ME-M B cells in response to TD and TI stimuli, secrete IgM, IgA and IgG. ELISA of IgM, IgA and IgG from supernatants of intestinal N and ME-M B cells cultured for 5 days with medium alone, CD40L, IL-21 and IL-10, CpG and IL-10 or CpG, IL-10, BAFF and APRIL (below graph). N, naïve; ME-M, IgM^+ memory B cells; BAFF, B-cell activating factor; APRIL, A proliferation-inducing ligand; CD40L, CD40 ligand. Error bars represent s.e.m; **P* < 0.05, **P<0,01, ***P<0,001 (two-tailed unpaired Student's *t*-test). Data includes two different experiments.

Given that FcRL4 is an inhibitory receptor expressed on activated human memory B cells in mucosal tissues[322,323], and that we had shown a subset

of ME-M B cells expressing this receptor (Fig. 14), we sorted FcRL4$^-$ and FcRL4$^+$ ME-M B cells from terminal ileum and cultured them for 5 days with or without TD stimuli. Although both subsets strongly differentiated to PBs, FcRL4$^+$ ME-M B cells underwent CSR to IgA more efficiently than their FcRL4$^-$ counterpart. Moreover, whereas the reduced number of class switched cells from the FcRL4$^-$ population were all IgA1, FcRL4$^+$ ME-M B cells generated both IgA1$^+$ and IgA2$^+$ cells (Fig. 26A). Analysis of AID (*AICDA*) gene expression by quantitative RT-PCR showed that FcRL4$^+$ ME-M B cells had higher AID expression than both N and FcRL4$^-$ ME-M B cells (Fig. 26B).

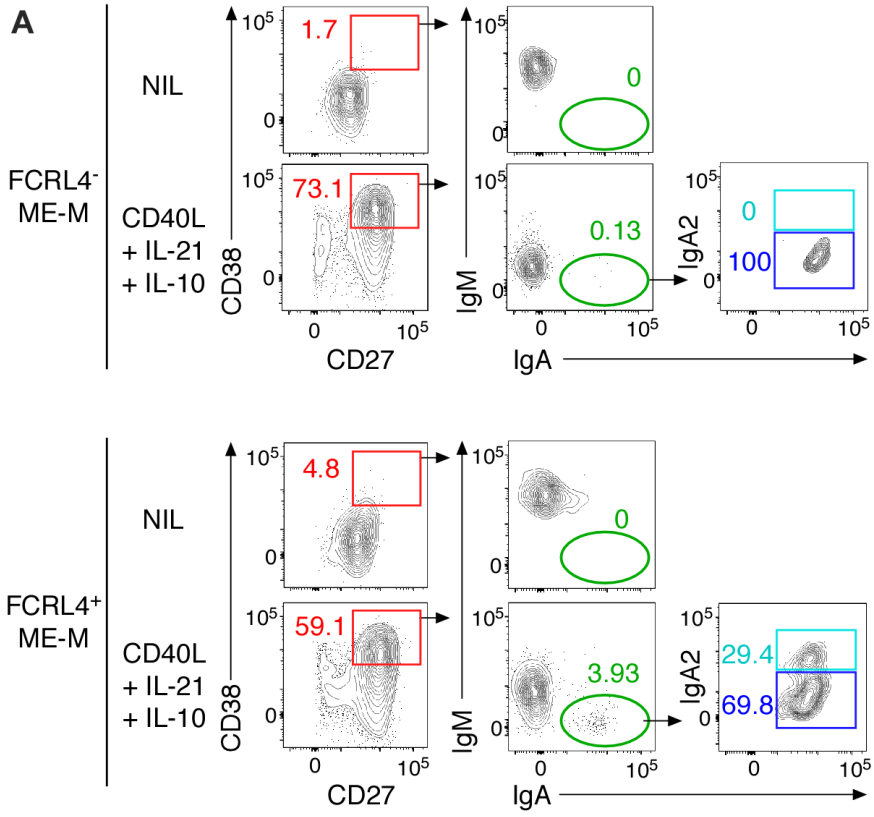

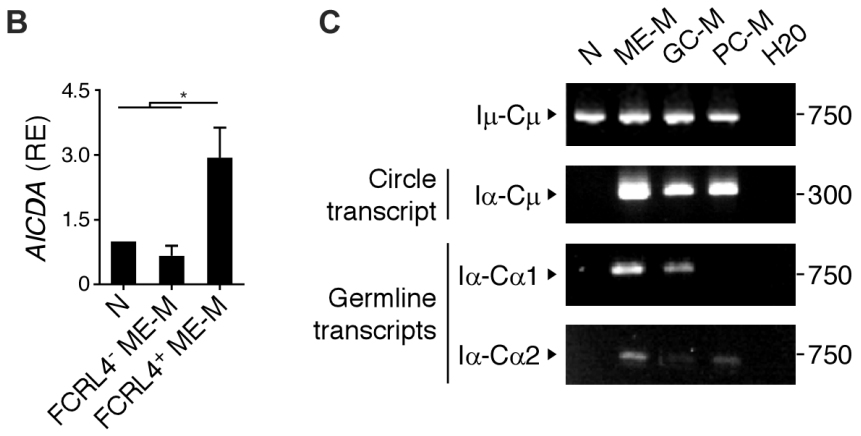


```
CLUSTAL O(1.2.1) multiple sequence alignment

ME-M          CTCAGCACTG-GGGCCCTCCAGCAGCCTGACCAGGGAGTGCATCCGCCCCAACCCTTT
GC            CTCAGCACTGCGGGCCCTCCAGCAGCCTGACCAGGGAGTGCATCCGCCCCAACCCTTT
Iα/Cμ         CTCAGCACTGCGGGCCCTCCAGCAGCCTGACCAGGGAGTGCATCCGCCCCAACCCTTT
              ********** **************************************************

ME-M        TCCCCCTCGTCTCCTGTGAGAATTCCCCGTCGGATACGAGCAGCGTGGCCGTTGGCTGCC
GC          TCCCCCTCGTCTCCTGTGAGAATTCCCCGTCGGATACGAGCAGCGTGGCCGTTGGCTGCC
Iα/Cμ       TCCCCCTCGTCTCCTGTGAGAATTCCCCGTCGGATACGAGCAGCGTGGCCGTTGGCTGCC
            ************************************************************

ME-M        TCGCACAGGACTTCCTTCCCGACTCCATCACTTTCTCCTGGAAATACAAGAACAACTCTG
GC          TCGCACAGGACTTCCTTCCCGACTCCATCACTTTCTCCTGGAAATACAAGAACAACTCTG
Iα/Cμ       TCGCACAGGACTTCCTTCCCGACTCCATCACTTTCTCCTGGAAATACAAGAACAACTCTG
            ************************************************************

ME-M        ACATCAGCAGCACCCGGGGCTTCCCATCAGTCCTGAGAGGGGGCAAGTACGCAGCCACCT
GC          ACATCAGCAGCACCCGGGGCTTCCCATCAGTCCTGAGAGGGGGCAAGTACGCAGCCACCT
Iα/Cμ       ACATCAGCAGCACCCGGGGCTTCCCATCAGTCCTGAGAGGGGGCAAGTACGCAGCCACCT
            ************************************************************

ME-M        CACAGGTGCTGCTGCCTTCCAAGGACGTCATGCAGGGCACAGACGAA-ACGTGGTGTG
GC          CACAGGTGCTGCTGCCTTCCAAGGACGTCATGCAGGGCACAGACGA-CACGTGGTGTG
Iα/Cμ       CACAGGTGCTGCTGCCTTCCAAGGACGTCATGCAGGGCACAGACGAACACGTGGTGTG
            ********************************************  **********
```

Iα primer (reverse complement)
Cμ primer (reverse complement)
Joint

Figure 26. FcRL4^{+} ME-M B cells have an increased capacity to undergo CSR to IgA. (A) Flow cytometric analysis of sorted intestinal FcRL4^{-} ME-M B cells

(top panel) and FcRL4$^+$ ME-M B cells (bottom panel) cultured for 5 days with medium alone (NIL, top row) or with CD40L, IL-21 and IL-10 (bottom row) stained for CD38, CD27, IgM, IgA and IgA2. Numbers in red next to outlined red areas indicate percentage of CD27^{hi}CD38^{hi} PBs. Numbers in green above outlined green areas indicate percentage of IgA$^+$ class-switched PBs. Numbers in blue next to outlined blue areas indicate percentage of IgA$^+$ PBs expressing IgA1 (dark blue) or IgA2 (light blue). (B) Quantitative RT-PCR analysis of mRNA encoding AID (*AICDA*) in sorted intestinal N, FcRL4$^-$ ME-M and FcRL4$^+$ ME-M B cells; results are normalized to those of mRNA encoding β-actin (*ACTB*) and presented as relative expression (RE) compared with that on N B cells, set as 1. (C) PCR of μ GLT (Iμ-Cμ), α switch circle transcript (Iα-Cμ) and α GLT (Iα-Cα1, Iα-Cα2) in N, ME-M, GC-M and PC-M. (D) Multiple sequence alignment of the α switch circle transcript (Iα-Cμ) PCR products from ME-M and GC B cells from ileum and their reference sequence. FcRL4, Fc Receptor-Like 4; CD40L, CD40 ligand. PCR, polymerase chain reaction; N, naïve; ME-M, IgM$^+$ memory B cells; GC-M, IgM$^+$ germinal center B cells; PB, plasmablast; PC-M, IgM$^+$ plasma cells; GLT, germline transcript. Error bars represent s.e.m; **P* < 0.05 (two-tailed unpaired Student's *t*-test). Data includes at least three different experiments (B).

Activation of B cells with IgA CSR inducing signals induces both AID expression and germline transcription of the Cμ and Cα genes[69]. This produces Iμ-Cμ and Iα-Cα germline transcripts (GLT) that associate with the template DNA strand of the targeted switch region and renders the Cμ and Cα genes substrate for AID. The subsequent DNA recombination process involves the excision of the noncoding intervening DNA and rearrangement of the IgH locus by replacement of Cμ with a downstream Cα gene. The excised circular DNA contains the I-promoter that is still active and directs the production of Iα-Cμ circle transcripts (CT), which are rapidly degraded[69]. Because of this, detection of CT is the most reliable method to demonstrate ongoing CSR in B cells.

After proving that ME-M B cells are able to undergo CSR *in vitro*, we wanted to assess whether there was ongoing CSR in our sorted intestinal ME-M B cell population. PCR amplification of Iα-Cμ CT, as well as Iμ-Cμ, Iα-Cα1 and Iα-Cα2 GLT cDNA in sorted naive, ME-M, GC-M and

PC-M showed a strong amplification of Iα-Cμ CT in ME-M, GC-M and PC-M, but not in naive B cells, confirming that some fractions of these B cell populations were undergoing active CSR (Figure 26C, D). Additionally, Iα-Cα1 GLT were amplified in ME-M and GC-M, indicating the induction of IgA1 CSR in these cellular subsets, and Iα-Cα2 GLT in ME-M and PC-M, pointing to the induction of IgA2 CSR. Iμ-Cμ GLTs were used as controls (Figure 26C). These data confirmed that intestinal ME-M B cells undergo CSR to both IgA1 and IgA2, as seen in the previous functional *in vitro* experiment, and that they preferentially undergo CSR to IgA1. Of note, GC-M B cells seem to class switch to IgA1 and PC-M to IgA2, although these findings varied amongst the different samples studied.

Finally, we wondered whether the ongoing DNA CSR detected in a fraction of these cells would translate into appropriate cell-surface protein expression. By performing flow cytometry of IgA1 and IgA2 in IgM^+ N and ME-M B cells, as well as in ME-SW, GC B cells and PB-PC, we detected a subset of cells co-expressing IgM and IgA1 on their surface, wich is usually interpreted as recent CSR, in the fraction of N and ME-M B cells. Of note, we also detected a small subset of ME-SW B cells co-expressing IgA1 and IgA2 in their surface, probably indicating sequential class switching from IgA1 to IgA2 (Fig. 27).

Collectively, these experiments indicate that human intestinal ME-M B cells respond to TD as well as TI stimuli by proliferating and differentiating into PBs, secreting IgM as well as IgA and IgG. Moreover, $FCRL4^+$ ME-M B cells have an increased capacity to undergo CSR to IgA, and at least a fraction of ME-M B cells is able to undergo CSR to IgA1 or IgA2 in the human gut.

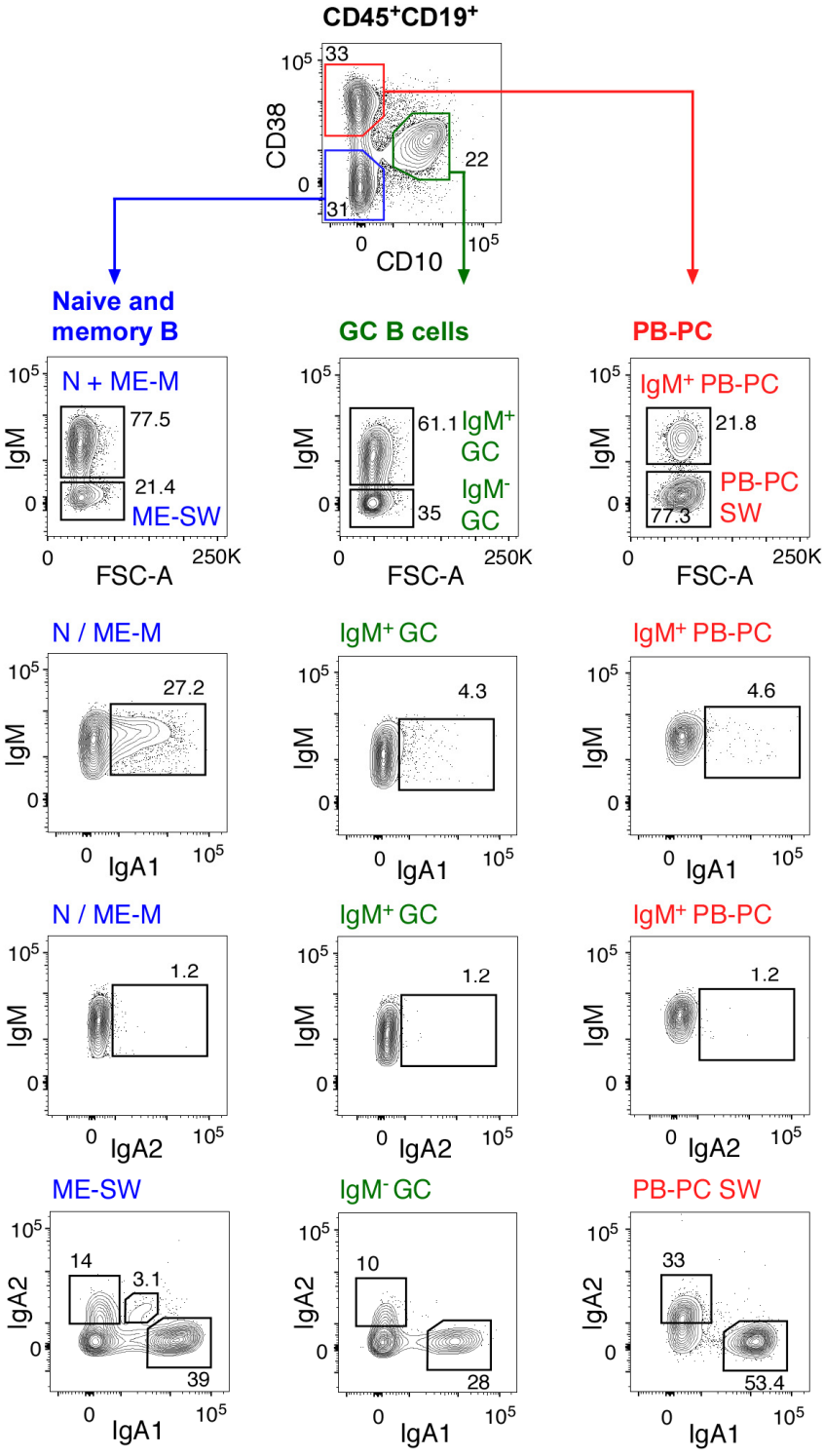
CD45+CD19+
CD38
CD10
33
22
31
Naive and memory B
GC B cells
PB-PC
N + ME-M
77.5
21.4
ME-SW
61.1
IgM+ GC
35
IgM- GC
IgM+ PB-PC
21.8
PB-PC SW
77.3
IgM
FSC-A
250K
N / ME-M
27.2
IgM+ GC
4.3
IgM+ PB-PC
4.6
IgA1
1.2
IgA2
ME-SW
14
3.1
39
IgM- GC
10
28
PB-PC SW
33
53.4

Figure 27. Human intestinal ME-M B cells preferentially class switch to IgA1. Flow cytometry of viable ($DAPI^-$) $CD45^+CD19^+$ intestinal lymphocytes stained for CD38, CD10, IgM, IgA1 and IgA2. Numbers adjacent to outlined areas indicate percentage of cells. Blue gate and captions refer to N and ME B cell populations. Green gate and captions refer to GC B cells. Red gate and captions refer to PB-PC populations. FSC-A, forward scatter area: N, naive; ME, memory B cells; ME-M, IgM^+ memory; ME-SW, switched memory; GC, germinal center; PB, plasmablast; PC, plasma cell; PB-PC SW, switched PB-PC.

A subset of ME-M B cells is clonally related to IgM^+ and IgA^+ PCs from ileum and colon

Once proved that ME-M B cells differentiate to PBs and that a fraction of them undergo CSR to IgA, we wanted to characterize the clonal architecture of ME-M B cells as well as their ontogenetic relationship with ME-SW B cells and PC expressing IgM or IgA. To this end, we performed high-throughput Ig repertoire analysis of sorted intestinal ME-M, ME-A, PC-M and PC-A from ileum and colon of 4 donors.

Analysis of relationships between clonal families revealed that the majority of the clonal families from human ileal ME-M B cells were unrelated to other B cell subsets, whereas the remaining 20% of clonal families were either related to PC-M or to switched ME B cells and PCs (Fig. 28A). In PC-M the proportion of unrelated clonal families varied between the four individuals studied, whereas in ME-A and PC-A the proportion of unrelated clonal families was smaller than in ME-M B cells.

Looking into the clonal families that include different populations, analysis of clonal relationships between ME-M and ME and PC from ileum indicated that a subset of ME-M B cells was clonally related to PC-M, ME-A and PC-A (Fig. 28B).

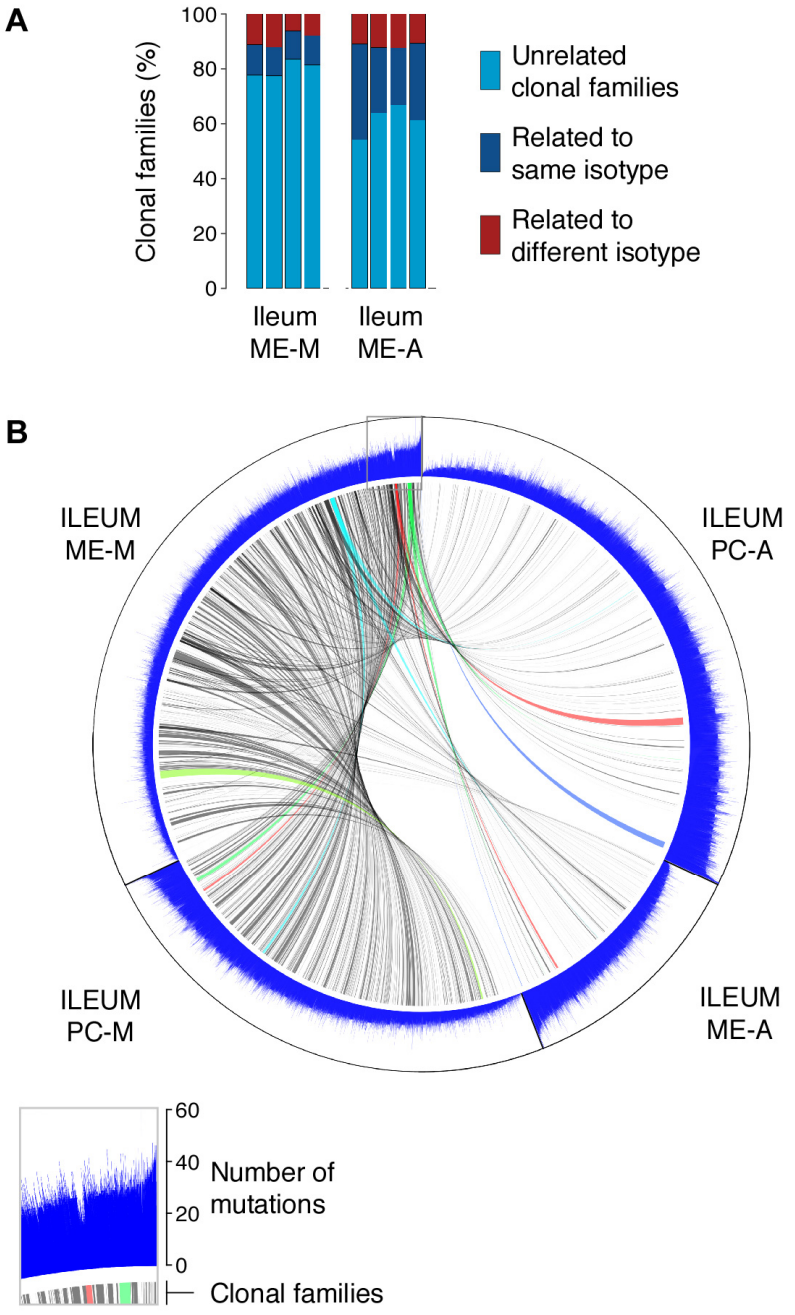

Figure 28. A subset of ileal ME-M B cells is clonally related to PC-M, ME-A and PC-A. (A) Proportion of clonal families in ME-M and ME-A B cell subsets from ileum, either unrelated to other clonal families, or related to different cell types of the same or different isotype. (B) Circos plot representing SHM and

clonal relationships for ileal ME-M, ME-A, PC-M and PC-A populations from one representative of four donors. The outer track illustrates the number of mutations per sequence. The inner space illustrates clonal relationships between populations for the ME-M B cell subset. The five biggest clonal families are shown in different colors.

Regarding ME-M B cells from ileum, four out of the five biggest clonal families with clonal relationships between populations were found amongst the clonal families with higher number of mutations and were related to highly mutated sequences in ME-A, PC-M and/or PC-A. On the other hand, one of the five biggest clonal families with clonal relationships between populations was found amongst the clonal families with low number of mutations and was only related to low mutated PC-M. Although some of the biggest clonal families in ME-M B cells were clonally related to switched ME or PCs, it is important to note that ME-M B cells were much more often related to PC-M than to the other B cell subsets (Fig. 28B).

When analyzing clonal relationships between cellular subsets in ileum and colon, we found that the majority of clonal families of ileal ME-M B cells were only found in the ileum, whereas 10 to 20% of the clonal families could be found in different subsets from ileum and colon (Fig. 29A). Further analysis of clonal relationships between ileal ME-M and ileal PC-M, colonic ME-M and colonic PC-M, indicated that a subset of ME-M B cells from ileum was clonally related to B cell subsets both in ileum and colon, pointing to the ability of these cells to recirculate between tissues (Fig. 29B). This time, regarding ME-M B cells from ileum, five out of the eight biggest clonal families with clonal relationships between populations were found amongst the clonal families with higher number of mutations and were related to highly mutated sequences in the rest of populations. On the other hand, three out of the eight biggest clonal families with

clonal relationships between populations were found amongst the clonal families with medium or low number of mutations and were related to low or medium mutated cellular subsets in both tissues (Fig. 29B).

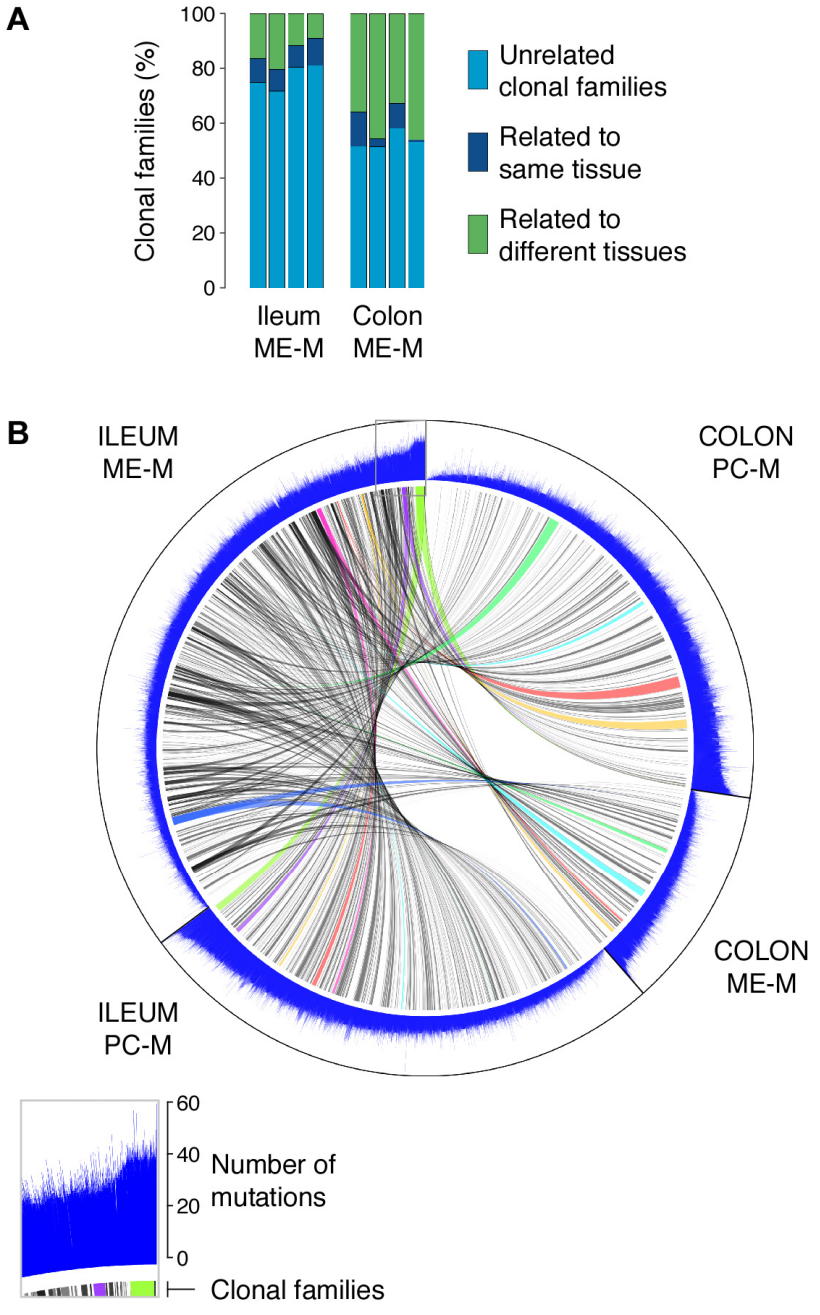

Figure 29. A subset of ileal ME-M B cells is clonally related to colonic ME-M and PC-M, suggesting dissemination between tissues. (A) Proportion of clonal families in ME-M B cells from ileum and colon, either unrelated to other clonal families, or related to different cell types of the same or different isotype. (B) Circos plot representing SHM and clonal relationships for ME-M and PC-M from ileum and ME-M and PC-M from colon, from one representative of four donors. The outer track illustrates the number of mutations per sequence. The inner space illustrates relationships between populations for the ME-M B cell subset from ileum. The eight biggest clonal families are shown in different colors.

As an illustration of these clonal relationships between cellular types and tissues, we identified one clonal family including sequences from colonic ME-M and PC-A with identical VDJ region, with different isotype but without accumulated mutations (Fig. 30A); another clonal family including sequences from ileal ME-M and ME-A showing accumulated mutations in the VDJ region, evidencing SHM and CSR (Fig. 30B); and one clonal family including sequences from two ME-M B cells from ileum and two PC-A from colon showing accumulated mutations in the VDJ region, thus evidencing SHM, CSR, PC differentiation and tissue dissemination (Fig. 30C).

As a summary, human ME-M B cells undergo PC differentiation and disseminate between ileum and colon. Moreover, a subset of ME-M B cells can undergo CSR to IgA with or without accumulating mutations.

A

```
CLUSTAL O(1.2.1) multiple sequence alignment


GERMLINE IGHV3-21 IGHJ5  GAGGTGCAGCTGGTGGAGTCTGGGGGAGGCCTGGTCAAGCCTGGGGGGTCCCTGAGACTC
Memory M - Colon         ------------------------------------------------------------
Plasma Cell A - Colon    ------------------------------------------------------------


GERMLINE IGHV3-21 IGHJ5  TCCTGTGCAGCCTCTGGATTCACCTTCAGTAGCTATAGCATGAACTGGGTCCGCCAGGCT
Memory M - Colon         ------GCAGCCTCTGGATTCACCTTCAGTAGCTATAGCATGAACTGGGTCCGCCAGGCT
Plasma Cell A - Colon    ------GCAGCCTCTGGATTCACCTTCAGTAGCTATAGCATGAACTGGGTCCGCCAGGCT
                               ************************************************************


GERMLINE IGHV3-21 IGHJ5  CCAGGGAAGGGGCTGGAGTGGGTCTCATCCATTAGTAGTAGTAGTAGTTACATATACTAC
Memory M - Colon         CCAGGGAAGGGGCTGGAGTGGGTCTCATCCATTAGTAGTAGTAGTAGTTACATATACTAC
Plasma Cell A - Colon    CCAGGGAAGGGGCTGGAGTGGGTCTCATCCATTAGTAGTAGTAGTAGTTACATATACTAC
                         ************************************************************


GERMLINE IGHV3-21 IGHJ5  GCAGACTCAGTGAAGGGCCGATTCACCATCTCCAGAGACAACGCCAAGAACTCACTGTAT
Memory M - Colon         GCAGACTCAGTGAAGGGCCGATTCACCATCTCCAGAGACAACGCCAAGAACTCACTGTAT
Plasma Cell A - Colon    GCAGACTCAGTGAAGGGCCGATTCACCATCTCCAGAGACAACGCCAAGAACTCACTGTAT
                         ************************************************************


GERMLINE IGHV3-21 IGHJ5  CTGCAAATGAACAGCCTGAGAGCCGAGGACACGGCTGTGTATTACTGTGCGAGAGANNNN
Memory M - Colon         CTGCAAATGAACAGCCTGAGAGCCGAGGACACGGCTGTGTATTACTGTGCGAGAGATGCA
Plasma Cell A - Colon    CTGCAAATGAACAGCCTGAGAGCCGAGGACACGGCTGTGTATTACTGTGCGAGAGATGCA
                         ************************************************************


GERMLINE IGHV3-21 IGHJ5  NNNNNNNNNNNNNNNNNNNNTTCGACCCCTGGGGCCAGGGAACCCTGGTCACCGTCTCC
Memory M - Colon         AGTGAACTGCCCAAGTCTCCTTTCGACCCCTGGGGCCAGGGAACCCTGGTCACCGTCTCC
Plasma Cell A - Colon    AGTGAACTGCCCAAGTCTCCTTTCGACCCCTGGGGCCAGGGAACCCTGGTCACCGTCTCC
                                              ****************************************


GERMLINE IGHV3-21 IGHJ5  TCAG----------------------------------------
Memory M - Colon         TCAGGGAGTGCATCCGCCCCAACCCTTTTCCCCCTCGTCTCCTG
Plasma Cell A - Colon    TCAGCATCCCCGACCAGCCCCAAGGTCTTC--------------
                         ****
```

CDR regions
IgM primer
IgA primer
(reverse complement)

B

```
CLUSTAL O(1.2.1) multiple sequence alignment

GERMLINE IGHV3-7 IGHJ4    TCCTGTGCAGCCTCTGGATTCACCTTTAGTAGCTATTGGATGAGCTGGGTCCGCCAGGCT
Memory M - Ileum          ------GCAGCCTCCGGATTCACATTTAGTAATTATTACATGAAGTGGGCCCGCCAGACT
Memory A - Ileum          ------GCAGCCTCCGGATTCACATTTGGTAATTATTACATGAAGTGGGCCCGCCAGACT
                                ******** ******** *** ***  ****  ****  **** ******* **

GERMLINE IGHV3-7 IGHJ4    CCAGGGAAGGGGCTGGAGTGGGTGGCCAACATAAAGCAAGATGGAAGTGAGAAATACTAT
Memory M - Ileum          CCAGAGAAGGGGCTGGAGTGGGTGGCCGACATAAATCATGATGGAAGTGAGACATCCTAT
Memory A - Ileum          CCAGAGAAGGGGCTGGAGTGGGTGGCCGACATAAATCCTGATGGAAGTAGGACAGCCTAT
                          **** ********************** ******* *  *********  ** *  ****

GERMLINE IGHV3-7 IGHJ4    GTGGACTCTGTGAAGGGCCGATTCACCATCTCCAGAGACAACGCCAAGAACTCACTGTAT
Memory M - Ileum          GTGGACTCTGTGAATGGCCGATTCACCATCTCCAGAGACAACGCCAAGAACTCACTGTAT
Memory A - Ileum          CTGGACTCTGTGAATGGCCGATTCACCATCTCCAGAGACAACGCCAAGAACTCACTCTTT
                           ************* ****************************************** * *

GERMLINE IGHV3-7 IGHJ4    CTGCAAATGAACAGCCTGAGAGCCGAGGACACGGCCGTGTATTACTGTGNNNNNNNNNN
Memory M - Ileum          TTACAAATGAACAGCCTGAGAGCCGAGGACACGGCCGTGTATTACTGTGTGTTGCACACG
Memory A - Ileum          TTACACATGAACAGCCTGAGAGCCGAGGACACGGCCGTGTATTATTGTGTGTTGCACACG
                           * ** ************************************* ****

GERMLINE IGHV3-7 IGHJ4    NNNNNNNNNNNNNTTGACTACTGGGGCCAGGGAACCCTGGTCACCGTCTCCTCAG-----
Memory M - Ileum          AGGGGGACTTCAATTGATTACTGGGGCCAGGGAACCCTGGTCACCGTCTCCTCAGGGAGT
Memory A - Ileum          AGGGGGACTTCATTTGATTACTGGGGCCAGGGAACCCTGCTCACCGTCTCCTCAGCATCC
                                    **** ********************** ***************

GERMLINE IGHV3-7 IGHJ4    -----------------------------------
Memory M - Ileum          GCATCCGCCCCAACCCTTTTCCCCCTCGTCTCCTG
Memory A - Ileum          CCGACCAGCCCCAAGGTCTTC--------------
```

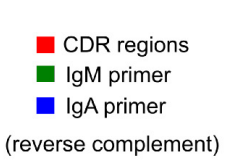

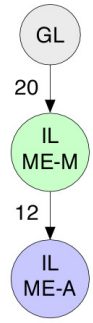

C

```
CLUSTAL O(1.2.1) multiple sequence alignment

GERMLINE IGHV3-72 IGHJ5    TCCTGTGCAGCCTCTGGATTCACCTTCAGTGACCACTACATGGACTGGGTCCGCCAGGCT
Memory M - Ileum           ------GCAACCTCTGGATTCACCTTCAGTGACGACAACATGGACTGGGTCCGCCAGGCT
Plasma Cell A - Colon      ------GCAACCTCTGGATTCACCTTCAGTGACGACAATATGGACTGGGTCCGCCAGGCT
Memory M - Ileum           ------GCAACCTCTGGATTCACCTTCAGTGACGACAACATGGACTGGGTCCGCCAGGCT
Plasma Cell A - Colon      ------GCAACCTCTGGATTCACCTTCAGTGACGACAACATGGACTGGGTCCGCCAGGCT
                                 *** ********************** ** * **********************

GERMLINE IGHV3-72 IGHJ5    CCAGGGAAGGGGCTGGAGTGGGTTGGCCGTACTAGAAACAAAGCTAACAGTTACACCACA
Memory M - Ileum           CCAGGGAAGGGACTGGAGTGGGTTGGCCGTACCAGAAACAAAGCTAACAGTTACACCACA
Plasma Cell A - Colon      CCAGGGAAGGGGCTGGAGTGGATTGGTCGTACTAGAAACAAAGCTAACAAATACACCACA
Memory M - Ileum           CCAGGGAAGGGACTGGAATGGGTTGGCCGTACCAGAAACAAAGCTAACAGTTACACCACA
Plasma Cell A - Colon      CCAGGGAAGGGACTGGAATGGGTTGGCCGTACCAGAAACAAGGCTAACAGTTACACCACA
                           *********** ***** *** **** ***** ******** *******  *********

GERMLINE IGHV3-72 IGHJ5    GAATACGCCGCGTCTGTGAAAGGCAGATTCACCATCTCAAGAGATGATTCAAAGAACTCA
Memory M - Ileum           GAATACGCCGCGTCTGTGAAAGGGAGATTCACCGTCGCAAGAGATGATTCAAAGAAGTCA
Plasma Cell A - Colon      GAATACGCCGCGTCTGTGAAAGGCAGATTCACCGTCGCAAGAGATGAGTCAAAGAAGTCA
Memory M - Ileum           GAATACGCCGCGTCTGTGAAAGGGAGATTCACCGTCGCAAGAGATGATTCAAAGAAGTCA
Plasma Cell A - Colon      GAATACGCCGCGTCTGTGAAAGGGAGATTCACCGTCGCAAGAGATGATTCAAAGAAGTCA
                           ********************** ********* ** ********** ******** ***

GERMLINE IGHV3-72 IGHJ5    CTGTATCTGCAAATGAACAGCCTGAAAACCGAGGACACGGCCGTGTATTACTGTGCTAGA
Memory M - Ileum           CTATATTTGCAAATGAACAGCCTGACAACCGAGGACACGGCCGTTTATTACTGTACTAGA
Plasma Cell A - Colon      TTTTATCTGCAAATGAACAGCCTGAAAACCGAGGACACGGCCGTTTATTACTGTACTAGA
Memory M - Ileum           CTATATTTGCAAATGAACAGCCTGACAACCGAGGACACGGCCGTTTATTACTGTACTAGA
Plasma Cell A - Colon      CTATATTTGCAAATGAACAGCCTGACAACCGAGGACACGGCCGTTTATTACTGTACTAGA
                            * *** ****************** ****************** ********* *****

GERMLINE IGHV3-72 IGHJ5    GNNNNNNNNNNNNNNNNNNNNNNNNNNNTGGGGCCAGGGAACCCTGGTCACCGTCTCC
Memory M - Ileum           GGGAGAATTGGGAGCGCCCCATGTGACAATTGGGGCCAGGGAACCCTGGTCACCGTCTCC
Plasma Cell A - Colon      GGGAGAATCGGGAGCGCCCCGTGTGACAATTGGGGCCAGGGAACTCTGGTCACCGTCTCC
Memory M - Ileum           GGGAGAATTGGGAGTGCCCCATGTGACAATTGGGGCCAGGGAACCCTGGTCACCGTCTCC
Plasma Cell A - Colon      GGGAGAATTGGGAGTGCCCCATGTGACAATTGGGGCCAGGGAACCCTGGTCACCGTCTCC
                           *                              ************** ***************

GERMLINE IGHV3-72 IGHJ5    TCAG----------------------------------------
Memory M - Ileum           TCAGGGAGTGCATCCGCCCCAACCCTTTTCCCCCTCGTCTCCTG
Plasma Cell A - Colon      TCAGCATCCCCGACCAGCCCCAAGGTCTTC--------------
Memory M - Ileum           TCAGGGAGTGCATCCGCCCCAACCCTTTTCCCCCTCGTCTCCTG
Plasma Cell A - Colon      TCAGCATCCCCGACCAGCCCCAAGGTCTTC--------------
                           ****
```

CDR regions
IgM primer
IgA primer
(reverse complement)

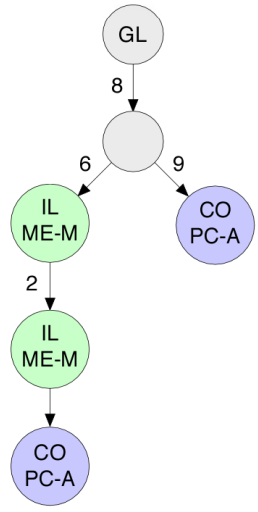

Figure 30. Human ME-M B cells are able to undergo PC differentiation and CSR to IgA with or without accumulating mutations. (A) Multiple sequence alignment of a colonic ME-M and PC-A clonal family and its germline sequence with identical VDJ region (no accumulated mutations). (B) Multiple sequence alignment and lineage tree of an ileal ME-M and ME-A clonal family and its germline sequence showing accumulated mutations in the VDJ region. (C) Multiple sequence alignment and lineage tree of an ileal ME-M and colonic PC-A clonal family and its germline sequence showing accumulated mutations in the VDJ region. Edges and numbers designate number of accumulated mutations along the lineage tree. CDR regions and primers are highlighted and color coded according to the legend. GL, germline sequence; ME-M, IgM^+ memory; ME-A, IgA^+ memory B cells; PC-M, IgM^+ plasma cells; PC-A, IgA^+ plasma cells.

The human intestinal mucosa harbors a significant proportion of PC-M, phenotypically similar to classical PC-A

Having demonstrated that ME-M B cells preferentially differentiate to PC-M in the human intestine, we next wanted to study human intestinal PC-M both in ileum and colon.

IFA of intestinal tissue sections including ILFs and LP from ileum and colon of patients of 1.5 months old, two years old and adult age, revealed that the human intestine harbors PC-M in the LP and around ILFs already at early life and throughout adulthood (Fig. 31A). Moreover, flow cytometric analysis of the ratio PC-M to PC-A also revealed that the proportion of PC-M in humans is higher in the ileum than in the colon, whereas the murine intestine showed a small proportion of PC-M (Fig. 31B).

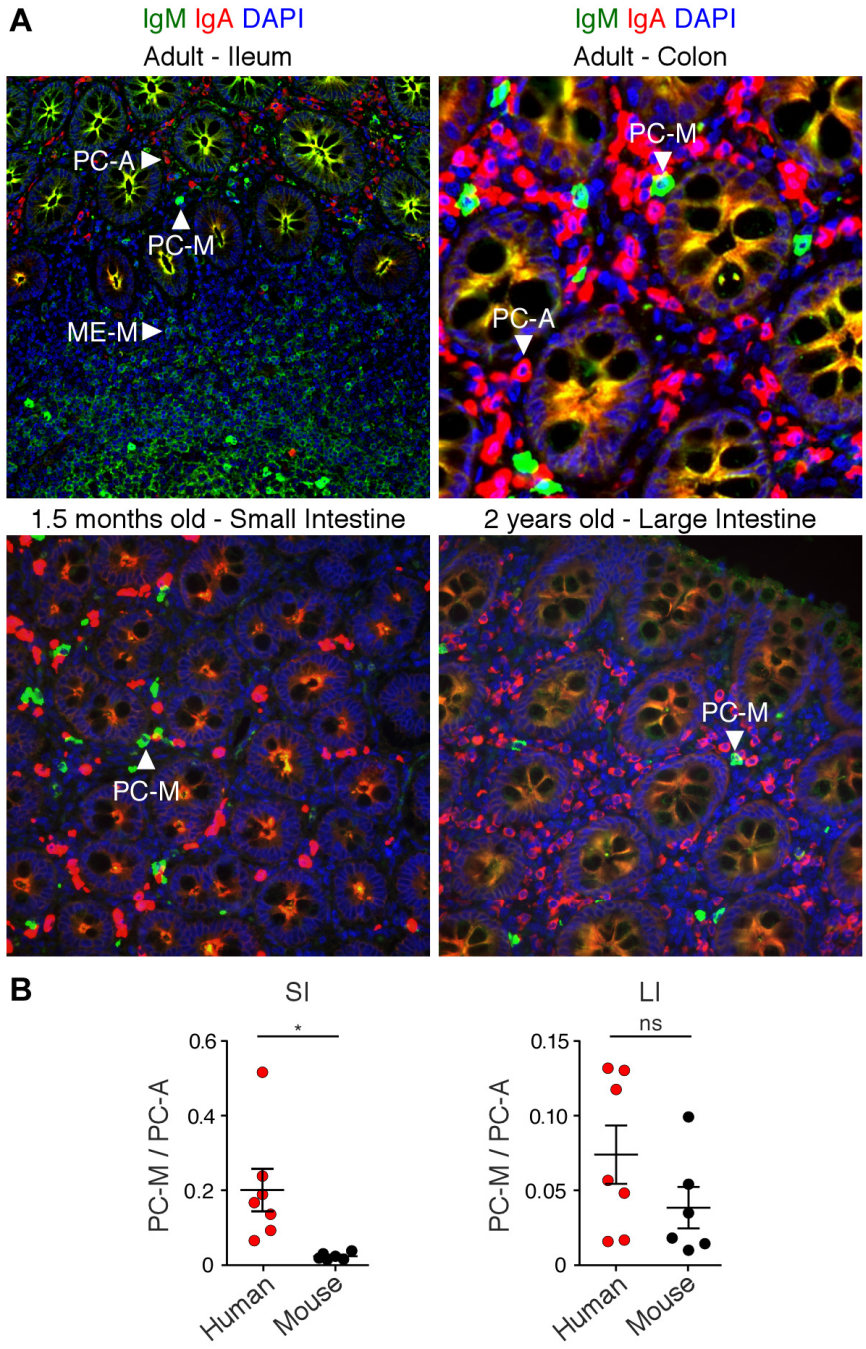

Figure 31. The human intestinal mucosa harbors a significant proportion of PC-M. (A) IFA of intestinal tissue sections including an area of LP close to a follicle (upper left) and sections of LP of an adult patient (upper right), a newborn

(1.5 months old, bottom left) and a two years old child (bottom right) stained for IgM (green), IgA (red) and DNA (with the DNA-binding dye DAPI; blue). Original magnification, 20X or 40X (upper right). (B) PC-M to PC-A ratio in human and mouse small intestine (left) and large intestine (right) by flow cytometry. IFA, immunofluorescence analysis; ME-M, IgM^+ memory B cell; PC-M, IgM^+ plasma cell; PC-A, IgA^+ plasma cell; SI, small intestine; LI, large intestine. Small horizontal lines indicate the mean (± s.e.m.); *P<0.05 (two-tailed unpaired Student's *t*-test). Data include 13 experiments (B).

IgM secreting cells are generally short lived PBs generated through an extrafollicular pathway before the GC formation[88]. We wanted to assess whether human intestinal PC-M had a phenotype comparable to PC-SW. Flow cytometric analysis showed that intestinal PC-M share phenotypic traits with PC-SW, which in the gut are mostly IgA^+ (Fig. 32A). Thus, PC-M expressed the gut homing chemokine receptors CCR9 and CCR10[337] and did not express CCR7 or CXCR4, confirming their localization in the LP. Moreover, PC-M did not express CD24, CD62L, HLA-DR or CD20, revealing a mature PC phenotype; and compared to PC-SW, expressed intermediate levels of CD138, considered to be a marker of terminal PC differentiation[338].

In addition, analysis of gene expression by quantitative RT-PCR revealed that intestinal PC-M displayed a phenotype comparable to PC-SW, with an abundant expression of BCMA (*TNFRSF17*), which recognizes BAFF and APRIL and is essential for the survival of PCs[339]; XBP1 (*XBP1*) that promotes Ig secretion[340]; and the transcription factor IRF4 (*IRF4*) that represses Bcl-6 and activates Blimp-1[341] (Fig. 32B).

However, compared to PC-SW, PC-M expressed lower levels of Bcl-2 (*BCL2*), TACI (*TNFRSF13B*) and the transcriptional repressor that promotes terminal differentiation of B cells Blimp-1 (*PRDM1*)[140],

suggesting a possible short lived phenotype or an enrichment of PBs in this population.

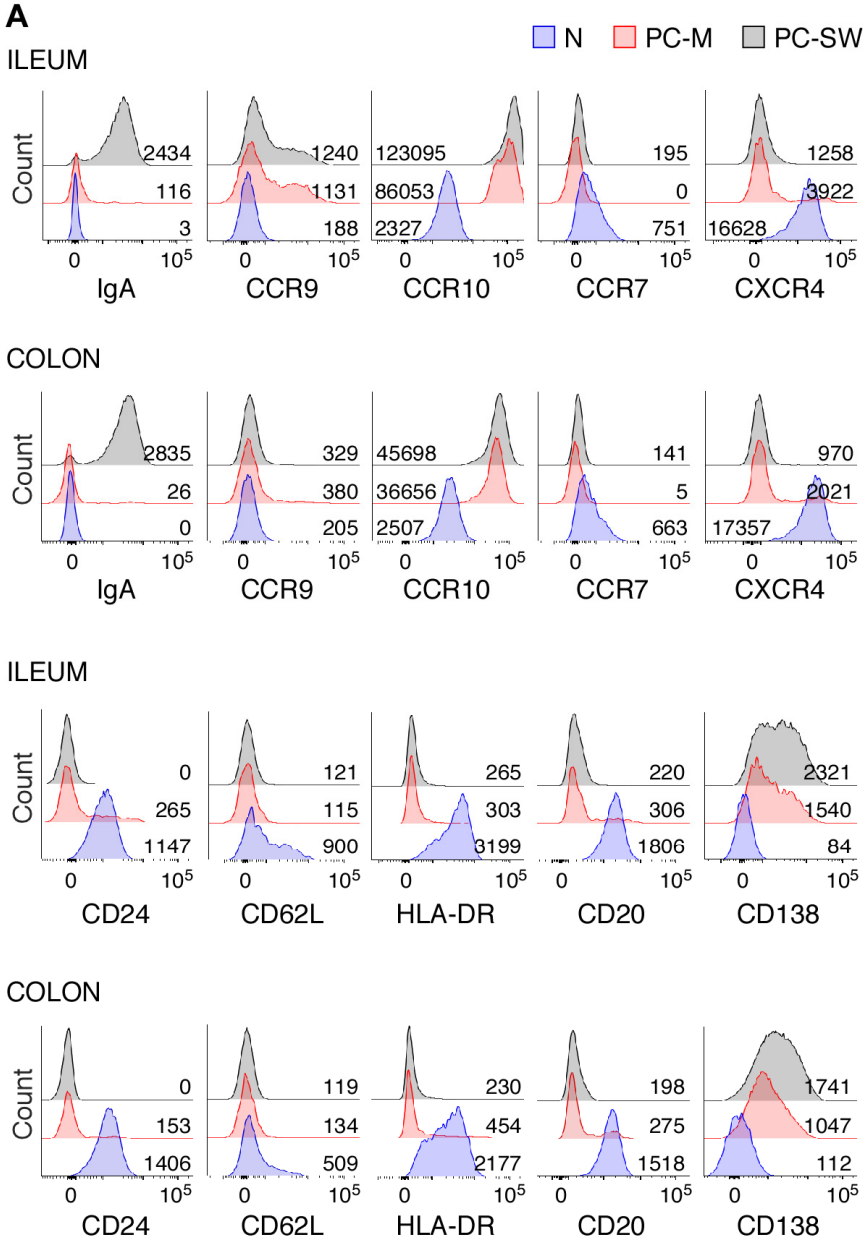

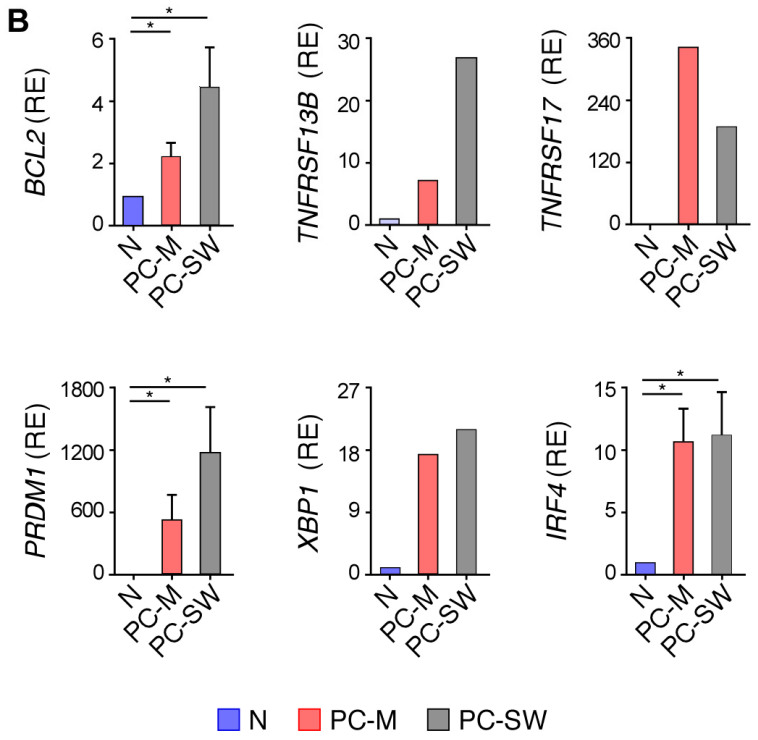

Figure 32. Human intestinal PC-M phenotypically resemble classical PC-A. Analysis of the expression of IgA, CCR9, CCR10, CCR7, CXCR4, CD24, CD62L, HLA-DR, CD20 and CD138 on intestinal N, PC-M and PC-SW, assessed by flow cytometry. Numbers in plots indicate mean fluorescence intensity (MFI). (B) Quantitative RT-PCR analysis of mRNA encoding Bcl-2 (*BCL2*), TACI (*TNFRSF13B*), BCMA (*TNFRSF17*), Blimp-1 (*PRDM1*), XBP1 (*XBP1*) and IRF4 (*IRF4*) in sorted intestinal N, PC-M and PC-SW; results are normalized to those of mRNA encoding β-actin (*ACTB*) and are presented as relative expression (RE) compared with that on N B cells, set as 1. N, naïve; PC-M, IgM^+ plasma cells; PC-SW, switched plasmas cells. Error bars represent s.e.m.; *P<0.05 (two-tailed unpaired Student's *t*-test). Data are representative (A) or include (B) at least three different experiments.

Therefore, these data prove that the human intestinal mucosa harbors a significant proportion of PC-M, which is higher in the ileum than in the colon, and in both cases higher than in mice. Moreover, human intestinal

PC-M are phenotypically similar to classical PC-A, and may be enriched in PBs.

The human intestinal mucus contains mostly IgA and IgM/IgA coated bacteria and fungi

The main function of PCs is the production of Ig, which in the intestine are secreted to the intestinal lumen across the epithelial barrier to interact with intestinal microbiota and establish mutualism[342]. Both PC-M and PC-A in the human intestine produce Ig with a J chain, a structure coupled to dimeric IgA and pentameric IgM that allows ligation of the Ig to the pIgR in the basal surface of IECs[343]. After transport across the epithelial cell and to the apical surface of IEC, the pIgR is cleaved and the Ig is released into the lumen as a complex including the Ig coupled with the J chain and a portion of the pIgR, termed secretory component[344].

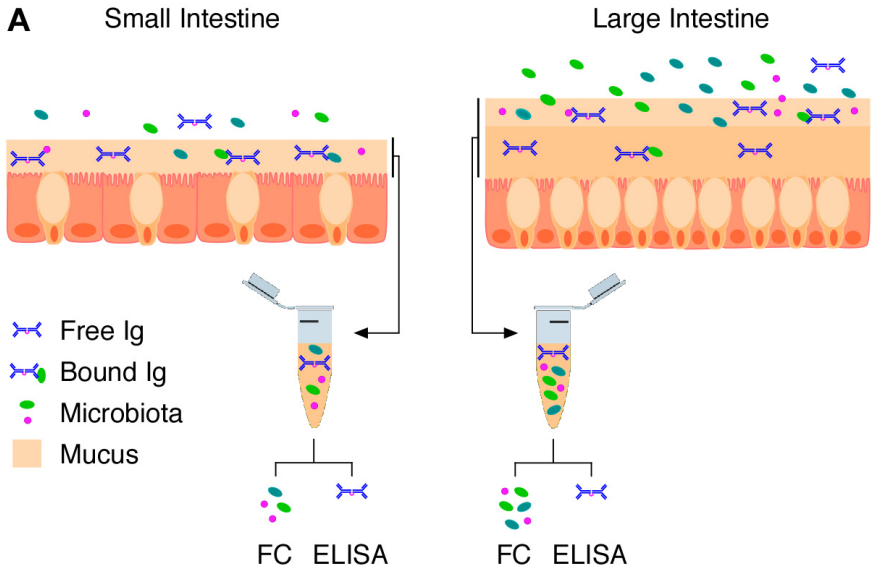

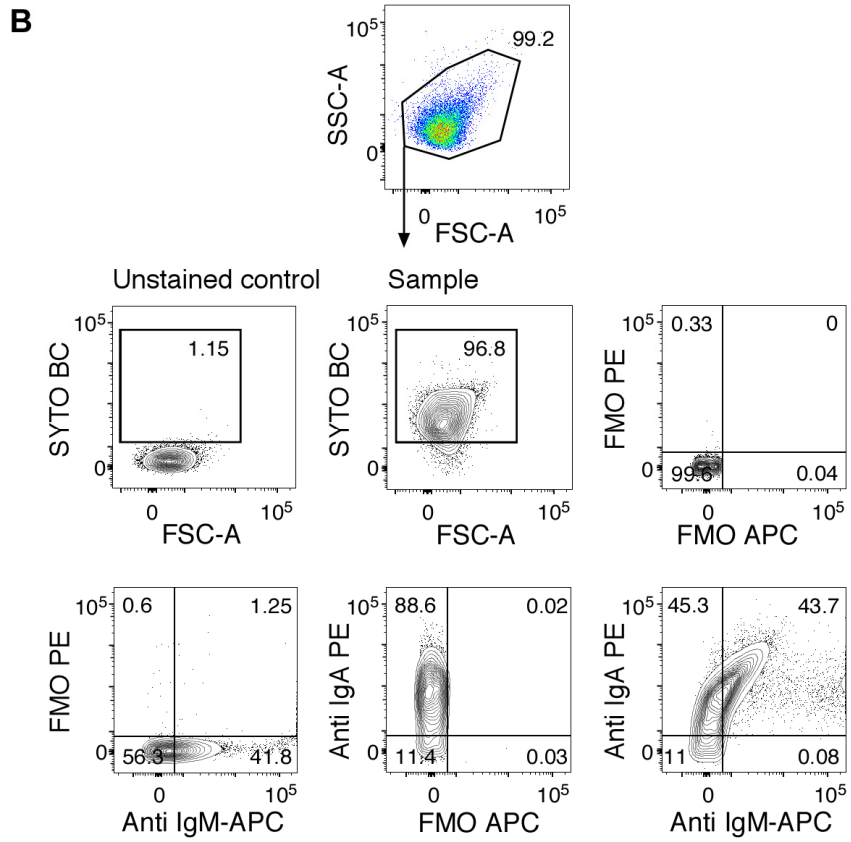

Figure 33. The human intestinal mucus contains mostly IgA and IgM/IgA coated microbes. (A) Experimental design used to analyze microbiota from human intestinal mucus. (B) Flow cytometry of intestinal microbiota stained for the nucleic acid stain SytoBC, isotype controls, IgM and IgA. Numbers in dot plots indicate percentage of cells. SSC-A, side scatter area; FSC-A, forward scatter area; FMO, fluorescence minus one. APC, allophycocyanin; PE, phycoerythrin; MB, microbiota.

To assess whether Igs produced by intestinal PC-M interact with the intestinal microbiota, we collected samples of mucus from terminal ileum and proximal colon and stained them with the nucleic acid stain SytoBC (Fig. 33A, B). By doing so, we confirmed that microbes present in human intestinal mucus are highly coated by Igs, both IgM and IgA (Fig. 33B).

The microbial Ig coating was highly variable between individuals and between ileal and colonic samples from the same individual, reflecting differences in the composition of the microbiota not only between individuals but also along the gut[345]. The majority of samples had a fraction of the microbiota double coated with IgA and IgM, a fraction coated only with IgA, and an uncoated fraction of microbes, whereas the amount of microbes coated only with IgM was very low (Fig. 34A).

Moreover, the percentage of double IgM and IgA coated microbes, was higher in the ileum than in the colon (Fig. 34B), whereas the amount of free IgA was much higher than free IgM in the mucus at both locations (Fig. 34C).

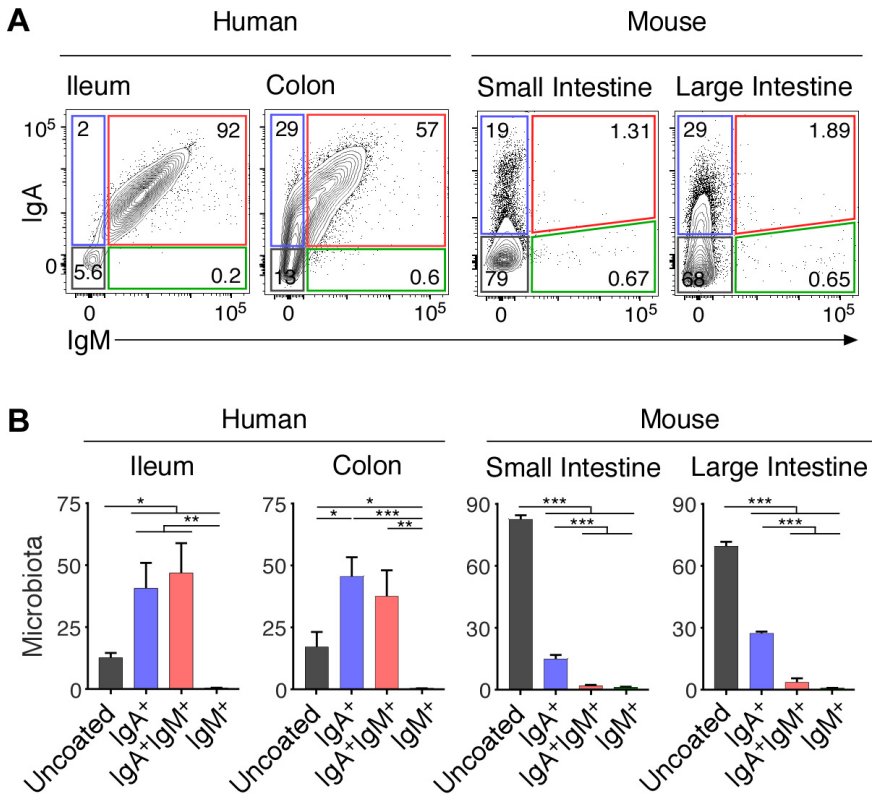

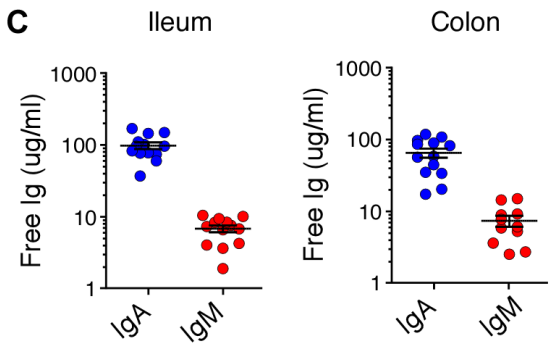

Figure 34. The human intestinal mucus contains a high proportion of IgA and IgM coated microbiota. (A) Flow cytometry of SytoBC^{+} intestinal microbiota stained for IgM and IgA in samples of mucus from human terminal ileum and proximal colon (left) and intestinal contents from murine small and large intestines (right). Numbers in dot plots indicate percentage of cells. (B) Frequency of SytoBC^{+} intestinal microbiota either uncoated, coated with IgA, IgA and IgM or IgM in the same type of samples from human and mice. (C) ELISA of free IgA and IgM from supernatants of intestinal mucus samples from human terminal ileum (left) and proximal colon (right). SytoBC, nucleic acid stain. Small horizontal lines indicate the mean (± s.e.m.); *P<0.05; **P<0.01; ***P<0.001 (two-tailed unpaired Student's t-test). Data show representatives (A) of 20 experiments (B) and 24 experiments (C).

On the other hand, analysis of murine small and large intestinal contents revealed that the amount of coated microbes was smaller in mice compared to humans (Fig. 34A, B). Moreover, the fraction of microbes coated with Igs was almost exclusively coated with IgA, indicating that in mice IgM does not participate in microbial coating as in humans.

Although SytoBC staining is mostly used to assess the presence of bacteria, a crystal violet staining of sorted microbes showed that all fractions contained different types of bacteria and probably fungi (Fig. 35A). To confirm that, we performed flow cytometry for a specific anti-fungal antibody and confirmed the presence of fungi in human mucus

samples with a similar Ig coating pattern than the one we have described with the SytoBC staining (Fig. 35B).

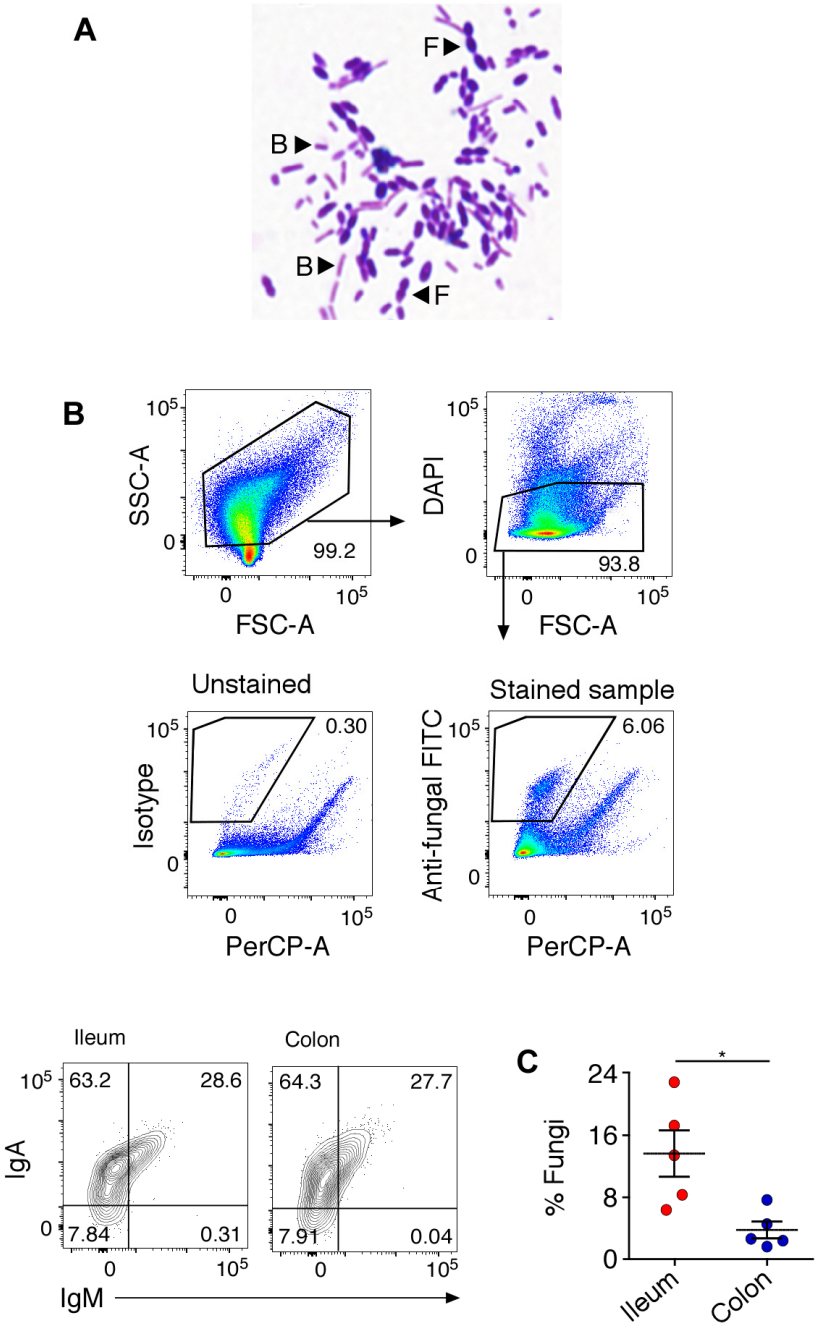

Figure 35. The human intestinal lumen contains IgM and IgA coated fungi. (A) Crystal violet staining of $Syto^{+}IgA^{+}IgM^{+}$ sorted intestinal microbiota. Original magnification 100X. (B) Flow cytometry of viable ($DAPI^{-}$) fungi stained for anti-fungal FITC antibody. (C) Frequency of $DAPI^{-}FITC^{+}$ fungi in mucus samples from ileum and colon. B, bacteria; F, fungi; SSC-A, side scatter area; FSC-A, forward scatter area; PerCP-A, peridinin chlorophyl area; FITC, fluorescein isothiocyanate. Numbers in dot plots indicate percentage of cells. Small horizontal lines indicate the mean (± s.e.m.) *P<0.05 (two-tailed unpaired Student's *t*-test). Data show representatives (A, B) of 10 experiments (C).

Importantly, we identified that mucus samples from terminal ileum contained a significantly higher frequency of fungi than colonic mucus samples from the same patients (Fig. 35C).

Taken together, these experiments showed that the human intestinal mucus contains a high portion of IgA and IgM/IgA coated bacteria and fungi. Importantly, and as expected, the proportion of IgM coated microbiota is highly variable between individuals and also varies from terminal ileum to proximal colon, reflecting variations of the microbiota.

CHAPTER 5
DISCUSSION

We have shown that human ME-M B cells formed a large intestinal reservoir of antigen-selected IgM^+ lymphocytes distinct from antigen-naïve IgM^+ lymphocytes positioned within lymphoid follicles. In humans, ME-M B cells colonized the intestine early in life, persisted throughout adulthood and predominantly inhabited mucosal sites of antigen entry, including PPs and ILFs. Remarkably, ME-M B cells comprised only a small fraction of gut lymphocytes in mice, suggesting that species-specific signals from the human gut mucosa are required for the establishment of a significant tissue-based repertoire of ME-M B cells.

Intestinal ME-M B cells shared a number of commonalities with splenic MZ B cells, including several phenotypic traits, multiple IgVH gene families and a pronounced reactivity against microbial carbohydrates and lipids. Despite these similarities, ME-M B cells expressed a gut-specific gene expression profile that revealed their closer affiliation to class-switched memory B cells. ME-M B cells further differed from MZ B cells by expressing an IgVH gene mutation profile that was consistent with a GC origin from gut inductive sites. Accordingly, ME-M B cells showed strong reactivity against mucus-embedded commensal antigens.

Intestinal ME-M B cells robustly proliferated in response to either TD or TI signals, which also induced prompt differentiation of intestinal ME-M B cells into PBs secreting IgM. In agreement with these findings, a subset of intestinal ME-M B cells showed extensive clonal relationships with intestinal PC-M. Of note, intestinal ME-M B cells extensively colonized both ileum and colon through a clonally organized response suggestive of centrifugal dissemination from follicular inductive sites. This possibility was further strengthened by the detection of abundant gut-homing receptors on circulating ME-M B cells.

A smaller population of intestinal ME-M B cells underwent IgM-to-IgA class switching to generate clonally related ME-A B cells along with PC-A. Accordingly, a fraction of freshly isolated ME-M B cells contained molecular hallmarks of ongoing IgM-to-IgA CSR, including switch circle and AID transcripts. Lastly, intestinal PC-M emerging from ME-M B cells colonized the ileum more extensively than the colon and released IgM antibodies that coated bacteria and fungi embedded within the mucus layer of the ileal mucosa. This IgM coating coexisted with and likely complemented IgA coating, at least in humans.

In summary, our data indicate that the human gut microenvironment engenders two parallel repertoires of follicular IgM^+ lymphocytes: one comprised of canonical antigen-naïve B cells and the other formed by antigen-selected B cells. After emerging from gut inductive sites, ME-M B cells may take advantage of their pre-existing specificities and functional plasticity to serve as immune sentinels at follicular entry sites. In particular, ME-M B cells may organize clonally coordinated IgM and IgA responses to accommodate antigenic changes in the prokaryotic and eukaryotic consortia inhabiting the human gut mucosa.

IgM^+ memory B cells in mice and humans

Memory B cells are antigen experienced quiescent cells that persist through long periods of time in the absence of antigen and respond more rapidly and with more affinity than naïve B cells in a secondary immune response[122,346,347].

In mice, the memory B cell compartment includes GC-dependent and GC-independent subsets. Early GC-independent memory B cells are unmutated and usually express IgM[134,135,313], whereas late GC-dependent memory B cells are mutated and can express either IgM or class-switched

antibodies, including IgG[6,131]. Upon secondary antigenic challenge, IgM^+ memory B cells re-enter the GC reaction to replenish the memory pool, whereas IgG^+ memory B cells promptly differentiate into IgG-secreting PBs[6,66,348]. Importantly, differences in antibody class expression and degree of SHM have been associated with differences in the longevity and fate of memory B cells[131]. Thus, IgM^+ memory B cells with fewer mutations are thought to have a longer life span than IgG^+ memory B cells with more mutations[349]. In addition, a recent study has shown that GC B cells expressing lower affinity BCRs are more prone to enter the memory B cell pool[350].

The fundamental tenets of memory B cell biology have emerged from studies performed in small animal models. In contrast, the human memory B cell compartment is less well understood[351].

In humans, memory B cells have been initially defined as $CD27^+$ class-switched B cells expressing mutated IgV genes[117,130,352]. However, recent studies have shown the existence of a small subset of mutated and class-switched $CD27^-$ memory B cells[277,353] as well as mutated but unswitched $CD27^+$ memory B cells[117]. In peripheral blood, the $CD27^+IgM^+$ B cell pool includes GC-derived ME-M B cells together with IgM^+IgD^+ MZ (or MZ-like) B cells, a recirculating memory B cell subset virtually identical to splenic MZ B cells and involved in systemic TI responses.

The origin and function of ME-M B cells in humans and mice are still debated. For instance, it is not clear whether ME-M B cells emerge from systemic immune responses to infection and/or vaccination as IgG^+ memory B cells do. It is also unknown whether ME-M B cells contribute to mucosal immune responses by IgA^+ memory B cells.

The present study is the first one to describe an enrichment of ME-M B cells in the human gut mucosa and to decipher the location, phenotype, transcriptome and function of human ME-M B cells.

ME-M B cells are enriched in the human gut

We found that human circulating ME-M B cells expressed the gut-homing receptors β7 and CCR9 and were enriched in the gut mucosa. In both human small and large intestines, ME-M B cells inhabited the follicular inductive sites of ILFs and PPs and expressed CCR7 and CXCR4, two chemokine receptors involved in B cell localization within lymphoid tissues.

PPs develop during embryonic life but undergo full maturation into GC-containing lymphoid aggregates following intestinal colonization by the gut microbiota, which occurs immediately after birth. On the other hand, ILFs develop only after birth[177] and their size and cellular composition are largely dependent on the amount and nature of the colonizing intestinal microbiota[183,184].

Interestingly, ME-M B cells were already present in the gut early in life and persisted throughout adulthood. Their location in ILFs and PPs as early as 1.5 months after birth suggests that the induction of ME-M B cells parallels the maturation of gut follicular structures in response to signals from bacteria. These intestinal ME-M B cells likely have fewer IgV gene mutations and could account for the generation of an initial wave of PC-M that may play a fundamental role in the initial control of the microbiota. Later, ME-M B cells may gradually accumulate an increasing number of IgV mutations through iterative rounds of proliferation and SHM in the GC of intestinal inductive sites, including PPs.

To determine whether intestinal colonization by ME-M B cells was conserved among species, we assessed the distribution and frequency of murine ME-M B cells expressing a canonical $IgM^{+}IgD^{-}CD80^{+}CD73^{+}$ memory phenotype in specific pathogen free (SPF) mice. Some of these ME-M B cells were indeed detected in the murine gut, but their frequency was consistently much lower than in humans.

The larger size of the ME-M B cell pool in the human gut compartment could stem from species-specific differences in the composition, richness and diversity of the gut microbiota. To further address this issue, we plan to generate humanized gnotobiotic mice by transplanting adult human fecal microbial communities into germ free mice.

ME-M B cells express a gut signature that includes MZ-like traits

Global gene transcriptome analysis determined that ME-M B cells had a gene expression profile consistent with that of canonical memory B cells and led to the identification of a gene signature common to memory B cells from both gut and spleen. In agreement with this finding, further molecular and functional assays demonstrated that intestinal ME-M B cells had phenotype, morphology and proliferation history similar to those of splenic memory B cells.

A deeper analysis of gene expression data revealed that intestinal ME-M B cells had a stronger affiliation to intestinal ME-SW B cells than to splenic MZ B cells. Further studies led to the identification of a tissue-specific gene signature common to all gut memory B cells. Genes belonging to this common signature included CCR9, IL-10, ITGAX (CD11c), AHR, SIGLEC6, RANKL and CD70 among others.

Additional hallmarks of gut memory B cells included FcRL4 and the IgA inducing transcription factor RUNX2, which have been associated earlier to memory B cells from the tonsillar mucosa[324]. Another gut memory B cell molecule was G protein-coupled receptor GPR15, an alternative HIV receptor[354] that regulates mucosal immune homeostasis and tolerance by controlling the homing of Treg cells to the large intestinal mucosa[355].

Gut memory B cells were also enriched in transcripts encoding IL-10, a powerful immnoregulatory cytokine involved in the control of inflammation and induction of Treg cells. Of note, IL-10 identifies B regulatory (Breg) cells capable to suppress immune responses potentially leading to uncontrolled inflammation[319-321]. Given that Breg cells typically secrete large amounts of IL-10, we determined whether ME-M B cells could do the same. When exposed to the TLR9 ligand CpG-DNA, ME-M B cells showed elevated release of Il-10.

Multiple subsets of Breg cells with various phenotypes have been described in both mice and humans. Currently, a common view is that Breg cells do not represent a distinct B cell lineage, but rather reflect an anti-inflammatory adaptation of B cells that are exposed to a highly pro-inflammatory environment. By showing elevated IL-10 production, our findings suggest that at least a fraction of intestinal ME-M B cells actively participate in the maintenance of a tolerogenic environment in the gut. Some intestinal ME-SW B cells may play a similar anti-inflammatory role.

Remarkably, a fraction of ME-M B cells showed signs of activation, including the expression of CD70, FcRL4, CD43 and CD11c. Previously published human studies have shown that the inhibitory IgA receptor FcRL4[356] is a hallmark of activated memory B cells inhabiting mucosal tissues, including mucosal sites invaded by pathogens[324]. In addition to

binding to IgA, FcRL4 dampens BCR but enhances TLR signaling in B cells chronically stimulated by antigen[322,357]. These observations suggest that FcRL4 plays some important regulatory role in mucosal tissues, possibly by modulating the magnitude and/or quality of secondary antibody responses, including IgA production[358].

We also found that a small fraction of ME-M B cells expressed CD11c. A recent report has shown that $CD11c^+$ B cells express high levels of CCR7 and localize at the T-B border of the spleen to present antigen to specific T cells[326]. This implies that ME-M B cells could promote homeostatic gut immune responses by presenting antigen to T cells in an IL-10-rich regulatory context that could lead to the generation of IgA-inducing Treg cells.

Besides expressing a large number of genes that were also detected in gut ME-SW B cells, intestinal ME-M B cells shared the expression of a smaller number of genes with splenic MZ B cells. Consistent with these transcriptional data, ME-M B cells showed some phenotypic and functional commonalities with MZ B cells. Regarding the phenotype, ME-M B cells expressed molecules typically associated with MZ B cells such as CD1c, CD1d and CD21. In addition, both ME-M and MZ B cells expressed CD148, a molecule typically expressed by memory B cells along with CD27 in humans[359]. Of note, CD148 is a tyrosine kinase receptor that serves as positive regulator of signals from ITAM-containing receptors in both B and myeloid cells[360]. ME-M B cells also expressed CD66a (CEACAM1), which belongs to a family of cell adhesion molecules involved in a variety of immune modulatory functions. Interestingly, a recently published study shows that activated neutrophils stimulate MZ B cells via homotypic CEACAM1 interactions which induce IgM secretion and class switching to IgG2[361].

Intestinal ME-M B cells expressed an IGHV gene family usage largely comparable to that of splenic MZ B cells but different from that of intestinal N and ME-SW B cells. This observation may reflect developmentally regulated processes involving mucosal antigens capable to target ME-M and MZ but not ME-SW B cell specificities. Alternatively, ME-M and MZ B cells may share a common progenitor. Of note, ME-M and MZ B cells showed a strong selection against IGHV1 gene usage and a concomitant pronounced enrichment in IGHV3-23 gene usage, which may account for the pronounced reactivity of IgM^+ memory B cells for certain antigenic determinants shared by both foreign and autologous antigens[362]. Consistent with this interpretation, ME-M B cells showed a robust reactivity for microbial carbohydrates and phospholipids also recognized by splenic MZ B cells.

ME-M B cells derive from gut GCs and recognize commensals

Notwithstanding their similarities, intestinal ME-M and splenic MZ B cells also exhibited a number of differences that point to their origin from different maturation processes. Indeed, gut ME-M but not splenic MZ B cells had reduced IGHJ6 gene usage compared to naïve B cells, which may reflect transition of ME-M B cells through GC-containing inductive sites. Indeed, IGHJ6 expression is associated with longer CDR3s[363] and thus its reduced usage may reflect selection of shorter CDR3s as a result of the GC reaction[362].

Consistent with their origin from GC-containing follicular structures, ME-M B cells expressed mutated IGHV genes, albeit less than ME-A, especially in the ileum. One possibility is that ME-M B cells represent a first wave of memory B cells that emerge from intestinal GCs engaged in homeostatic antibody responses to intraluminal antigens. Besides showing

less IGHJ6 gene usage, intestinal ME-M and ME-SW B cells expressed less Igλ compared to splenic MZ and ME-SW B cells. These findings indicate that selection forces operating in intestinal GCs are different from the ones present in splenic GCs. In particular, gut ME-M B cells may experience iterative rounds of GC selection as gut ME-SW B cells do[364].

Our demonstration that ME-M B cells could recognize several conserved microbial antigens as MZ B cells did prompted us to further explore the reactivity of ME-M B cells for gut antigens. To accomplish this goal, we developed a protocol to assess the reactivity of intestinal ME-M B cells and control naive B cells for commensal microbes embedded within autologous intestinal mucus layer. Thus, antigen-selected intestinal ME-M B cells specifically recognize gut bacteria, whereas non-antigen-selected naive B cells do not.

ME-M B cells differentiate to PC-M and switch to ME-A and PC-A

ME-M B cells vigorously proliferated and differentiated into PBs secreting IgM or class-switched IgA and IgG antibodies upon exposure to either TD or TI stimuli. In agreement with these *in vitro* data, in vivo activated $FcRL4^+$ ME-M B cells expressed more AID than resting $FcRL4^-$ ME-M B cells and showed an increased capacity to undergo switching from IgM to IgA. Indeed, at least a fraction of ME-M B cells showed signs of ongoing CSR from IgM to IgA1 or IgA2.

ME-M B cells positioned at the T-B border of intestinal lymphoid follicles, including ILFs, may receive IgA CSR-inducing signals from T cells. Accordingly, several studies have shown that CSR can initiate prior to the initiation of the GC reaction either in the early extrafollicular phase of primary TD responses[365] or 12-24 hours after secondary B cell

activation[56]. Along the same lines, a recent study has shown that mucosal pre-GC B cells up-regulate CCR6 expression to migrate into the SED of PPs, where they initiate IgA CSR upon interacting with TGF-β-expressing DCs[366]. This process further involves group 3 ILCs, which promote DC survival and activation through the release of LTβ. By showing that ME-M B cells respond to either TD or TI stimuli and by demonstrating that ME-M B cells inhabit both extrafollicular and follicular areas of PP and ILF sites specialized in antigen entry, our findings suggest that ME-M B cells are ideally positioned to promptly respond to antigenic changes occurring within the intestinal microbiota.

High-throughput analysis of the clonal architecture of ME-M B cells showed that the majority of these antigen-selected lymphocytes were organized in clonal families largely unrelated to other B cell subsets, particularly within the ileal mucosa. This observation may reflect the sentinel activity of ME-M B cells, which may acquire a semi-quiescent state of active readiness at mucosal sites of antigen entry. Remarkably, the remaining ME-M B cells were clonally linked to PC-M and to a lesser extent ME-A and PC-A. This observation nicely correlated with in vitro data showing that mucosal ME-M B cells could generate IgM^+ PBs or undergo CSR from IgM to IgA upon exposure to TD and TI stimuli. The in vivo differentiation of ME-M B cells along an extrafollicular GC-independent pathway fueled by TI or TD signals inducing CSR but not SHM was corroborated by the identification of some ME-M and PC-A clonotypes expressing identical VDJ genes. Additional evidence indicated in vivo differentiation of some ME-M clonotypes into more mutated ME-A clones through a follicular GC-dependent pathway inducing SHM in addition to CSR. Further analysis revealed that one of the largest clonal families from our set of ileal mucosa samples included poorly mutated ME-M B cells that had differentiated into PC-M. However, four additional

large clonal families included ME-M B cells that had differentiated into highly mutated PC-M, ME-A B cells and/or PC-A.

In general, these data indicate that the multilayered nature of gut antibody responses is not limited to the continuous diversification of pre-existing ME-A B cells in gut inductive sites[309], but it may further involve iterative entry of pre-existing ME-M specificities into GCs supporting class switching and affinity maturation in addition to PC differentiation. This implies that gut follicles include two parallel repertoires of IgM^+ lymphocytes: one composed of antigen-inexperienced naive B cells and the other one encompassing antigen-experienced ME-M B cells. The former are likely recruited into de novo responses to initiate protective humoral immunity against pathogens, whereas the latter may mostly contribute to homeostatic IgM and IgA responses against commensals. Such responses would further involve IgM and IgA production by pre-existing ME-M specificities transiting through extrafollicular compartments without undergoing affinity maturation.

Of note, the majority of ileal ME-M clonal families exclusively inhabited the ileum and showed a larger degree of unrelatedness to ME-A and PC-A compared to colonic ME-M clonotypes. However, a subset of clonally related ME-M B cells could be detected in both ileum and colon, which indicates that some ME-M B cells undergo dissemination from GC-containing inductive sites to both ileal and colonic effector sites through the general circulation. Consistent with this possibility, circulating ME-M B cells expressed high levels of gut-homing receptors.

By showing the presence of similarly mutated IgA clones in separate regions of the intestine, previously published studies suggest that GC-driven dissemination of clonally expanded and recirculating ME-A and PC-A clones are a hallmark of gut IgA responses[309]. Other published

works have shown that re-utilization of pre-existing GCs by antigen-specific ME-A B cells following oral immunization establishes synchronized oligoclonal IgA responses to cholera toxin along the whole length of the mouse small intestine[364].

Our findings add further complexity to this picture and suggest that the ileum contains a large repertoire of ME-M specificities that emerge from an early phase of GC reactions in central gut inductive sites, including PPs. Most of these ME-M clonotypes likely patrol ileal follicular sites without further undergoing CSR, SHM and/or PC differentiation, whereas others disseminate to the colon via the general circulation to participate in local GC reactions. The resulting IgM as well as IgA responses would reflect the accommodation of ileal ME-M clonotypes to the colonic antigenic environment. Consistent with this scenario, the overall mutational load of ME-M and ME-A clonotypes was less different in the colon than in the ileum.

PC-M similar to PC-A secrete antibodies to gut bacteria and fungi

Human intestinal samples contained PC-M in the LP and around ILFs early in life and throughout adulthood. In these samples, the proportion of PC-M was higher in the ileum than in the colon. In contrast, mouse intestinal samples contained way fewer PC-M, which showed comparable (low) frequencies in both ileum and colon.

Intestinal PC-M expressed transcripts for the BAFF/APRIL receptor BCMA along with transcripts encoding the PC-inducing transcription factors XBP1 and IRF4. This gene expression profile was grossly similar to that of classical long-lived PC-A. However, compared to PC-A, PC-M showed lower expression of transcripts for BCL2, TACI and BLIMP1 as

well as intermediate levels of transcripts for CD138, which may indicate the presence of some relatively short-lived PB-M within a classically long-lived PC-M population.

Recent mouse studies show that lymphoid follicles generate memory B cells and PCs by following a sequential order[367]. Unswitched memory B cells appear prior to the GC reaction, followed by the emergence of unswitched and switched memory B cells at the peak of the GC reaction and by a delayed wave of switched long-lived PCs, which migrate to extrafollicular sites and have the highest affinity for antigen. This complexity may reflect the need of the GC to support affinity maturation over time while adapting to changes in the magnitude of the antigenic input. One way of achieving this is to use an antibody feedback mechanism involving affinity-dependent equilibrium of GC-associated antibodies with antibodies released outside the GC[368]. Antibodies produced by PCs would compete for antigen with antibodies present in the GC, thus enhancing GC selection and pressuring towards increasing affinity. This mechanism would also explain how spatially separated GCs exchange information as to the level of the intruding antigen.

In humans, the LZ of gut GCs contained abundant FDCs that were seemingly bound by IgM-containing ICs. Thus, we speculate that gut PC-M derived from antigen-specific ME-M B cells generate specific IgM that competes for antigen with other GC-associated antibodies, including IgA. Should this be the case, PC-M may contribute to the regulation of GC-based B cell selection processes required for the generation of antibodies with progressively increasing affinity for antigen.

That said, the majority of intestinal PC-M were located in the LP, an effector site specialized in the release of secretory antibodies across the epithelial barrier[342]. While the role of SIgA in gut homeostasis is well

established, that of SIgM remains largely unknown. In particular, it is unclear whether SIgM binds to the gut microbiota as much as SIgA does. In IgA-deficient patients, SIgM coating of commensal bacteria likely increases to compensate for the lack of SIgA, which could explain why many of these patients remain asymptomatic. Conversely, the lack of SIgM may explain the presence of gut inflammation and allergy in patients with selective IgM deficiency, a recently described disorder also associated with respiratory infections[369].

We found that both bacteria and fungi embedded within human intestinal mucus were highly coated by SIgM. Of note, the majority of mucus samples was characterized by three distinct microbiota fractions: one double coated with SIgA and SIgM, another one coated with SIgA but not SIgM, and a third one that was completely uncoated. The amount of microbes coated by SIgM but not SIgA was very low. Of note, the degree of microbial coating was highly variable among individuals and between ileal and colonic samples from the same individual, which probably reflects tissue-specific in addition to inter-individual differences in the composition of the microbiota[345]. Unlike human samples, mouse samples showed IgA-coated and uncoated but no IgM-coated commensal microbes in both small and large intestinal segments.

In humans, the amount of free (unbound) SIgA was much higher than the amount of free SIgM both in ileal and colonic mucus samples. However, the percentage of microbes dually coated by SIgM and SIgA was higher in the ileum. This intestinal segment also contained a significantly higher amount of fungi, suggesting that the magnitude of SIgM release may be adjusted by the gut mucosa to the local demand for high-avidity immune exclusion by eukaryotic commensals.

Previously published studies have demonstrated the importance of SIgA in maintaining appropriate gut commensal communities through the use of murine models of global or partial AID deficiency that involved either combined loss of CSR and SHM[370] or selective loss of SHM, respectively[371]. Of note, both these models led to the development of intestinal dysbiosis, which indicates that SHM plays a more prominent role than CSR in the maintenance of gut homeostasis. Given that a fraction of gut PC-M are clonally related to ME-M expressing mutated IgM, it is likely that SIgM cooperates with SIgA to regulate the gut microbiota. Consistent with this possibility, selective IgM deficiency is often complicated by the onset of intestinal inflammation.

Remarkably, unmutated SIgA emerging from TI pathways recognizes commensals as specifically as mutated SIgA emerging from TD pathways, although the latter probably coat different sets of bacteria[260,372]. Indeed, it has been recently proposed that bacteria living in closer contact with the gut epithelium predominantly induce SIgA in a TD manner, whereas all the other commensals elicit SIgA responses through the TI pathway. Our high-throughput sequencing data suggest that also SIgM responses may arise from either TD or TI pathways. Accordingly, in vitro experiments show that ME-M B cells can differentiate into PC-M in response to either TD or TI stimuli. These IgM responses likely provide the gut mucosa with an additional layer of humoral defense, which may be necessary for the optimal control of larger commensals, including fungi.

Besides specifically recognizing bacteria through its Fab segment, SIgA may coat microbes through nonspecific mechanisms involving its Fc region as well as N-glycans associated with its secretory component[373]. Similarly, pentameric SIgM complexes may integrate their specificity for commensal bacteria with similar non-specific binding modalities, which may be further increased by the recruitment of complement proteins.

Besides releasing SIgA and SIgM, intestinal epithelial cells, including Paneth cells, secrete large amounts of antimicrobial peptides that contribute to the establishment of immune exclusion. Moreover, intestinal goblet cells release secretory gel-forming mucins that polymerize to generate a mucus layer that shields the epithelial surface from commensal microbes. This mucus layer is poorly organized and patchy in the small intestine, but becomes completely impervious to bacteria in the colon, where a loose bacteria-inhabited layer tops a dense sterile layer. Accordingly, it has been proposed that SIgA predominantly targets commensal bacteria from the small intestine[372]. However, our studies show that the majority of bacteria and fungi embedded within either ileal or colonic mucus were coated with SIgM and/or SIgA.

Unlike human SIgM, mouse SIgM did not coat bacteria from either the small or large gut segments, which were almost exclusively recognized by SIgA. This finding correlated with the relative paucity of PC-M in the mouse gut, which may stem from species-specific differences in the composition of the gut microbiota. These differences include a reduced frequency of fungi in mice compared to humans. However, it must be noted that microbe-coating SIgM was measured in mice using whole intestinal contents instead of mucus, which could account for some of the observed differences.

Clinical implications

Besides playing an important role in gut homeostasis, ME-M B cells could also contribute to pathobiological processes leading to the onset of mucosal or systemic inflammation. These processes may involve dysregulation of FCRL4, an inhibitory receptor that likely controls the activation of ME-M as well as class-switched subsets of tissue-based

memory B cells. Indeed, FCRL4 has been shown to dampen signals emanating from BCR in B cells chronically exposed to antigen[357,358]. Though important for the generation of non-inflammatory antibody responses at mucosal sites of antigen entry, FCRL4 may contribute to B-cell mediated immunopathology when "locked" in dysregulated immune circuitries.

In agreement with this possibility, viremic individuals chronically infected with HIV show an increased frequency of circulating $FCRL4^+$ memory B cells, which is considered to reflect immune exhaustion. Indeed, this B cell abnormality emerges in response to chronic immune activation, which in turn fuels viral replication through a mechanism involving enhanced microbial translocation from mucosal surfaces[374]. Similarly, $FCRL4^+$ memory B cells are increased in patients chronically infected with malaria and this increase correlates with immune exhaustion brought about by chronic parasitemia[375]. $FCRL4^+$ memory B cells are also increased in autoimmune disorders such as rheumatoid arthritis, where $FcRL4^+$ memory B cells could play a role in the activation of pro-inflammatory T cells by self-antigen[376] .

It is very likely that $FCRL4^+$ ME-M B cells are further involved in additional clinical conditions associated with chronic antigenic stimulation, including inflammatory bowel disease. In this chronic disorder, impairment of the epithelial mucosal barrier resulting from genetic and environmental predisposing factor is thought to determine continuous "leak" of intraluminal contents into the mucosal tissue, which may alter $FCRL4^+$ memory B cell function. In this pathological context, ME-M B cells may dysregulate their tolerogenic CSR program to mount pro-inflammatory IgG instead of non-inflammatory IgA responses.

Finally, our discovery of intestinal ME-M B cells may have far-reaching implications with respect to the development of mucosal vaccines. In general, the longevity and robust anamnestic responsiveness of memory B cells are key factors in the development of vaccine-induced immune protection. A more complete understanding of the reactivity and tolerogenic properties of ME-M B cells could lead to the development of novel vaccines against certain mucosal pathogens and personalized commensal-targeting anti-IBD strategies aimed at restoring a balanced microbiota.

Concluding remarks

Our studies indicate that the human gut mucosa includes two categories of follicular IgM^+ lymphocytes: canonical naive B cells with no prior exposure to antigen and a large repertoire of antigen-experienced ME-M B cells that may cooperate with ME-A B cells to promote gut homeostasis, including coating of prokaryotic and eukaryotic commensals by SIgM and SIgA. While naive B cells could be mostly recruited in de novo antibody responses against pathogens, ME-M B cells would be predominantly engaged in homeostatic antibody responses aimed at maintaining host-commensal mutualism. In particular, ME-M B cells may be strategically positioned at follicular sites of antigen entry to rapidly accommodate small antigenic changes occurring in the prevailing non-invasive microbiota. In contrast, more pronounced antigenic challenges brought about by invasive microbes would require the emergency recall of germ line specificities from the naive B cell repertoire.

Together with ME-A B cells, the ME-M B cells identified in this study may provide the intestinal mucosa with an additional layer of humoral protection that could be deployed through the activation of either TD or TI

pathways. Indeed, the predominant location of gut ME-M B cells in follicular areas containing both T cells and antigen-sampling DCs may facilitates the coordination of clonotypically organized IgM and class-switched IgA responses through either GC-dependent or less dominant GC-independent pathways. In the GC pathway, iterative entry of ME-M B cells into pre-existing GCs may allow the continuous replenishment of local memory B cell pools with more "microbiota-actualized" affinities and specificities by induction of DNA editing through SHM. Ultimately, the coordinated induction of PC-M and PC-A by ME-M B cells may lead to the combined release of SIgM and SIgA antibodies required for the control of the complex prokaryotic and eukaryotic communities inhabiting gut mucus.

CHAPTER 6
CONCLUSIONS

1. Human ME-M B cells form a large reservoir of intestinal antigen-selected IgM^+ lymphocytes distinct from antigen-naïve IgM^+ lymphocytes.

2. In humans, ME-M B cells colonize the intestine early in life, persist throughout adulthood and predominantly inhabit mucosal sites of antigen entry, including PPs and ILFs.

3. Intestinal ME-M B cells share a number of commonalities with splenic MZ B cells, but express a gut-specific gene expression profile that reveals their closer affiliation to class-switched memory B cells.

4. ME-M B cells express an IgVH gene mutation profile consistent with a GC origin from gut inductive sites. Accordingly, ME-M B cells show strong reactivity against mucus-embedded commensal antigens.

5. Intestinal ME-M B cells robustly proliferate in response to either TD or TI signals and differentiate into PBs secreting IgM.

6. ME-M B cells extensively colonize both ileum and colon through a clonally organized response suggestive of centrifugal dissemination from follicular inductive sites.

7. A smaller population of intestinal ME-M B cells undergoes IgM-to-IgA class switching to generate clonally related ME-A B cells along with PC-A.

8. Intestinal PC-M emerging from ME-M B cells colonize the ileum more extensively than the colon and release SIgM that along with SIgA, coats bacteria and fungi embedded within the mucus layer of the gut mucosa.

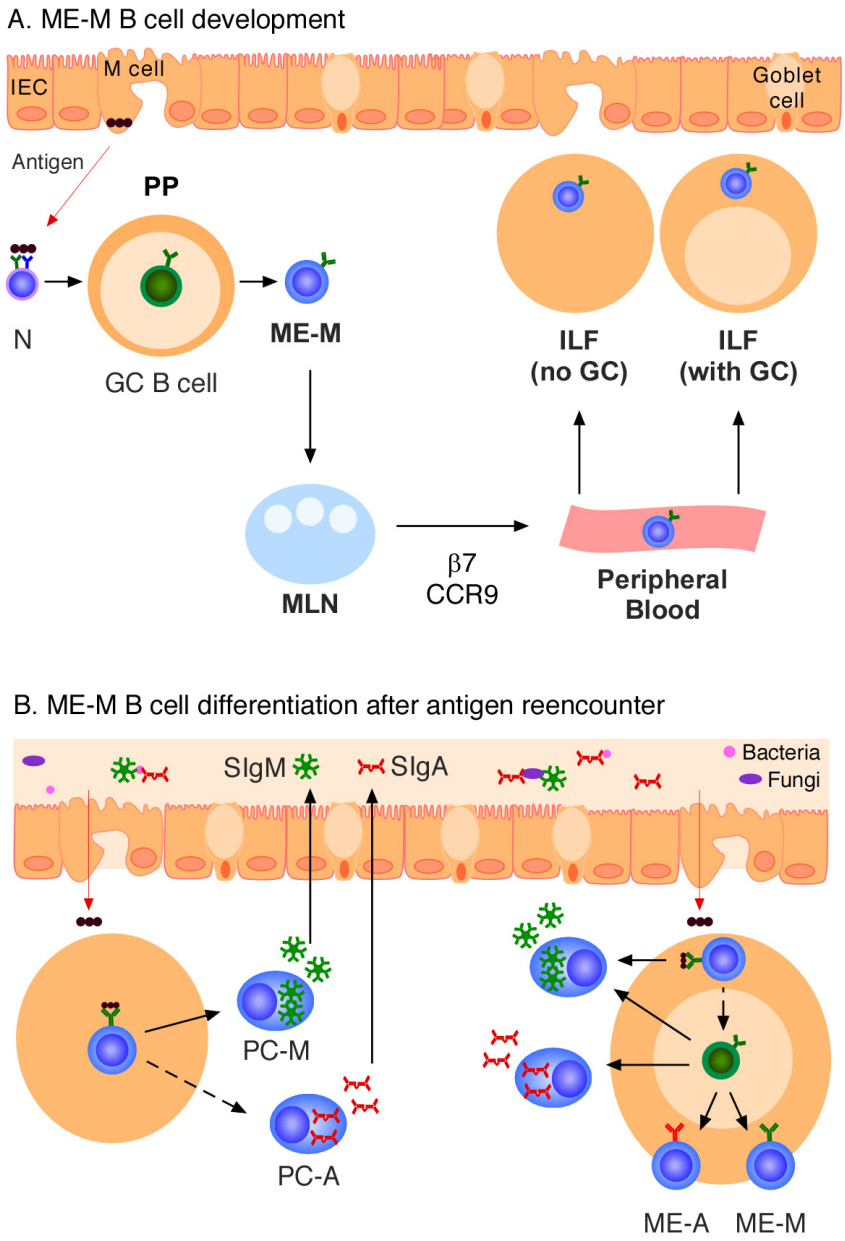

Figure 36. Model of ME-M B cell development and differentiation in the gut mucosa. A) After antigenic stimulation from intestinal microbiota, naïve B cells become activated and through a GC reaction differentiate into ME-M B cells in the follicular inductive sites of the small intestine, which include PP and ILFs

with GCs. Recently generated ME-M B cells enter the circulation and through the expression of the gut-homing receptors β7 and CCR9 relocate to mucosal sites of antigen entry, such as PPs and ILFs (with and without GCs). There, ME-M B cells may take advantage of their pre-existing specificities and functional plasticity to serve as immune sentinels at follicular entry sites. B) Upon antigen re-encounter, ME-M B cells can follow several differentiation pathways. ME-M B cells located in ILFs without GC promptly differentiate into antibody producing PC-M. A fraction of ME-M B cells can undergo CSR to IgA and differentiate into PC-A. On the other hand, ME-M B cells located in ILFs with GC, can follow the same PC differentiation pathway or may eventually reenter the GC where they undergo proliferation and additional SHM. In the GC-dependent pathway, the initial ME-M B cell may differentiate into either IgM or class-switched memory or PC. The resulting ME-M B cells recirculate to the ileum and colon to replenish the memory B cell pool. In both pathways, the resulting PC-M and PC-A produce IgM and IgA that are secreted to the gut lumen and coat bacteria and fungi embedded in the intestinal mucus layer. GC, germinal center; ME-M, IgM^+ memory; PP, Peyer's patches; ILF, isolated lymphoid follicles; CCR, chemokine receptor; PC-M, IgM^+ plasma cell; PC-A, IgA^+ plasma cell; CSR, class switch recombination; SHM, somatic hypermutation.

ANNEX I

References

1. Janeway, C.A., Jr. Approaching the asymptote? Evolution and revolution in immunology. *Cold Spring Harb Symp Quant Biol* **54 Pt 1**, 1-13 (1989).
2. Gallo, R.L. & Nakatsuji, T. Microbial symbiosis with the innate immune defense system of the skin. *J Invest Dermatol* **131**, 1974-1980 (2011).
3. Grivennikov, S.I., Greten, F.R. & Karin, M. Immunity, inflammation, and cancer. *Cell* **140**, 883-899 (2010).
4. Hoebe, K., Janssen, E. & Beutler, B. The interface between innate and adaptive immunity. *Nat Immunol* **5**, 971-974 (2004).
5. Janeway, C.A., Jr. & Medzhitov, R. Innate immune recognition. *Annu Rev Immunol* **20**, 197-216 (2002).
6. Dogan, I*., et al.* Multiple layers of B cell memory with different effector functions. *Nat Immunol* **10**, 1292-1299 (2009).
7. Cooper, M.D., Raymond, D.A., Peterson, R.D., South, M.A. & Good, R.A. The functions of the thymus system and the bursa system in the chicken. *J Exp Med* **123**, 75-102 (1966).
8. Hardy, R.R. & Hayakawa, K. B cell development pathways. *Annu Rev Immunol* **19**, 595-621 (2001).
9. Edelman, G.M. Antibody structure and molecular immunology. *Science* **180**, 830-840 (1973).
10. Bassing, C.H., Swat, W. & Alt, F.W. The mechanism and regulation of chromosomal V(D)J recombination. *Cell* **109 Suppl**, S45-55 (2002).
11. Schatz, D.G. & Swanson, P.C. V(D)J recombination: mechanisms of initiation. *Annu Rev Genet* **45**, 167-202 (2011).
12. Davis, A.C. & Shulman, M.J. IgM--molecular requirements for its assembly and function. *Immunol Today* **10**, 118-122; 127-118 (1989).
13. Goodnow, C.C., Adelstein, S. & Basten, A. The need for central and peripheral tolerance in the B cell repertoire. *Science* **248**, 1373-1379 (1990).
14. von Boehmer, H. & Melchers, F. Checkpoints in lymphocyte development and autoimmune disease. *Nat Immunol* **11**, 14-20 (2010).
15. Chen, K. & Cerutti, A. The function and regulation of immunoglobulin D. *Curr Opin Immunol* **23**, 345-352 (2011).

16. Chung, J.B., Silverman, M. & Monroe, J.G. Transitional B cells: step by step towards immune competence. *Trends Immunol* **24**, 343-349 (2003).
17. Batista, F.D. & Harwood, N.E. The who, how and where of antigen presentation to B cells. *Nat Rev Immunol* **9**, 15-27 (2009).
18. Batista, F.D., Iber, D. & Neuberger, M.S. B cells acquire antigen from target cells after synapse formation. *Nature* **411**, 489-494 (2001).
19. Lanzavecchia, A. Antigen-specific interaction between T and B cells. *Nature* **314**, 537-539 (1985).
20. Forster, R., Davalos-Misslitz, A.C. & Rot, A. CCR7 and its ligands: balancing immunity and tolerance. *Nat Rev Immunol* **8**, 362-371 (2008).
21. Kerfoot, S.M.*, et al.* Germinal center B cell and T follicular helper cell development initiates in the interfollicular zone. *Immunity* **34**, 947-960 (2011).
22. Okada, T.*, et al.* Antigen-engaged B cells undergo chemotaxis toward the T zone and form motile conjugates with helper T cells. *PLoS Biol* **3**, e150 (2005).
23. Qi, H., Cannons, J.L., Klauschen, F., Schwartzberg, P.L. & Germain, R.N. SAP-controlled T-B cell interactions underlie germinal centre formation. *Nature* **455**, 764-769 (2008).
24. Foy, T.M.*, et al.* gp39-CD40 interactions are essential for germinal center formation and the development of B cell memory. *J Exp Med* **180**, 157-163 (1994).
25. Allen, C.D., Okada, T. & Cyster, J.G. Germinal-center organization and cellular dynamics. *Immunity* **27**, 190-202 (2007).
26. De Silva, N.S. & Klein, U. Dynamics of B cells in germinal centres. *Nat Rev Immunol* **15**, 137-148 (2015).
27. Allen, C.D. & Cyster, J.G. Follicular dendritic cell networks of primary follicles and germinal centers: phenotype and function. *Semin Immunol* **20**, 14-25 (2008).
28. Tew, J.G., Kosco, M.H., Burton, G.F. & Szakal, A.K. Follicular dendritic cells as accessory cells. *Immunol Rev* **117**, 185-211 (1990).
29. Heesters, B.A., Myers, R.C. & Carroll, M.C. Follicular dendritic cells: dynamic antigen libraries. *Nat Rev Immunol* **14**, 495-504 (2014).
30. Ansel, K.M.*, et al.* A chemokine-driven positive feedback loop organizes lymphoid follicles. *Nature* **406**, 309-314 (2000).
31. Kopf, M., Herren, S., Wiles, M.V., Pepys, M.B. & Kosco-Vilbois, M.H. Interleukin 6 influences germinal center development and antibody production via a contribution of C3 complement component. *J Exp Med* **188**, 1895-1906 (1998).

32. Wu, Y.*, et al.* IL-6 produced by immune complex-activated follicular dendritic cells promotes germinal center reactions, IgG responses and somatic hypermutation. *Int Immunol* **21**, 745-756 (2009).
33. Garin, A.*, et al.* Toll-like receptor 4 signaling by follicular dendritic cells is pivotal for germinal center onset and affinity maturation. *Immunity* **33**, 84-95 (2010).
34. Johnston, R.J.*, et al.* Bcl6 and Blimp-1 are reciprocal and antagonistic regulators of T follicular helper cell differentiation. *Science* **325**, 1006-1010 (2009).
35. Nurieva, R.I.*, et al.* Bcl6 mediates the development of T follicular helper cells. *Science* **325**, 1001-1005 (2009).
36. Yu, D.*, et al.* The transcriptional repressor Bcl-6 directs T follicular helper cell lineage commitment. *Immunity* **31**, 457-468 (2009).
37. Crotty, S. Follicular helper CD4 T cells (TFH). *Annu Rev Immunol* **29**, 621-663 (2011).
38. Ramiscal, R.R. & Vinuesa, C.G. T-cell subsets in the germinal center. *Immunol Rev* **252**, 146-155 (2013).
39. Vinuesa, C.G., Linterman, M.A., Goodnow, C.C. & Randall, K.L. T cells and follicular dendritic cells in germinal center B-cell formation and selection. *Immunol Rev* **237**, 72-89 (2010).
40. Allen, C.D.*, et al.* Germinal center dark and light zone organization is mediated by CXCR4 and CXCR5. *Nat Immunol* **5**, 943-952 (2004).
41. Caron, G., Le Gallou, S., Lamy, T., Tarte, K. & Fest, T. CXCR4 expression functionally discriminates centroblasts versus centrocytes within human germinal center B cells. *J Immunol* **182**, 7595-7602 (2009).
42. Bannard, O.*, et al.* Germinal center centroblasts transition to a centrocyte phenotype according to a timed program and depend on the dark zone for effective selection. *Immunity* **39**, 912-924 (2013).
43. Muramatsu, M.*, et al.* Specific expression of activation-induced cytidine deaminase (AID), a novel member of the RNA-editing deaminase family in germinal center B cells. *J Biol Chem* **274**, 18470-18476 (1999).
44. Muramatsu, M.*, et al.* Class switch recombination and hypermutation require activation-induced cytidine deaminase (AID), a potential RNA editing enzyme. *Cell* **102**, 553-563 (2000).
45. Klein, U.*, et al.* Transcriptional analysis of the B cell germinal center reaction. *Proc Natl Acad Sci U S A* **100**, 2639-2644 (2003).

46. Liu, Y.J., *et al.* Germinal center cells express bcl-2 protein after activation by signals which prevent their entry into apoptosis. *Eur J Immunol* **21**, 1905-1910 (1991).
47. Liu, Y.J., *et al.* Mechanism of antigen-driven selection in germinal centres. *Nature* **342**, 929-931 (1989).
48. Liu, Y.J. & Arpin, C. Germinal center development. *Immunol Rev* **156**, 111-126 (1997).
49. Victora, G.D. & Nussenzweig, M.C. Germinal centers. *Annu Rev Immunol* **30**, 429-457 (2012).
50. Breitfeld, D., *et al.* Follicular B helper T cells express CXC chemokine receptor 5, localize to B cell follicles, and support immunoglobulin production. *J Exp Med* **192**, 1545-1552 (2000).
51. Gunn, M.D., *et al.* A B-cell-homing chemokine made in lymphoid follicles activates Burkitt's lymphoma receptor-1. *Nature* **391**, 799-803 (1998).
52. Schaerli, P., *et al.* CXC chemokine receptor 5 expression defines follicular homing T cells with B cell helper function. *J Exp Med* **192**, 1553-1562 (2000).
53. Klein, U. & Dalla-Favera, R. Germinal centres: role in B-cell physiology and malignancy. *Nat Rev Immunol* **8**, 22-33 (2008).
54. Kolar, G.R., Mehta, D., Pelayo, R. & Capra, J.D. A novel human B cell subpopulation representing the initial germinal center population to express AID. *Blood* **109**, 2545-2552 (2007).
55. Pape, K.A., *et al.* Visualization of the genesis and fate of isotype-switched B cells during a primary immune response. *J Exp Med* **197**, 1677-1687 (2003).
56. Toellner, K.M., Gulbranson-Judge, A., Taylor, D.R., Sze, D.M. & MacLennan, I.C. Immunoglobulin switch transcript production in vivo related to the site and time of antigen-specific B cell activation. *J Exp Med* **183**, 2303-2312 (1996).
57. Allen, C.D., Okada, T., Tang, H.L. & Cyster, J.G. Imaging of germinal center selection events during affinity maturation. *Science* **315**, 528-531 (2007).
58. Hauser, A.E., *et al.* Definition of germinal-center B cell migration in vivo reveals predominant intrazonal circulation patterns. *Immunity* **26**, 655-667 (2007).
59. Schwickert, T.A., *et al.* In vivo imaging of germinal centres reveals a dynamic open structure. *Nature* **446**, 83-87 (2007).
60. Linterman, M.A., *et al.* IL-21 acts directly on B cells to regulate Bcl-6 expression and germinal center responses. *J Exp Med* **207**, 353-363 (2010).
61. Vinuesa, C.G., Sanz, I. & Cook, M.C. Dysregulation of germinal centres in autoimmune disease. *Nat Rev Immunol* **9**, 845-857 (2009).

62. Gitlin, A.D., Shulman, Z. & Nussenzweig, M.C. Clonal selection in the germinal centre by regulated proliferation and hypermutation. *Nature* **509**, 637-640 (2014).
63. Victora, G.D.*, et al.* Germinal center dynamics revealed by multiphoton microscopy with a photoactivatable fluorescent reporter. *Cell* **143**, 592-605 (2010).
64. Avery, D.T.*, et al.* B cell-intrinsic signaling through IL-21 receptor and STAT3 is required for establishing long-lived antibody responses in humans. *J Exp Med* **207**, 155-171 (2010).
65. Blink, E.J.*, et al.* Early appearance of germinal center-derived memory B cells and plasma cells in blood after primary immunization. *J Exp Med* **201**, 545-554 (2005).
66. Phan, T.G.*, et al.* High affinity germinal center B cells are actively selected into the plasma cell compartment. *J Exp Med* **203**, 2419-2424 (2006).
67. Shapiro-Shelef, M.*, et al.* Blimp-1 is required for the formation of immunoglobulin secreting plasma cells and pre-plasma memory B cells. *Immunity* **19**, 607-620 (2003).
68. Chaudhuri, J. & Alt, F.W. Class-switch recombination: interplay of transcription, DNA deamination and DNA repair. *Nat Rev Immunol* **4**, 541-552 (2004).
69. Stavnezer, J., Guikema, J.E. & Schrader, C.E. Mechanism and regulation of class switch recombination. *Annu Rev Immunol* **26**, 261-292 (2008).
70. Cerutti, A.*, et al.* CD30 is a CD40-inducible molecule that negatively regulates CD40-mediated immunoglobulin class switching in non-antigen-selected human B cells. *Immunity* **9**, 247-256 (1998).
71. Hodgkin, P.D., Lee, J.H. & Lyons, A.B. B cell differentiation and isotype switching is related to division cycle number. *J Exp Med* **184**, 277-281 (1996).
72. Hasbold, J., Lyons, A.B., Kehry, M.R. & Hodgkin, P.D. Cell division number regulates IgG1 and IgE switching of B cells following stimulation by CD40 ligand and IL-4. *Eur J Immunol* **28**, 1040-1051 (1998).
73. Deenick, E.K., Hasbold, J. & Hodgkin, P.D. Switching to IgG3, IgG2b, and IgA is division linked and independent, revealing a stochastic framework for describing differentiation. *J Immunol* **163**, 4707-4714 (1999).
74. Rush, J.S., Liu, M., Odegard, V.H., Unniraman, S. & Schatz, D.G. Expression of activation-induced cytidine deaminase is regulated by cell division, providing a mechanistic basis for division-linked class switch recombination. *Proc Natl Acad Sci U S A* **102**, 13242-13247 (2005).

75. Liu, Y.J., *et al.* Within germinal centers, isotype switching of immunoglobulin genes occurs after the onset of somatic mutation. *Immunity* **4**, 241-250 (1996).
76. Cattoretti, G., *et al.* Nuclear and cytoplasmic AID in extrafollicular and germinal center B cells. *Blood* **107**, 3967-3975 (2006).
77. Cunningham, A.F., *et al.* Salmonella induces a switched antibody response without germinal centers that impedes the extracellular spread of infection. *J Immunol* **178**, 6200-6207 (2007).
78. Castigli, E., *et al.* TACI and BAFF-R mediate isotype switching in B cells. *J Exp Med* **201**, 35-39 (2005).
79. Xu, W., *et al.* Epithelial cells trigger frontline immunoglobulin class switching through a pathway regulated by the inhibitor SLPI. *Nat Immunol* **8**, 294-303 (2007).
80. He, B., *et al.* Intestinal bacteria trigger T cell-independent immunoglobulin A(2) class switching by inducing epithelial-cell secretion of the cytokine APRIL. *Immunity* **26**, 812-826 (2007).
81. Jacob, J., Kelsoe, G., Rajewsky, K. & Weiss, U. Intraclonal generation of antibody mutants in germinal centres. *Nature* **354**, 389-392 (1991).
82. Berek, C., Berger, A. & Apel, M. Maturation of the immune response in germinal centers. *Cell* **67**, 1121-1129 (1991).
83. Wagner, S.D. & Neuberger, M.S. Somatic hypermutation of immunoglobulin genes. *Annu Rev Immunol* **14**, 441-457 (1996).
84. Odegard, V.H. & Schatz, D.G. Targeting of somatic hypermutation. *Nat Rev Immunol* **6**, 573-583 (2006).
85. Di Noia, J.M. & Neuberger, M.S. Molecular mechanisms of antibody somatic hypermutation. *Annu Rev Biochem* **76**, 1-22 (2007).
86. Lehmann, A.R., *et al.* Translesion synthesis: Y-family polymerases and the polymerase switch. *DNA Repair (Amst)* **6**, 891-899 (2007).
87. Peled, J.U., *et al.* The biochemistry of somatic hypermutation. *Annu Rev Immunol* **26**, 481-511 (2008).
88. MacLennan, I.C., *et al.* Extrafollicular antibody responses. *Immunol Rev* **194**, 8-18 (2003).
89. Cerutti, A., Puga, I. & Cols, M. Innate control of B cell responses. *Trends Immunol* **32**, 202-211 (2011).
90. Chorny, A. & Cerutti, A. A gut triumvirate rules homeostasis. *Nat Med* **17**, 1549-1550 (2011).
91. Dillon, S.R., Gross, J.A., Ansell, S.M. & Novak, A.J. An APRIL to remember: novel TNF ligands as therapeutic targets. *Nat Rev Drug Discov* **5**, 235-246 (2006).

92. Mackay, F. & Schneider, P. Cracking the BAFF code. *Nat Rev Immunol* **9**, 491-502 (2009).
93. Cerutti, A., Cols, M. & Puga, I. Activation of B cells by non-canonical helper signals. *EMBO Rep* **13**, 798-810 (2012).
94. Xu, W.*, et al.* Viral double-stranded RNA triggers Ig class switching by activating upper respiratory mucosa B cells through an innate TLR3 pathway involving BAFF. *J Immunol* **181**, 276-287 (2008).
95. Cols, M.*, et al.* Stromal endothelial cells establish a bidirectional crosstalk with chronic lymphocytic leukemia cells through the TNF-related factors BAFF, APRIL, and CD40L. *J Immunol* **188**, 6071-6083 (2012).
96. He, B.*, et al.* The transmembrane activator TACI triggers immunoglobulin class switching by activating B cells through the adaptor MyD88. *Nat Immunol* **11**, 836-845 (2010).
97. Baumgarth, N. The double life of a B-1 cell: self-reactivity selects for protective effector functions. *Nat Rev Immunol* **11**, 34-46 (2011).
98. Martin, F. & Kearney, J.F. Marginal-zone B cells. *Nat Rev Immunol* **2**, 323-335 (2002).
99. Weill, J.C., Weller, S. & Reynaud, C.A. Human marginal zone B cells. *Annu Rev Immunol* **27**, 267-285 (2009).
100. Bendelac, A., Bonneville, M. & Kearney, J.F. Autoreactivity by design: innate B and T lymphocytes. *Nat Rev Immunol* **1**, 177-186 (2001).
101. Cerutti, A., Cols, M. & Puga, I. Marginal zone B cells: virtues of innate-like antibody-producing lymphocytes. *Nat Rev Immunol* **13**, 118-132 (2013).
102. Descatoire, M., Weill, J.C., Reynaud, C.A. & Weller, S. A human equivalent of mouse B-1 cells? *J Exp Med* **208**, 2563-2564 (2011).
103. Martin, F., Oliver, A.M. & Kearney, J.F. Marginal zone and B1 B cells unite in the early response against T-independent blood-borne particulate antigens. *Immunity* **14**, 617-629 (2001).
104. Steiniger, B.S. Human spleen microanatomy: why mice do not suffice. *Immunology* **145**, 334-346 (2015).
105. Puga, I.*, et al.* B cell-helper neutrophils stimulate the diversification and production of immunoglobulin in the marginal zone of the spleen. *Nat Immunol* **13**, 170-180 (2012).
106. Joo, H.*, et al.* C-type lectin-like receptor LOX-1 promotes dendritic cell-mediated class-switched B cell responses. *Immunity* **41**, 592-604 (2014).

107. Litinskiy, M.B., *et al.* DCs induce CD40-independent immunoglobulin class switching through BLyS and APRIL. *Nat Immunol* **3**, 822-829 (2002).
108. Xu, W., *et al.* Macrophages induce differentiation of plasma cells through CXCL10/IP-10. *J Exp Med* **209**, 1813-1823, S1811-1812 (2012).
109. William, J., Euler, C., Christensen, S. & Shlomchik, M.J. Evolution of autoantibody responses via somatic hypermutation outside of germinal centers. *Science* **297**, 2066-2070 (2002).
110. Weller, S., *et al.* Human blood IgM "memory" B cells are circulating splenic marginal zone B cells harboring a prediversified immunoglobulin repertoire. *Blood* **104**, 3647-3654 (2004).
111. Cerutti, A. The regulation of IgA class switching. *Nat Rev Immunol* **8**, 421-434 (2008).
112. Magri, G., *et al.* Innate lymphoid cells integrate stromal and immunological signals to enhance antibody production by splenic marginal zone B cells. *Nat Immunol* **15**, 354-364 (2014).
113. Steiniger, B., Timphus, E.M. & Barth, P.J. The splenic marginal zone in humans and rodents: an enigmatic compartment and its inhabitants. *Histochem Cell Biol* **126**, 641-648 (2006).
114. Timens, W., Boes, A. & Poppema, S. Human marginal zone B cells are not an activated B cell subset: strong expression of CD21 as a putative mediator for rapid B cell activation. *Eur J Immunol* **19**, 2163-2166 (1989).
115. Kruetzmann, S., *et al.* Human immunoglobulin M memory B cells controlling Streptococcus pneumoniae infections are generated in the spleen. *J Exp Med* **197**, 939-945 (2003).
116. Dunn-Walters, D.K., Isaacson, P.G. & Spencer, J. Analysis of mutations in immunoglobulin heavy chain variable region genes of microdissected marginal zone (MGZ) B cells suggests that the MGZ of human spleen is a reservoir of memory B cells. *J Exp Med* **182**, 559-566 (1995).
117. Klein, U., Rajewsky, K. & Kuppers, R. Human immunoglobulin (Ig)M+IgD+ peripheral blood B cells expressing the CD27 cell surface antigen carry somatically mutated variable region genes: CD27 as a general marker for somatically mutated (memory) B cells. *J Exp Med* **188**, 1679-1689 (1998).
118. Seifert, M. & Kuppers, R. Molecular footprints of a germinal center derivation of human IgM+(IgD+)CD27+ B cells and the dynamics of memory B cell generation. *J Exp Med* **206**, 2659-2669 (2009).
119. Spencer, J., Finn, T., Pulford, K.A., Mason, D.Y. & Isaacson, P.G. The human gut contains a novel population of B

lymphocytes which resemble marginal zone cells. *Clin Exp Immunol* **62**, 607-612 (1985).
120. Tierens, A., Delabie, J., Michiels, L., Vandenberghe, P. & De Wolf-Peeters, C. Marginal-zone B cells in the human lymph node and spleen show somatic hypermutations and display clonal expansion. *Blood* **93**, 226-234 (1999).
121. Dono, M.*, et al.* Heterogeneity of tonsillar subepithelial B lymphocytes, the splenic marginal zone equivalents. *J Immunol* **164**, 5596-5604 (2000).
122. Kurosaki, T., Kometani, K. & Ise, W. Memory B cells. *Nat Rev Immunol* **15**, 149-159 (2015).
123. Ahmed, R. & Gray, D. Immunological memory and protective immunity: understanding their relation. *Science* **272**, 54-60 (1996).
124. Tarlinton, D. B-cell memory: are subsets necessary? *Nat Rev Immunol* **6**, 785-790 (2006).
125. Berkowska, M.A.*, et al.* Human memory B cells originate from three distinct germinal center-dependent and -independent maturation pathways. *Blood* **118**, 2150-2158 (2011).
126. Schwickert, T.A.*, et al.* A dynamic T cell-limited checkpoint regulates affinity-dependent B cell entry into the germinal center. *J Exp Med* **208**, 1243-1252 (2011).
127. Dent, A.L., Shaffer, A.L., Yu, X., Allman, D. & Staudt, L.M. Control of inflammation, cytokine expression, and germinal center formation by BCL-6. *Science* **276**, 589-592 (1997).
128. Fischer, S.F.*, et al.* Proapoptotic BH3-only protein Bim is essential for developmentally programmed death of germinal center-derived memory B cells and antibody-forming cells. *Blood* **110**, 3978-3984 (2007).
129. Clybouw, C.*, et al.* Regulation of memory B-cell survival by the BH3-only protein Puma. *Blood* **118**, 4120-4128 (2011).
130. Tarlinton, D. & Good-Jacobson, K. Diversity among memory B cells: origin, consequences, and utility. *Science* **341**, 1205-1211 (2013).
131. Pape, K.A., Taylor, J.J., Maul, R.W., Gearhart, P.J. & Jenkins, M.K. Different B cell populations mediate early and late memory during an endogenous immune response. *Science* **331**, 1203-1207 (2011).
132. Zuccarino-Catania, G.V.*, et al.* CD80 and PD-L2 define functionally distinct memory B cell subsets that are independent of antibody isotype. *Nat Immunol* **15**, 631-637 (2014).
133. Anderson, S.M., Tomayko, M.M., Ahuja, A., Haberman, A.M. & Shlomchik, M.J. New markers for murine memory B cells that

define mutated and unmutated subsets. *J Exp Med* **204**, 2103-2114 (2007).
134. Taylor, J.J., Pape, K.A. & Jenkins, M.K. A germinal center-independent pathway generates unswitched memory B cells early in the primary response. *J Exp Med* **209**, 597-606 (2012).
135. Kaji, T.*, et al.* Distinct cellular pathways select germline-encoded and somatically mutated antibodies into immunological memory. *J Exp Med* **209**, 2079-2097 (2012).
136. Takemori, T., Kaji, T., Takahashi, Y., Shimoda, M. & Rajewsky, K. Generation of memory B cells inside and outside germinal centers. *Eur J Immunol* **44**, 1258-1264 (2014).
137. Fairfax, K.A., Kallies, A., Nutt, S.L. & Tarlinton, D.M. Plasma cell development: from B-cell subsets to long-term survival niches. *Semin Immunol* **20**, 49-58 (2008).
138. Shlomchik, M.J. & Weisel, F. Germinal center selection and the development of memory B and plasma cells. *Immunol Rev* **247**, 52-63 (2012).
139. Radbruch, A.*, et al.* Competence and competition: the challenge of becoming a long-lived plasma cell. *Nat Rev Immunol* **6**, 741-750 (2006).
140. Shaffer, A.L.*, et al.* Blimp-1 orchestrates plasma cell differentiation by extinguishing the mature B cell gene expression program. *Immunity* **17**, 51-62 (2002).
141. Shaffer, A.L.*, et al.* BCL-6 represses genes that function in lymphocyte differentiation, inflammation, and cell cycle control. *Immunity* **13**, 199-212 (2000).
142. Nutt, S.L., Taubenheim, N., Hasbold, J., Corcoran, L.M. & Hodgkin, P.D. The genetic network controlling plasma cell differentiation. *Semin Immunol* **23**, 341-349 (2011).
143. Basso, K. & Dalla-Favera, R. Roles of BCL6 in normal and transformed germinal center B cells. *Immunol Rev* **247**, 172-183 (2012).
144. Morrison, A.M.*, et al.* Deregulated PAX-5 transcription from a translocated IgH promoter in marginal zone lymphoma. *Blood* **92**, 3865-3878 (1998).
145. Pasqualucci, L.*, et al.* Inactivation of the PRDM1/BLIMP1 gene in diffuse large B cell lymphoma. *J Exp Med* **203**, 311-317 (2006).
146. Afshar-Sterle, S.*, et al.* Fas ligand-mediated immune surveillance by T cells is essential for the control of spontaneous B cell lymphomas. *Nat Med* **20**, 283-290 (2014).
147. Mandelbaum, J.*, et al.* BLIMP1 is a tumor suppressor gene frequently disrupted in activated B cell-like diffuse large B cell lymphoma. *Cancer Cell* **18**, 568-579 (2010).

148. Calado, D.P., *et al.* Constitutive canonical NF-kappaB activation cooperates with disruption of BLIMP1 in the pathogenesis of activated B cell-like diffuse large cell lymphoma. *Cancer Cell* **18**, 580-589 (2010).
149. Lohr, J.G., *et al.* Widespread genetic heterogeneity in multiple myeloma: implications for targeted therapy. *Cancer Cell* **25**, 91-101 (2014).
150. Leung-Hagesteijn, C., *et al.* Xbp1s-negative tumor B cells and pre-plasmablasts mediate therapeutic proteasome inhibitor resistance in multiple myeloma. *Cancer Cell* **24**, 289-304 (2013).
151. Shaffer, A.L., *et al.* IRF4 addiction in multiple myeloma. *Nature* **454**, 226-231 (2008).
152. Fairfax, K.A., *et al.* Different kinetics of blimp-1 induction in B cell subsets revealed by reporter gene. *J Immunol* **178**, 4104-4111 (2007).
153. Genestier, L., *et al.* TLR agonists selectively promote terminal plasma cell differentiation of B cell subsets specialized in thymus-independent responses. *J Immunol* **178**, 7779-7786 (2007).
154. Shapiro-Shelef, M. & Calame, K. Regulation of plasma-cell development. *Nat Rev Immunol* **5**, 230-242 (2005).
155. Kallies, A., *et al.* Plasma cell ontogeny defined by quantitative changes in blimp-1 expression. *J Exp Med* **200**, 967-977 (2004).
156. Angelin-Duclos, C., Cattoretti, G., Lin, K.I. & Calame, K. Commitment of B lymphocytes to a plasma cell fate is associated with Blimp-1 expression in vivo. *J Immunol* **165**, 5462-5471 (2000).
157. Soro, P.G., *et al.* Differential involvement of the transcription factor Blimp-1 in T cell-independent and -dependent B cell differentiation to plasma cells. *J Immunol* **163**, 611-617 (1999).
158. Chu, V.T., *et al.* Eosinophils are required for the maintenance of plasma cells in the bone marrow. *Nat Immunol* **12**, 151-159 (2011).
159. Winter, O., *et al.* Megakaryocytes constitute a functional component of a plasma cell niche in the bone marrow. *Blood* **116**, 1867-1875 (2010).
160. Cassese, G., *et al.* Plasma cell survival is mediated by synergistic effects of cytokines and adhesion-dependent signals. *J Immunol* **171**, 1684-1690 (2003).
161. Xiang, Z., *et al.* FcgammaRIIb controls bone marrow plasma cell persistence and apoptosis. *Nat Immunol* **8**, 419-429 (2007).
162. Macpherson, A.J. & Harris, N.L. Interactions between commensal intestinal bacteria and the immune system. *Nat Rev Immunol* **4**, 478-485 (2004).

163. Cerutti, A., Chen, K. & Chorny, A. Immunoglobulin responses at the mucosal interface. *Annu Rev Immunol* **29**, 273-293 (2011).
164. Mills, S.E. *Histology for pathologists*, (Lippincott Williams & Wilkins, Philadelphia, 2007).
165. Mowat, A.M. & Agace, W.W. Regional specialization within the intestinal immune system. *Nat Rev Immunol* **14**, 667-685 (2014).
166. Cornes, J.S. Number, size, and distribution of Peyer's patches in the human small intestine: Part I The development of Peyer's patches. *Gut* **6**, 225-229 (1965).
167. Shan, M.*, et al.* Mucus enhances gut homeostasis and oral tolerance by delivering immunoregulatory signals. *Science* **342**, 447-453 (2013).
168. Johansson, M.E., Larsson, J.M. & Hansson, G.C. The two mucus layers of colon are organized by the MUC2 mucin, whereas the outer layer is a legislator of host-microbial interactions. *Proc Natl Acad Sci U S A* **108 Suppl 1**, 4659-4665 (2011).
169. Yoshida, H.*, et al.* IL-7 receptor alpha+ CD3(-) cells in the embryonic intestine induces the organizing center of Peyer's patches. *Int Immunol* **11**, 643-655 (1999).
170. Eberl, G. & Littman, D.R. The role of the nuclear hormone receptor RORgammat in the development of lymph nodes and Peyer's patches. *Immunol Rev* **195**, 81-90 (2003).
171. Eberl, G.*, et al.* An essential function for the nuclear receptor RORgamma(t) in the generation of fetal lymphoid tissue inducer cells. *Nat Immunol* **5**, 64-73 (2004).
172. Spits, H.*, et al.* Innate lymphoid cells--a proposal for uniform nomenclature. *Nat Rev Immunol* **13**, 145-149 (2013).
173. Jung, C., Hugot, J.P. & Barreau, F. Peyer's Patches: The Immune Sensors of the Intestine. *Int J Inflam* **2010**, 823710 (2010).
174. Mabbott, N.A., Donaldson, D.S., Ohno, H., Williams, I.R. & Mahajan, A. Microfold (M) cells: important immunosurveillance posts in the intestinal epithelium. *Mucosal Immunol* **6**, 666-677 (2013).
175. Owen, R.L., Piazza, A.J. & Ermak, T.H. Ultrastructural and cytoarchitectural features of lymphoreticular organs in the colon and rectum of adult BALB/c mice. *Am J Anat* **190**, 10-18 (1991).
176. Perry, G.A. & Sharp, J.G. Characterization of proximal colonic lymphoid tissue in the mouse. *Anat Rec* **220**, 305-312 (1988).
177. Hamada, H.*, et al.* Identification of multiple isolated lymphoid follicles on the antimesenteric wall of the mouse small intestine. *J Immunol* **168**, 57-64 (2002).
178. Trepel, F. Number and distribution of lymphocytes in man. A critical analysis. *Klin Wochenschr* **52**, 511-515 (1974).

179. Moghaddami, M., Cummins, A. & Mayrhofer, G. Lymphocyte-filled villi: comparison with other lymphoid aggregations in the mucosa of the human small intestine. *Gastroenterology* **115**, 1414-1425 (1998).
180. O'Leary, A.D. & Sweeney, E.C. Lymphoglandular complexes of the colon: structure and distribution. *Histopathology* **10**, 267-283 (1986).
181. Kanamori, Y.*, et al.* Identification of novel lymphoid tissues in murine intestinal mucosa where clusters of c-kit+ IL-7R+ Thy1+ lympho-hemopoietic progenitors develop. *J Exp Med* **184**, 1449-1459 (1996).
182. Taylor, R.T., Lugering, A., Newell, K.A. & Williams, I.R. Intestinal cryptopatch formation in mice requires lymphotoxin alpha and the lymphotoxin beta receptor. *J Immunol* **173**, 7183-7189 (2004).
183. Bouskra, D.*, et al.* Lymphoid tissue genesis induced by commensals through NOD1 regulates intestinal homeostasis. *Nature* **456**, 507-510 (2008).
184. Pabst, O.*, et al.* Adaptation of solitary intestinal lymphoid tissue in response to microbiota and chemokine receptor CCR7 signaling. *J Immunol* **177**, 6824-6832 (2006).
185. Tsuji, M.*, et al.* Requirement for lymphoid tissue-inducer cells in isolated follicle formation and T cell-independent immunoglobulin A generation in the gut. *Immunity* **29**, 261-271 (2008).
186. Brandtzaeg, P. & Johansen, F.E. Mucosal B cells: phenotypic characteristics, transcriptional regulation, and homing properties. *Immunol Rev* **206**, 32-63 (2005).
187. Maynard, C.L. & Weaver, C.T. Intestinal effector T cells in health and disease. *Immunity* **31**, 389-400 (2009).
188. Murphy, K.M. & Stockinger, B. Effector T cell plasticity: flexibility in the face of changing circumstances. *Nat Immunol* **11**, 674-680 (2010).
189. Weaver, C.T., Hatton, R.D., Mangan, P.R. & Harrington, L.E. IL-17 family cytokines and the expanding diversity of effector T cell lineages. *Annu Rev Immunol* **25**, 821-852 (2007).
190. Maynard, C.L.*, et al.* Regulatory T cells expressing interleukin 10 develop from Foxp3+ and Foxp3- precursor cells in the absence of interleukin 10. *Nat Immunol* **8**, 931-941 (2007).
191. Ziegler, S.F. & Buckner, J.H. Influence of FOXP3 on CD4+CD25+ regulatory T cells. *Expert Rev Clin Immunol* **2**, 639-647 (2006).

192. Bilate, A.M. & Lafaille, J.J. Induced CD4+Foxp3+ regulatory T cells in immune tolerance. *Annu Rev Immunol* **30**, 733-758 (2012).
193. Artis, D. & Spits, H. The biology of innate lymphoid cells. *Nature* **517**, 293-301 (2015).
194. Yagi, R.*, et al.* The transcription factor GATA3 is critical for the development of all IL-7Ralpha-expressing innate lymphoid cells. *Immunity* **40**, 378-388 (2014).
195. Klose, C.S.*, et al.* Differentiation of type 1 ILCs from a common progenitor to all helper-like innate lymphoid cell lineages. *Cell* **157**, 340-356 (2014).
196. Constantinides, M.G., McDonald, B.D., Verhoef, P.A. & Bendelac, A. A committed precursor to innate lymphoid cells. *Nature* **508**, 397-401 (2014).
197. Bernink, J.H.*, et al.* Human type 1 innate lymphoid cells accumulate in inflamed mucosal tissues. *Nat Immunol* **14**, 221-229 (2013).
198. Hoyler, T.*, et al.* The transcription factor GATA-3 controls cell fate and maintenance of type 2 innate lymphoid cells. *Immunity* **37**, 634-648 (2012).
199. Moro, K.*, et al.* Innate production of T(H)2 cytokines by adipose tissue-associated c-Kit(+)Sca-1(+) lymphoid cells. *Nature* **463**, 540-544 (2010).
200. Cella, M.*, et al.* A human natural killer cell subset provides an innate source of IL-22 for mucosal immunity. *Nature* **457**, 722-725 (2009).
201. Sawa, S.*, et al.* Lineage relationship analysis of RORgammat+ innate lymphoid cells. *Science* **330**, 665-669 (2010).
202. Sonnenberg, G.F., Monticelli, L.A., Elloso, M.M., Fouser, L.A. & Artis, D. CD4(+) lymphoid tissue-inducer cells promote innate immunity in the gut. *Immunity* **34**, 122-134 (2011).
203. Vonarbourg, C.*, et al.* Regulated expression of nuclear receptor RORgammat confers distinct functional fates to NK cell receptor-expressing RORgammat(+) innate lymphocytes. *Immunity* **33**, 736-751 (2010).
204. McKenzie, A.N., Spits, H. & Eberl, G. Innate lymphoid cells in inflammation and immunity. *Immunity* **41**, 366-374 (2014).
205. Cerovic, V., Bain, C.C., Mowat, A.M. & Milling, S.W. Intestinal macrophages and dendritic cells: what's the difference? *Trends Immunol* **35**, 270-277 (2014).
206. Persson, E.K., Jaensson, E. & Agace, W.W. The diverse ontogeny and function of murine small intestinal dendritic cell/macrophage subsets. *Immunobiology* **215**, 692-697 (2010).

207. Nagashima, R., Maeda, K., Imai, Y. & Takahashi, T. Lamina propria macrophages in the human gastrointestinal mucosa: their distribution, immunohistological phenotype, and function. *J Histochem Cytochem* **44**, 721-731 (1996).
208. Ueda, Y.*, et al.* Commensal microbiota induce LPS hyporesponsiveness in colonic macrophages via the production of IL-10. *Int Immunol* **22**, 953-962 (2010).
209. Varol, C., Zigmond, E. & Jung, S. Securing the immune tightrope: mononuclear phagocytes in the intestinal lamina propria. *Nat Rev Immunol* **10**, 415-426 (2010).
210. McDole, J.R.*, et al.* Goblet cells deliver luminal antigen to CD103+ dendritic cells in the small intestine. *Nature* **483**, 345-349 (2012).
211. Iwata, M.*, et al.* Retinoic acid imprints gut-homing specificity on T cells. *Immunity* **21**, 527-538 (2004).
212. Johansson-Lindbom, B.*, et al.* Functional specialization of gut CD103+ dendritic cells in the regulation of tissue-selective T cell homing. *J Exp Med* **202**, 1063-1073 (2005).
213. Jaensson, E.*, et al.* Small intestinal CD103+ dendritic cells display unique functional properties that are conserved between mice and humans. *J Exp Med* **205**, 2139-2149 (2008).
214. Uematsu, S.*, et al.* Regulation of humoral and cellular gut immunity by lamina propria dendritic cells expressing Toll-like receptor 5. *Nat Immunol* **9**, 769-776 (2008).
215. Schulz, O.*, et al.* Intestinal CD103+, but not CX3CR1+, antigen sampling cells migrate in lymph and serve classical dendritic cell functions. *J Exp Med* **206**, 3101-3114 (2009).
216. Diehl, G.E.*, et al.* Microbiota restricts trafficking of bacteria to mesenteric lymph nodes by CX(3)CR1(hi) cells. *Nature* **494**, 116-120 (2013).
217. Niess, J.H.*, et al.* CX3CR1-mediated dendritic cell access to the intestinal lumen and bacterial clearance. *Science* **307**, 254-258 (2005).
218. Rescigno, M.*, et al.* Dendritic cells express tight junction proteins and penetrate gut epithelial monolayers to sample bacteria. *Nat Immunol* **2**, 361-367 (2001).
219. Mishra, A., Hogan, S.P., Lee, J.J., Foster, P.S. & Rothenberg, M.E. Fundamental signals that regulate eosinophil homing to the gastrointestinal tract. *J Clin Invest* **103**, 1719-1727 (1999).
220. Bischoff, S.C. Physiological and pathophysiological functions of intestinal mast cells. *Semin Immunopathol* **31**, 185-205 (2009).
221. Miller, H.R. & Pemberton, A.D. Tissue-specific expression of mast cell granule serine proteinases and their role in inflammation in the lung and gut. *Immunology* **105**, 375-390 (2002).

222. Macpherson, A.J., Geuking, M.B., Slack, E., Hapfelmeier, S. & McCoy, K.D. The habitat, double life, citizenship, and forgetfulness of IgA. *Immunol Rev* **245**, 132-146 (2012).
223. Macpherson, A.J., Hunziker, L., McCoy, K. & Lamarre, A. IgA responses in the intestinal mucosa against pathogenic and non-pathogenic microorganisms. *Microbes Infect* **3**, 1021-1035 (2001).
224. Swarbrick, E.T., Stokes, C.R. & Soothill, J.F. Absorption of antigens after oral immunisation and the simultaneous induction of specific systemic tolerance. *Gut* **20**, 121-125 (1979).
225. Worbs, T.*, et al.* Oral tolerance originates in the intestinal immune system and relies on antigen carriage by dendritic cells. *J Exp Med* **203**, 519-527 (2006).
226. Pierce, N.F. & Gowans, J.L. Cellular kinetics of the intestinal immune response to cholera toxoid in rats. *J Exp Med* **142**, 1550-1563 (1975).
227. Macpherson, A.J., Geuking, M.B. & McCoy, K.D. Immune responses that adapt the intestinal mucosa to commensal intestinal bacteria. *Immunology* **115**, 153-162 (2005).
228. Ahmed, S.*, et al.* Mucosa-associated bacterial diversity in relation to human terminal ileum and colonic biopsy samples. *Appl Environ Microbiol* **73**, 7435-7442 (2007).
229. Eckburg, P.B.*, et al.* Diversity of the human intestinal microbial flora. *Science* **308**, 1635-1638 (2005).
230. Hill, D.A. & Artis, D. Intestinal bacteria and the regulation of immune cell homeostasis. *Annu Rev Immunol* **28**, 623-667 (2010).
231. Sansonetti, P.J. War and peace at mucosal surfaces. *Nat Rev Immunol* **4**, 953-964 (2004).
232. Belkaid, Y. & Hand, T.W. Role of the microbiota in immunity and inflammation. *Cell* **157**, 121-141 (2014).
233. Cerutti, A.*, et al.* Regulation of mucosal IgA responses: lessons from primary immunodeficiencies. *Ann N Y Acad Sci* **1238**, 132-144 (2011).
234. Mestecky, J., Russell, M.W. & Elson, C.O. Intestinal IgA: novel views on its function in the defence of the largest mucosal surface. *Gut* **44**, 2-5 (1999).
235. Macpherson, A.J., McCoy, K.D., Johansen, F.E. & Brandtzaeg, P. The immune geography of IgA induction and function. *Mucosal Immunol* **1**, 11-22 (2008).
236. Gibbons, D.L. & Spencer, J. Mouse and human intestinal immunity: same ballpark, different players; different rules, same score. *Mucosal Immunol* **4**, 148-157 (2011).
237. Pabst, O. New concepts in the generation and functions of IgA. *Nat Rev Immunol* **12**, 821-832 (2012).

238. Flanagan, J.G., Lefranc, M.P. & Rabbitts, T.H. Mechanisms of divergence and convergence of the human immunoglobulin alpha 1 and alpha 2 constant region gene sequences. *Cell* **36**, 681-688 (1984).
239. Plaut, A.G., Wistar, R., Jr. & Capra, J.D. Differential susceptibility of human IgA immunoglobulins to streptococcal IgA protease. *J Clin Invest* **54**, 1295-1300 (1974).
240. Bonner, A., Almogren, A., Furtado, P.B., Kerr, M.A. & Perkins, S.J. The nonplanar secretory IgA2 and near planar secretory IgA1 solution structures rationalize their different mucosal immune responses. *J Biol Chem* **284**, 5077-5087 (2009).
241. Brandtzaeg, P. Presence of J chain in human immunocytes containing various immunoglobulin classes. *Nature* **252**, 418-420 (1974).
242. Brandtzaeg, P., Baekkevold, E.S. & Morton, H.C. From B to A the mucosal way. *Nat Immunol* **2**, 1093-1094 (2001).
243. Fagarasan, S. Intestinal IgA synthesis: a primitive form of adaptive immunity that regulates microbial communities in the gut. *Curr Top Microbiol Immunol* **308**, 137-153 (2006).
244. Mostov, K.E. & Simister, N.E. Transcytosis. *Cell* **43**, 389-390 (1985).
245. Corthesy, B. Multi-faceted functions of secretory IgA at mucosal surfaces. *Front Immunol* **4**, 185 (2013).
246. Duc, M., Johansen, F.E. & Corthesy, B. Antigen binding to secretory immunoglobulin A results in decreased sensitivity to intestinal proteases and increased binding to cellular Fc receptors. *J Biol Chem* **285**, 953-960 (2010).
247. Mantis, N.J. & Forbes, S.J. Secretory IgA: arresting microbial pathogens at epithelial borders. *Immunol Invest* **39**, 383-406 (2010).
248. Forbes, S.J., Eschmann, M. & Mantis, N.J. Inhibition of Salmonella enterica serovar typhimurium motility and entry into epithelial cells by a protective antilipopolysaccharide monoclonal immunoglobulin A antibody. *Infect Immun* **76**, 4137-4144 (2008).
249. Forbes, S.J., Bumpus, T., McCarthy, E.A., Corthesy, B. & Mantis, N.J. Transient suppression of Shigella flexneri type 3 secretion by a protective O-antigen-specific monoclonal IgA. *MBio* **2**, e00042-00011 (2011).
250. Kadaoui, K.A. & Corthesy, B. Secretory IgA mediates bacterial translocation to dendritic cells in mouse Peyer's patches with restriction to mucosal compartment. *J Immunol* **179**, 7751-7757 (2007).

251. Mantis, N.J., Rol, N. & Corthesy, B. Secretory IgA's complex roles in immunity and mucosal homeostasis in the gut. *Mucosal Immunol* **4**, 603-611 (2011).
252. Harriman, G.R*., et al.* Targeted deletion of the IgA constant region in mice leads to IgA deficiency with alterations in expression of other Ig isotypes. *J Immunol* **162**, 2521-2529 (1999).
253. Yel, L. Selective IgA deficiency. *J Clin Immunol* **30**, 10-16 (2010).
254. Macpherson, A.J., Koller, Y. & McCoy, K.D. The bilateral responsiveness between intestinal microbes and IgA. *Trends Immunol* **36**, 460-470 (2015).
255. Palm, N.W*., et al.* Immunoglobulin A coating identifies colitogenic bacteria in inflammatory bowel disease. *Cell* **158**, 1000-1010 (2014).
256. Suzuki, K., Kawamoto, S., Maruya, M. & Fagarasan, S. GALT: organization and dynamics leading to IgA synthesis. *Adv Immunol* **107**, 153-185 (2010).
257. Benveniste, J., Lespinats, G. & Salomon, J. Serum and secretory IgA in axenic and holoxenic mice. *J Immunol* **107**, 1656-1662 (1971).
258. Benveniste, J., Lespinats, G., Adam, C. & Salomon, J.C. Immunoglobulins in intact, immunized, and contaminated axenic mice: study of serum IgA. *J Immunol* **107**, 1647-1655 (1971).
259. Moreau, M.C., Ducluzeau, R., Guy-Grand, D. & Muller, M.C. Increase in the population of duodenal immunoglobulin A plasmocytes in axenic mice associated with different living or dead bacterial strains of intestinal origin. *Infect Immun* **21**, 532-539 (1978).
260. Macpherson, A.J*., et al.* A primitive T cell-independent mechanism of intestinal mucosal IgA responses to commensal bacteria. *Science* **288**, 2222-2226 (2000).
261. Lycke, N., Eriksen, L. & Holmgren, J. Protection against cholera toxin after oral immunization is thymus-dependent and associated with intestinal production of neutralizing IgA antitoxin. *Scand J Immunol* **25**, 413-419 (1987).
262. Suzuki, K. & Fagarasan, S. How host-bacterial interactions lead to IgA synthesis in the gut. *Trends Immunol* **29**, 523-531 (2008).
263. Cerutti, A. & Rescigno, M. The biology of intestinal immunoglobulin A responses. *Immunity* **28**, 740-750 (2008).
264. Fagarasan, S., Kawamoto, S., Kanagawa, O. & Suzuki, K. Adaptive immune regulation in the gut: T cell-dependent and T cell-independent IgA synthesis. *Annu Rev Immunol* **28**, 243-273 (2010).

265. Cazac, B.B. & Roes, J. TGF-beta receptor controls B cell responsiveness and induction of IgA in vivo. *Immunity* **13**, 443-451 (2000).
266. Hirota, K.*, et al.* Plasticity of Th17 cells in Peyer's patches is responsible for the induction of T cell-dependent IgA responses. *Nat Immunol* **14**, 372-379 (2013).
267. Avery, D.T., Bryant, V.L., Ma, C.S., de Waal Malefyt, R. & Tangye, S.G. IL-21-induced isotype switching to IgG and IgA by human naive B cells is differentially regulated by IL-4. *J Immunol* **181**, 1767-1779 (2008).
268. Bryant, V.L.*, et al.* Cytokine-mediated regulation of human B cell differentiation into Ig-secreting cells: predominant role of IL-21 produced by CXCR5+ T follicular helper cells. *J Immunol* **179**, 8180-8190 (2007).
269. Seo, G.Y., Youn, J. & Kim, P.H. IL-21 ensures TGF-beta 1-induced IgA isotype expression in mouse Peyer's patches. *J Leukoc Biol* **85**, 744-750 (2009).
270. Tokuyama, H. & Tokuyama, Y. The regulatory effects of all-trans-retinoic acid on isotype switching: retinoic acid induces IgA switch rearrangement in cooperation with IL-5 and inhibits IgG1 switching. *Cell Immunol* **192**, 41-47 (1999).
271. Sato, A.*, et al.* CD11b+ Peyer's patch dendritic cells secrete IL-6 and induce IgA secretion from naive B cells. *J Immunol* **171**, 3684-3690 (2003).
272. Defrance, T.*, et al.* Interleukin 10 and transforming growth factor beta cooperate to induce anti-CD40-activated naive human B cells to secrete immunoglobulin A. *J Exp Med* **175**, 671-682 (1992).
273. Masahata, K.*, et al.* Generation of colonic IgA-secreting cells in the caecal patch. *Nat Commun* **5**, 3704 (2014).
274. Tezuka, H.*, et al.* Prominent role for plasmacytoid dendritic cells in mucosal T cell-independent IgA induction. *Immunity* **34**, 247-257 (2011).
275. Gourzi, P., Leonova, T. & Papavasiliou, F.N. Viral induction of AID is independent of the interferon and the Toll-like receptor signaling pathways but requires NF-kappaB. *J Exp Med* **204**, 259-265 (2007).
276. He, B., Qiao, X. & Cerutti, A. CpG DNA induces IgG class switch DNA recombination by activating human B cells through an innate pathway that requires TLR9 and cooperates with IL-10. *J Immunol* **173**, 4479-4491 (2004).
277. Berkowska, M.A.*, et al.* Circulating Human CD27-IgA+ Memory B Cells Recognize Bacteria with Polyreactive Igs. *J Immunol* **195**, 1417-1426 (2015).

278. Tezuka, H.*, et al.* Regulation of IgA production by naturally occurring TNF/iNOS-producing dendritic cells. *Nature* **448**, 929-933 (2007).
279. Jang, M.H.*, et al.* Intestinal villous M cells: an antigen entry site in the mucosal epithelium. *Proc Natl Acad Sci U S A* **101**, 6110-6115 (2004).
280. Massacand, J.C.*, et al.* Intestinal bacteria condition dendritic cells to promote IgA production. *PLoS One* **3**, e2588 (2008).
281. Nardelli, B.*, et al.* Synthesis and release of B-lymphocyte stimulator from myeloid cells. *Blood* **97**, 198-204 (2001).
282. Craxton, A., Magaletti, D., Ryan, E.J. & Clark, E.A. Macrophage- and dendritic cell--dependent regulation of human B-cell proliferation requires the TNF family ligand BAFF. *Blood* **101**, 4464-4471 (2003).
283. Suzuki, K.*, et al.* The sensing of environmental stimuli by follicular dendritic cells promotes immunoglobulin A generation in the gut. *Immunity* **33**, 71-83 (2010).
284. Kruglov, A.A.*, et al.* Nonredundant function of soluble LTalpha3 produced by innate lymphoid cells in intestinal homeostasis. *Science* **342**, 1243-1246 (2013).
285. Rimoldi, M.*, et al.* Intestinal immune homeostasis is regulated by the crosstalk between epithelial cells and dendritic cells. *Nat Immunol* **6**, 507-514 (2005).
286. Peterson, D.A., McNulty, N.P., Guruge, J.L. & Gordon, J.I. IgA response to symbiotic bacteria as a mediator of gut homeostasis. *Cell Host Microbe* **2**, 328-339 (2007).
287. Benckert, J.*, et al.* The majority of intestinal IgA+ and IgG+ plasmablasts in the human gut are antigen-specific. *J Clin Invest* **121**, 1946-1955 (2011).
288. Washington, K., Stenzel, T.T., Buckley, R.H. & Gottfried, M.R. Gastrointestinal pathology in patients with common variable immunodeficiency and X-linked agammaglobulinemia. *Am J Surg Pathol* **20**, 1240-1252 (1996).
289. Jesus, A.A., Duarte, A.J. & Oliveira, J.B. Autoimmunity in hyper-IgM syndrome. *J Clin Immunol* **28 Suppl 1**, S62-66 (2008).
290. Malamut, G.*, et al.* The enteropathy associated with common variable immunodeficiency: the delineated frontiers with celiac disease. *Am J Gastroenterol* **105**, 2262-2275 (2010).
291. Knight, A.K. & Cunningham-Rundles, C. Inflammatory and autoimmune complications of common variable immune deficiency. *Autoimmun Rev* **5**, 156-159 (2006).
292. Cunningham-Rundles, C. Physiology of IgA and IgA deficiency. *J Clin Immunol* **21**, 303-309 (2001).

293. Agarwal, S., Smereka, P., Harpaz, N., Cunningham-Rundles, C. & Mayer, L. Characterization of immunologic defects in patients with common variable immunodeficiency (CVID) with intestinal disease. *Inflamm Bowel Dis* **17**, 251-259 (2011).
294. de Villartay, J.P., Fischer, A. & Durandy, A. The mechanisms of immune diversification and their disorders. *Nat Rev Immunol* **3**, 962-972 (2003).
295. Cunningham-Rundles, C. & Ponda, P.P. Molecular defects in T- and B-cell primary immunodeficiency diseases. *Nat Rev Immunol* **5**, 880-892 (2005).
296. Bastlein, C.*, et al.* Common variable immunodeficiency syndrome and nodular lymphoid hyperplasia in the small intestine. *Endoscopy* **20**, 272-275 (1988).
297. Fagarasan, S. & Honjo, T. Intestinal IgA synthesis: regulation of front-line body defences. *Nat Rev Immunol* **3**, 63-72 (2003).
298. Castigli, E.*, et al.* Reexamining the role of TACI coding variants in common variable immunodeficiency and selective IgA deficiency. *Nat Genet* **39**, 430-431 (2007).
299. Castigli, E.*, et al.* TACI is mutant in common variable immunodeficiency and IgA deficiency. *Nat Genet* **37**, 829-834 (2005).
300. Salzer, U.*, et al.* Mutations in TNFRSF13B encoding TACI are associated with common variable immunodeficiency in humans. *Nat Genet* **37**, 820-828 (2005).
301. Zhang, L.*, et al.* Transmembrane activator and calcium-modulating cyclophilin ligand interactor mutations in common variable immunodeficiency: clinical and immunologic outcomes in heterozygotes. *J Allergy Clin Immunol* **120**, 1178-1185 (2007).
302. Vander Heiden, J.A.*, et al.* pRESTO: a toolkit for processing high-throughput sequencing raw reads of lymphocyte receptor repertoires. *Bioinformatics* **30**, 1930-1932 (2014).
303. Ye, J., Ma, N., Madden, T.L. & Ostell, J.M. IgBLAST: an immunoglobulin variable domain sequence analysis tool. *Nucleic Acids Res* **41**, W34-40 (2013).
304. Gupta, N.T.*, et al.* Change-O: a toolkit for analyzing large-scale B cell immunoglobulin repertoire sequencing data. *Bioinformatics* **31**, 3356-3358 (2015).
305. Zhang, H., Meltzer, P. & Davis, S. RCircos: an R package for Circos 2D track plots. *BMC Bioinformatics* **14**, 244 (2013).
306. Barak, M., Zuckerman, N.S., Edelman, H., Unger, R. & Mehr, R. IgTree: creating Immunoglobulin variable region gene lineage trees. *J Immunol Methods* **338**, 67-74 (2008).
307. van Zelm, M.C., Szczepanski, T., van der Burg, M. & van Dongen, J.J. Replication history of B lymphocytes reveals

homeostatic proliferation and extensive antigen-induced B cell expansion. *J Exp Med* **204**, 645-655 (2007).
308. Iliev, I.D.*, et al.* Interactions between commensal fungi and the C-type lectin receptor Dectin-1 influence colitis. *Science* **336**, 1314-1317 (2012).
309. Lindner, C.*, et al.* Diversification of memory B cells drives the continuous adaptation of secretory antibodies to gut microbiota. *Nat Immunol* **16**, 880-888 (2015).
310. Farstad, I.N.*, et al.* Human intestinal B-cell blasts and plasma cells express the mucosal homing receptor integrin alpha 4 beta 7. *Scand J Immunol* **42**, 662-672 (1995).
311. Pabst, O.*, et al.* Chemokine receptor CCR9 contributes to the localization of plasma cells to the small intestine. *J Exp Med* **199**, 411-416 (2004).
312. Okada, T.*, et al.* Chemokine requirements for B cell entry to lymph nodes and Peyer's patches. *J Exp Med* **196**, 65-75 (2002).
313. Toyama, H.*, et al.* Memory B cells without somatic hypermutation are generated from Bcl6-deficient B cells. *Immunity* **17**, 329-339 (2002).
314. Obukhanych, T.V. & Nussenzweig, M.C. T-independent type II immune responses generate memory B cells. *J Exp Med* **203**, 305-310 (2006).
315. Oliver, A.M., Martin, F., Gartland, G.L., Carter, R.H. & Kearney, J.F. Marginal zone B cells exhibit unique activation, proliferative and immunoglobulin secretory responses. *Eur J Immunol* **27**, 2366-2374 (1997).
316. Agematsu, K.*, et al.* Absence of IgD-CD27(+) memory B cell population in X-linked hyper-IgM syndrome. *J Clin Invest* **102**, 853-860 (1998).
317. Notarangelo, L.D., Duse, M. & Ugazio, A.G. Immunodeficiency with hyper-IgM (HIM). *Immunodefic Rev* **3**, 101-121 (1992).
318. Kobata, T.*, et al.* CD27-CD70 interactions regulate B-cell activation by T cells. *Proc Natl Acad Sci U S A* **92**, 11249-11253 (1995).
319. Mizoguchi, A., Mizoguchi, E., Takedatsu, H., Blumberg, R.S. & Bhan, A.K. Chronic intestinal inflammatory condition generates IL-10-producing regulatory B cell subset characterized by CD1d upregulation. *Immunity* **16**, 219-230 (2002).
320. Mauri, C., Gray, D., Mushtaq, N. & Londei, M. Prevention of arthritis by interleukin 10-producing B cells. *J Exp Med* **197**, 489-501 (2003).
321. Mauri, C. & Menon, M. The expanding family of regulatory B cells. *Int Immunol* **27**, 479-486 (2015).

322. Ehrhardt, G.R.*, et al.* Expression of the immunoregulatory molecule FcRH4 defines a distinctive tissue-based population of memory B cells. *J Exp Med* **202**, 783-791 (2005).
323. Falini, B.*, et al.* Expression of the IRTA1 receptor identifies intraepithelial and subepithelial marginal zone B cells of the mucosa-associated lymphoid tissue (MALT). *Blood* **102**, 3684-3692 (2003).
324. Ehrhardt, G.R.*, et al.* Discriminating gene expression profiles of memory B cell subpopulations. *J Exp Med* **205**, 1807-1817 (2008).
325. Wiken, M., Bjorck, P., Axelsson, B. & Perlmann, P. Induction of CD43 expression during activation and terminal differentiation of human B cells. *Scand J Immunol* **28**, 457-464 (1988).
326. Rubtsov, A.V.*, et al.* CD11c-Expressing B Cells Are Located at the T Cell/B Cell Border in Spleen and Are Potent APCs. *J Immunol* **195**, 71-79 (2015).
327. Jackson, T.A., Haga, C.L., Ehrhardt, G.R., Davis, R.S. & Cooper, M.D. FcR-like 2 Inhibition of B cell receptor-mediated activation of B cells. *J Immunol* **185**, 7405-7412 (2010).
328. de la Fuente-Garcia, M.A.*, et al.* CD148 is a membrane protein tyrosine phosphatase present in all hematopoietic lineages and is involved in signal transduction on lymphocytes. *Blood* **91**, 2800-2809 (1998).
329. Ettinger, R.*, et al.* IL-21 induces differentiation of human naive and memory B cells into antibody-secreting plasma cells. *J Immunol* **175**, 7867-7879 (2005).
330. Engels, N.*, et al.* The immunoglobulin tail tyrosine motif upgrades memory-type BCRs by incorporating a Grb2-Btk signalling module. *Nat Commun* **5**, 5456 (2014).
331. Elgueta, R.*, et al.* Molecular mechanism and function of CD40/CD40L engagement in the immune system. *Immunol Rev* **229**, 152-172 (2009).
332. Noelle, R.J.*, et al.* A 39-kDa protein on activated helper T cells binds CD40 and transduces the signal for cognate activation of B cells. *Proc Natl Acad Sci U S A* **89**, 6550-6554 (1992).
333. Hartmann, G. & Krieg, A.M. Mechanism and function of a newly identified CpG DNA motif in human primary B cells. *J Immunol* **164**, 944-953 (2000).
334. Bernasconi, N.L., Traggiai, E. & Lanzavecchia, A. Maintenance of serological memory by polyclonal activation of human memory B cells. *Science* **298**, 2199-2202 (2002).
335. Katsenelson, N.*, et al.* Synthetic CpG oligodeoxynucleotides augment BAFF- and APRIL-mediated immunoglobulin secretion. *Eur J Immunol* **37**, 1785-1795 (2007).

336. Schneider, P. The role of APRIL and BAFF in lymphocyte activation. *Curr Opin Immunol* **17**, 282-289 (2005).
337. Hieshima, K.*, et al.* CC chemokine ligands 25 and 28 play essential roles in intestinal extravasation of IgA antibody-secreting cells. *J Immunol* **173**, 3668-3675 (2004).
338. Medina, F., Segundo, C., Campos-Caro, A., Gonzalez-Garcia, I. & Brieva, J.A. The heterogeneity shown by human plasma cells from tonsil, blood, and bone marrow reveals graded stages of increasing maturity, but local profiles of adhesion molecule expression. *Blood* **99**, 2154-2161 (2002).
339. O'Connor, B.P.*, et al.* BCMA is essential for the survival of long-lived bone marrow plasma cells. *J Exp Med* **199**, 91-98 (2004).
340. Shaffer, A.L.*, et al.* XBP1, downstream of Blimp-1, expands the secretory apparatus and other organelles, and increases protein synthesis in plasma cell differentiation. *Immunity* **21**, 81-93 (2004).
341. Klein, U.*, et al.* Transcription factor IRF4 controls plasma cell differentiation and class-switch recombination. *Nat Immunol* **7**, 773-782 (2006).
342. Pabst, O., Cerovic, V. & Hornef, M. Secretory IgA in the Coordination of Establishment and Maintenance of the Microbiota. *Trends Immunol* **37**, 287-296 (2016).
343. Johansen, F.E., Braathen, R. & Brandtzaeg, P. The J chain is essential for polymeric Ig receptor-mediated epithelial transport of IgA. *J Immunol* **167**, 5185-5192 (2001).
344. Corthesy, B. Role of secretory immunoglobulin A and secretory component in the protection of mucosal surfaces. *Future Microbiol* **5**, 817-829 (2010).
345. Donaldson, G.P., Lee, S.M. & Mazmanian, S.K. Gut biogeography of the bacterial microbiota. *Nat Rev Microbiol* **14**, 20-32 (2016).
346. Maruyama, M., Lam, K.P. & Rajewsky, K. Memory B-cell persistence is independent of persisting immunizing antigen. *Nature* **407**, 636-642 (2000).
347. Tangye, S.G., Avery, D.T., Deenick, E.K. & Hodgkin, P.D. Intrinsic differences in the proliferation of naive and memory human B cells as a mechanism for enhanced secondary immune responses. *J Immunol* **170**, 686-694 (2003).
348. Davey, A.M. & Pierce, S.K. Intrinsic differences in the initiation of B cell receptor signaling favor responses of human IgG(+) memory B cells over IgM(+) naive B cells. *J Immunol* **188**, 3332-3341 (2012).

349. Gitlin, A.D.*, et al.* Independent Roles of Switching and Hypermutation in the Development and Persistence of B Lymphocyte Memory. *Immunity* **44**, 769-781 (2016).
350. Shinnakasu, R.*, et al.* Regulated selection of germinal-center cells into the memory B cell compartment. *Nat Immunol* (2016).
351. Reynaud, C.A.*, et al.* IgM memory B cells: a mouse/human paradox. *Cell Mol Life Sci* **69**, 1625-1634 (2012).
352. Sanz, I., Wei, C., Lee, F.E. & Anolik, J. Phenotypic and functional heterogeneity of human memory B cells. *Semin Immunol* **20**, 67-82 (2008).
353. Fecteau, J.F., Cote, G. & Neron, S. A new memory CD27-IgG+ B cell population in peripheral blood expressing VH genes with low frequency of somatic mutation. *J Immunol* **177**, 3728-3736 (2006).
354. Farzan, M.*, et al.* Two orphan seven-transmembrane segment receptors which are expressed in CD4-positive cells support simian immunodeficiency virus infection. *J Exp Med* **186**, 405-411 (1997).
355. Kim, S.V.*, et al.* GPR15-mediated homing controls immune homeostasis in the large intestine mucosa. *Science* **340**, 1456-1459 (2013).
356. Wilson, T.J., Fuchs, A. & Colonna, M. Cutting edge: human FcRL4 and FcRL5 are receptors for IgA and IgG. *J Immunol* **188**, 4741-4745 (2012).
357. Sohn, H.W., Krueger, P.D., Davis, R.S. & Pierce, S.K. FcRL4 acts as an adaptive to innate molecular switch dampening BCR signaling and enhancing TLR signaling. *Blood* **118**, 6332-6341 (2011).
358. Ehrhardt, G.R.*, et al.* The inhibitory potential of Fc receptor homolog 4 on memory B cells. *Proc Natl Acad Sci U S A* **100**, 13489-13494 (2003).
359. Tangye, S.G., Liu, Y.J., Aversa, G., Phillips, J.H. & de Vries, J.E. Identification of functional human splenic memory B cells by expression of CD148 and CD27. *J Exp Med* **188**, 1691-1703 (1998).
360. Zhu, J.W., Brdicka, T., Katsumoto, T.R., Lin, J. & Weiss, A. Structurally distinct phosphatases CD45 and CD148 both regulate B cell and macrophage immunoreceptor signaling. *Immunity* **28**, 183-196 (2008).
361. Seifert, M.*, et al.* Functional capacities of human IgM memory B cells in early inflammatory responses and secondary germinal center reactions. *Proc Natl Acad Sci U S A* **112**, E546-555 (2015).

362. Wu, Y.C., *et al.* High-throughput immunoglobulin repertoire analysis distinguishes between human IgM memory and switched memory B-cell populations. *Blood* **116**, 1070-1078 (2010).
363. Stamatopoulos, K., *et al.* Over 20% of patients with chronic lymphocytic leukemia carry stereotyped receptors: Pathogenetic implications and clinical correlations. *Blood* **109**, 259-270 (2007).
364. Bergqvist, P., *et al.* Re-utilization of germinal centers in multiple Peyer's patches results in highly synchronized, oligoclonal, and affinity-matured gut IgA responses. *Mucosal Immunol* **6**, 122-135 (2013).
365. Toellner, K.M., *et al.* T helper 1 (Th1) and Th2 characteristics start to develop during T cell priming and are associated with an immediate ability to induce immunoglobulin class switching. *J Exp Med* **187**, 1193-1204 (1998).
366. Reboldi, A., *et al.* IgA production requires B cell interaction with subepithelial dendritic cells in Peyer's patches. *Science* **352**, aaf4822 (2016).
367. Weisel, F.J., Zuccarino-Catania, G.V., Chikina, M. & Shlomchik, M.J. A Temporal Switch in the Germinal Center Determines Differential Output of Memory B and Plasma Cells. *Immunity* **44**, 116-130 (2016).
368. Zhang, Y., *et al.* Germinal center B cells govern their own fate via antibody feedback. *J Exp Med* **210**, 457-464 (2013).
369. Louis, A.G. & Gupta, S. Primary selective IgM deficiency: an ignored immunodeficiency. *Clin Rev Allergy Immunol* **46**, 104-111 (2014).
370. Fagarasan, S., *et al.* Critical roles of activation-induced cytidine deaminase in the homeostasis of gut flora. *Science* **298**, 1424-1427 (2002).
371. Wei, M., *et al.* Mice carrying a knock-in mutation of Aicda resulting in a defect in somatic hypermutation have impaired gut homeostasis and compromised mucosal defense. *Nat Immunol* **12**, 264-270 (2011).
372. Bunker, J.J., *et al.* Innate and Adaptive Humoral Responses Coat Distinct Commensal Bacteria with Immunoglobulin A. *Immunity* **43**, 541-553 (2015).
373. Mathias, A. & Corthesy, B. Recognition of gram-positive intestinal bacteria by hybridoma- and colostrum-derived secretory immunoglobulin A is mediated by carbohydrates. *J Biol Chem* **286**, 17239-17247 (2011).
374. Moir, S., *et al.* Evidence for HIV-associated B cell exhaustion in a dysfunctional memory B cell compartment in HIV-infected viremic individuals. *J Exp Med* **205**, 1797-1805 (2008).

375. Weiss, G.E.*, et al.* Atypical memory B cells are greatly expanded in individuals living in a malaria-endemic area. *J Immunol* **183**, 2176-2182 (2009).
376. Yeo, L.*, et al.* Expression of FcRL4 defines a pro-inflammatory, RANKL-producing B cell subset in rheumatoid arthritis. *Ann Rheum Dis* **74**, 928-935 (2015).

ANNEX II

Publications

Shan M, Carrillo J, Chen K, Walland AC, Yeiser JR, van de Veen V, Gutzeit C, Yeste A, Comerma L, Boonpiyathad T, Grasset E, Lee H, Faith JJ, Blanco J, Osborne L, Siracusa MC, Akdis M, Artis D, Mehandru S, Sampson HA, Berin C, Cerutti A. IgD uncouples TH2 immunity from inflammation and enhances allergen protection by binding basophils via galectin-9.
Immunity. *Under revision.*

Magri G, Miyajima M, Bascones S, Mortha A, Puga I, Cassis L, Barra CM, Comerma L, Chudnovskiy A, Gentile M, Llige D, Cols M, Serrano S, Aróstegui JI, Juan M, Yagüe J, Merad M, Fagarasan S, Cerutti A. Innate lymphoid cells integrate stromal and immunological signals to enhance antibody production by splenic marginal zone B cells.
Nature Immunology. 2014 Apr;15(4):354-64. .ñ

Shan M, Gentile M, Yeiser JR, Walland AC, Bornstein VU, Chen K, He B, Cassis L, Bigas A, Cols M, Comerma L, Huang B, Blander JM, Xiong H, Mayer L, Berin C, Augenlicht LH, Velcich A, Cerutti A. Mucus enhances gut homeostasis and oral tolerance by delivering immunoregulatory signals.
Science. 2013 Oct 25;342(6157):447-53.

Castillo D, Puig S, Iglesias M, Seoane A, de Bolós C, Munitiz V, Parrilla P, Comerma L, Poulsom R, Krishnadath KK, Grande L, Pera M. Activation of the BMP4 pathway and early expression of CDX2 characterize non-specialized columnar metaplasia in a human model of Barrett's esophagus.
Journal of Gastrointestinal Surgery. 2012 Feb;16(2):227-37.

Puga I, Cols M, Barra CM, He B, Cassis L, Gentile M, Comerma L, Chorny A, Shan M, Xu W, Magri G, Knowles DM, Tam W, Chiu A, Bussel JB, Serrano S, Lorente JA, Bellosillo B, Lloreta J, Juanpere N, Alameda F, Baró T, de Heredia CD, Torán N, Català A, Torrebadell M, Fortuny C, Cusí V, Carreras C, Diaz GA, Blander JM, Farber CM, Silvestri G, Cunningham-Rundles C, Calvillo M, Dufour C, Notarangelo LD, Lougaris V, Plebani A, Casanova JL, Ganal SC, Diefenbach A, Aróstegui JI, Juan M, Yagüe J, Mahlaoui N, Donadieu J, Chen K, Cerutti A. B cell-helper neutrophils stimulate the diversification and production of immunoglobulin in the marginal zone of the spleen.
Nature Immunology. 2011 Dec 25;13(2):170-80.